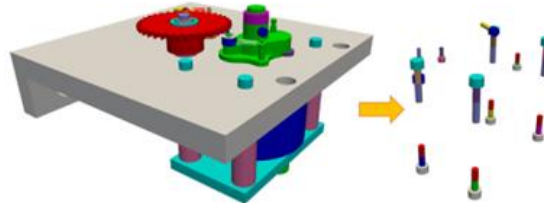
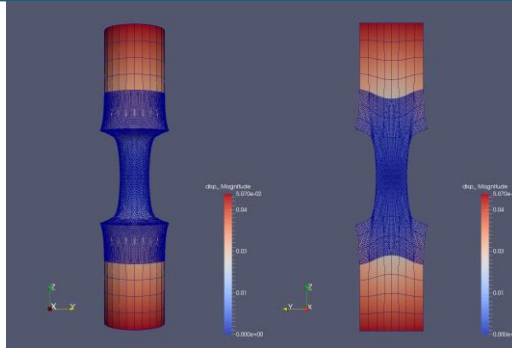
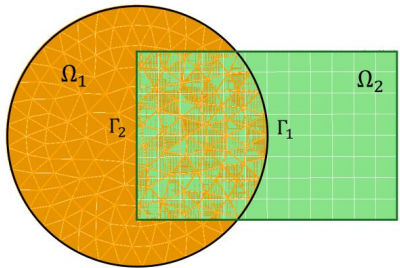


Accelerating analyst workflows via alternating Schwarz-based coupling and (non-intrusive Operator Inference-based) model order reduction



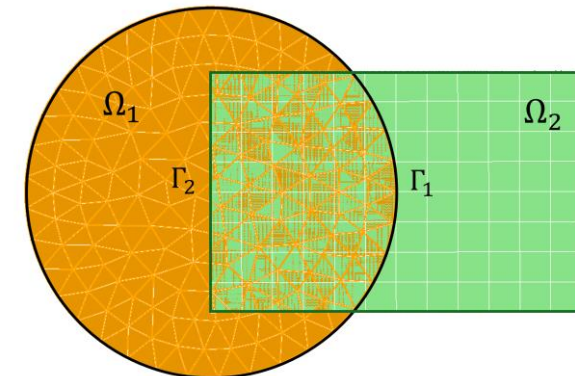
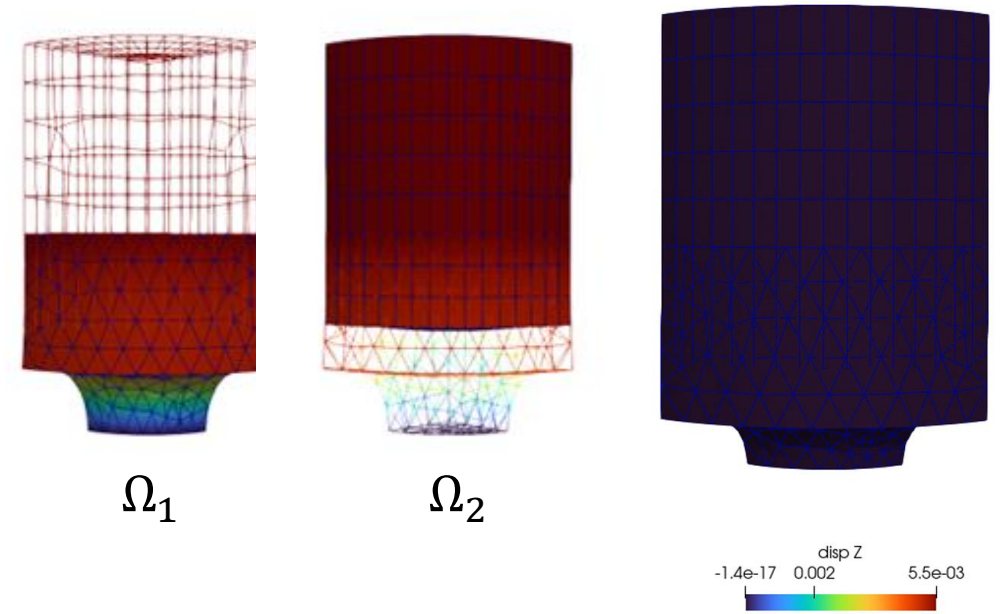
I. Tezaur¹, E. Parish¹, A. Gruber¹, I. Moore^{1,2}, C. Wentland¹, C. Rodriguez³, A. Mota¹

¹Sandia National Laboratories, USA. ²Virginia Tech, USA.

³Columbia University, USA

Outline

1. Preliminaries
 - Motivation
 - The Schwarz Alternating Method (SAM) for Multi-Scale Coupling
 - Non-Intrusive Operator Inference (OpInf)
2. Overlapping SAM for OpInf Reduced Order Model (ROM) Coupling
 - Methodology
 - Numerical Examples
3. Non-overlapping SAM for OpInf ROM Coupling
 - Methodology
 - Numerical Example
4. Summary
5. Ongoing & Future Work



Outline

1. Preliminaries

- Motivation
- The Schwarz Alternating Method (SAM) for Multi-Scale Coupling
- Non-Intrusive Operator Inference (OpInf)

2. Overlapping SAM for OpInf Reduced Order Model (ROM) Coupling

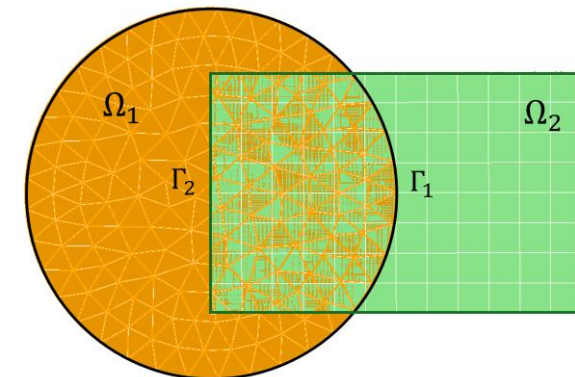
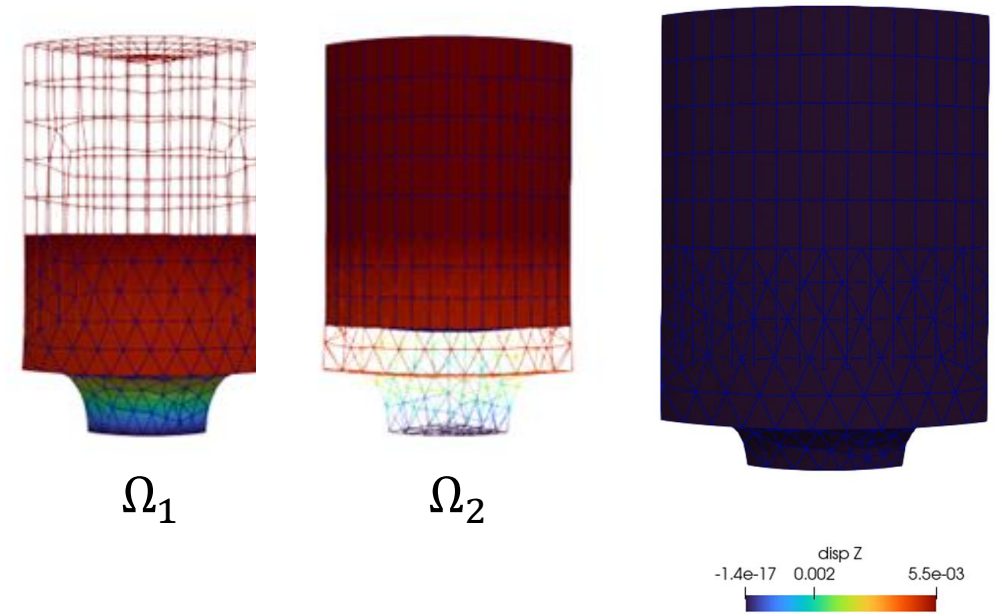
- Methodology
- Numerical Examples

3. Non-overlapping SAM for OpInf ROM Coupling

- Methodology
- Numerical Example

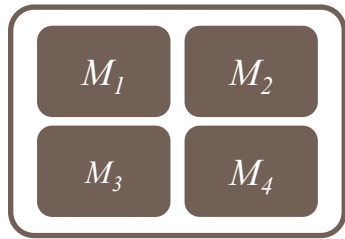
4. Summary

5. Ongoing & Future Work



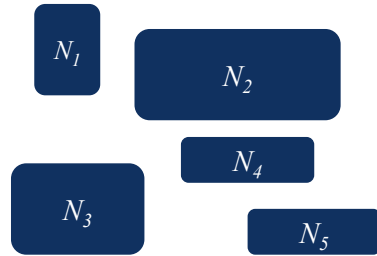
Motivation: Multiscale & Multiphysics Coupling for Predictive Digital Twins

There exist established rigorous mathematical theories for coupling multiscale/multiphysics components based on traditional discretization methods (FOMs).



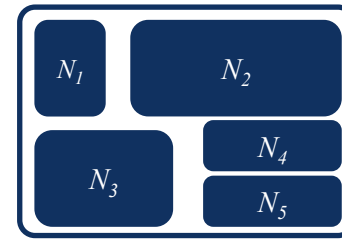
Complex System Model

- PDEs, ODEs
- Nonlocal integral
- Classical DFT
- Atomistic, ...



Traditional Methods

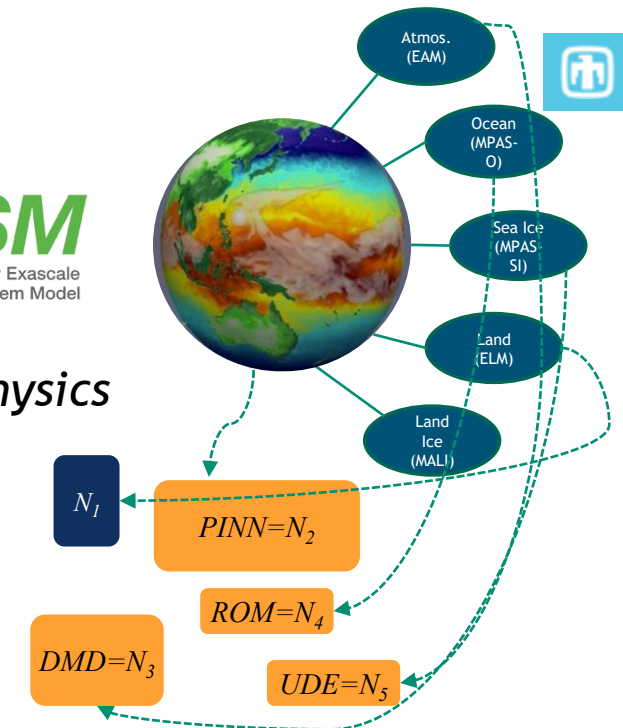
- Mesh-based (FE, FV, FD)
- Meshless (SPH, MLS)
- Implicit, explicit
- Eulerian, Lagrangian, ...



Coupled Numerical Model

- Monolithic (Lagrange multipliers)
- Partitioned (loose) coupling
- Iterative (Schwarz, optimization)

Multiphysics

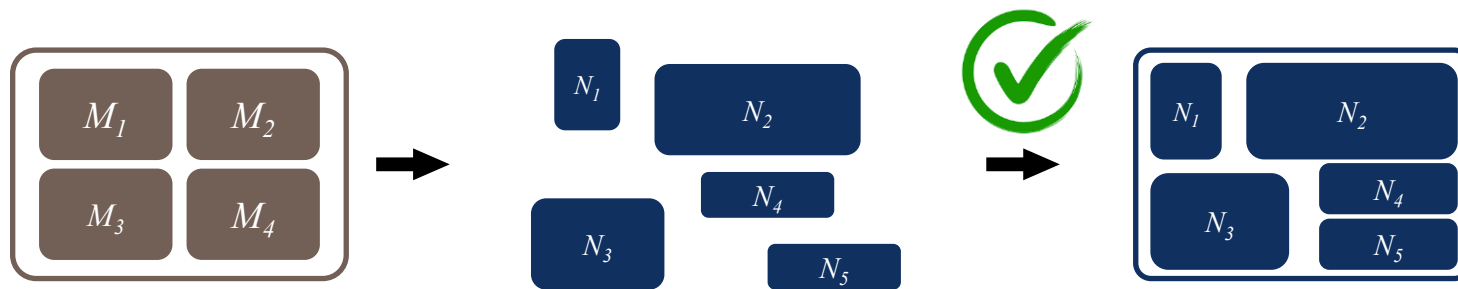


Traditional + Data-Driven Methods

- PINNs
- Neural ODEs
- Projection-based ROMs, ...

Motivation: Multiscale & Multiphysics Coupling for Predictive Digital Twins

There exist established rigorous mathematical theories for coupling multiscale/multiphysics components based on traditional discretization methods (FOMs).



Complex System Model

- PDEs, ODEs
- Nonlocal integral
- Classical DFT
- Atomistic, ...

Traditional Methods

- Mesh-based (FE, FV, FD)
- Meshless (SPH, MLS)
- Implicit, explicit
- Eulerian, Lagrangian, ...

Coupled Numerical Model

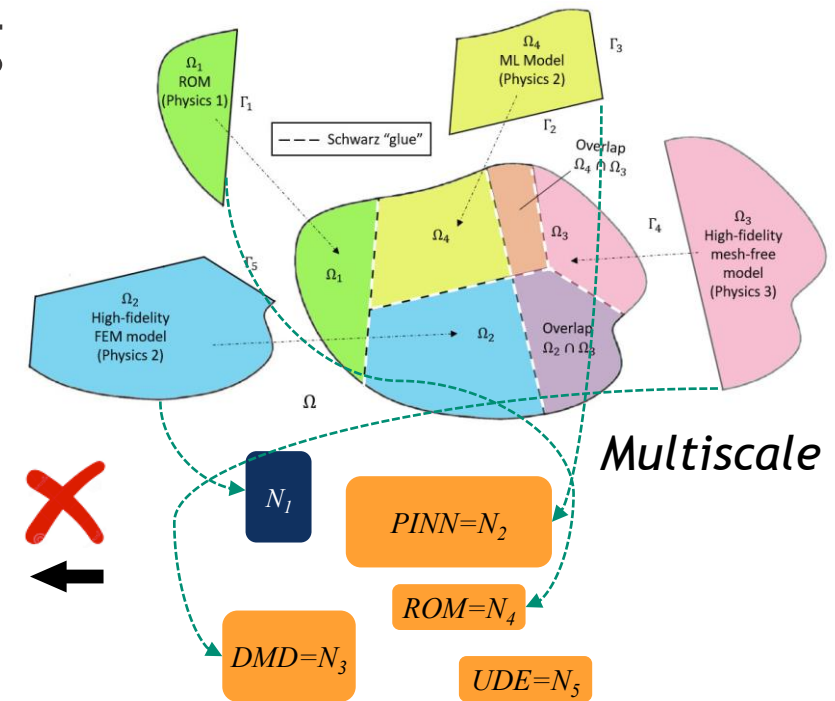
- Monolithic (Lagrange multipliers)
- Partitioned (loose) coupling
- Iterative (Schwarz, optimization)

Traditional + Data-Driven Methods

- PINNs
- Neural ODEs
- Projection-based ROMs, ...

Deficiencies of data-driven models and couplings involving them:

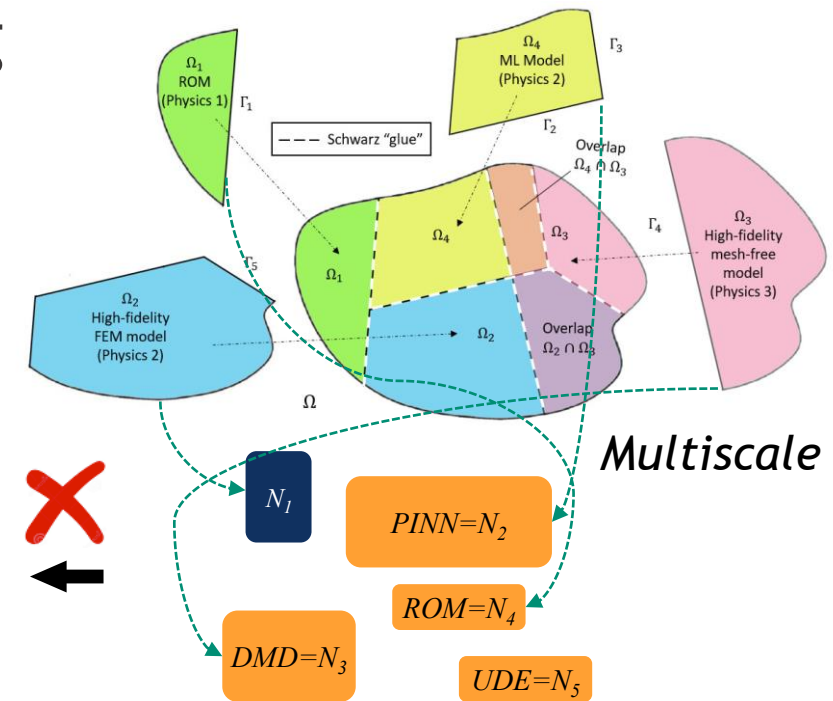
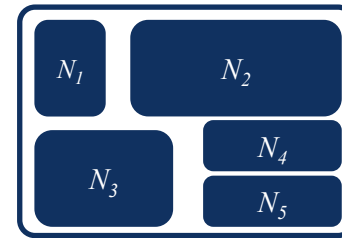
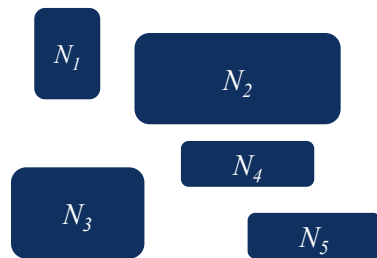
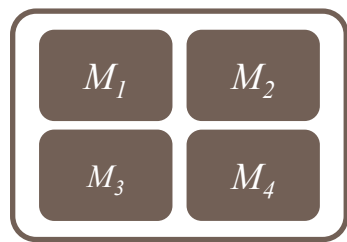
- Existing coupling methods for high-fidelity models may not work out-of-the-box when including data-driven models
- ROMs can suffer from lack of robustness, stability and accuracy, and cannot be easily refined to achieve a specified accuracy



Multiscale

Motivation: Multiscale & Multiphysics Coupling for Predictive Digital Twins

There exist established rigorous mathematical theories for coupling multiscale/multiphysics components based on traditional discretization methods (FOMs).



Complex System Model

- PDEs, ODEs
- Nonlocal integral
- Classical DFT
- Atomistic, ...

Traditional Methods

- Mesh-based (FE, FV, FD)
- Meshless (SPH, MLS)
- Implicit, explicit
- Eulerian, Lagrangian, ...

Coupled Numerical Model

- Monolithic (Lagrange multipliers)
- Partitioned (loose) coupling
- Iterative (Schwarz, optimization)

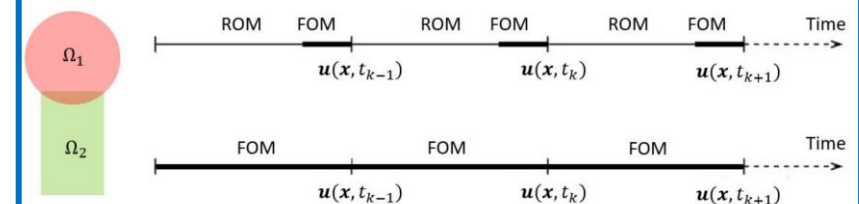
Traditional + Data-Driven Methods

- PINNs
- Neural ODEs
- Projection-based ROMs, ...

Deficiencies of data-driven models and couplings involving them:

- Existing coupling methods for high-fidelity models may not work out-of-the-box when including data-driven models
- ROMs can suffer from lack of robustness, stability and accuracy, and cannot be easily refined to achieve a specified accuracy

Proposed solution: domain decomposition- (DD-) based coupling via SAM & (soon) online model switching



Outline

1. Preliminaries

- Motivation
- **The Schwarz Alternating Method (SAM) for Multi-Scale Coupling**
- Non-Intrusive Operator Inference (OpInf)

2. Overlapping SAM for OpInf Reduced Order Model (ROM) Coupling

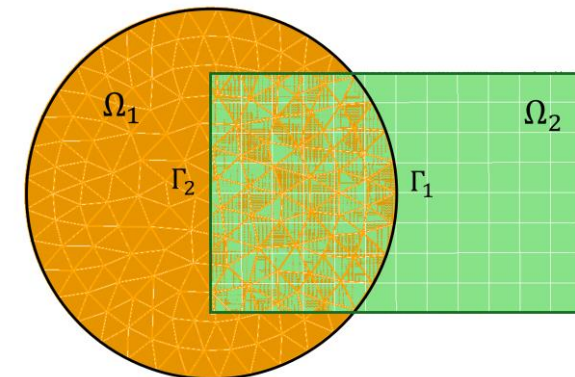
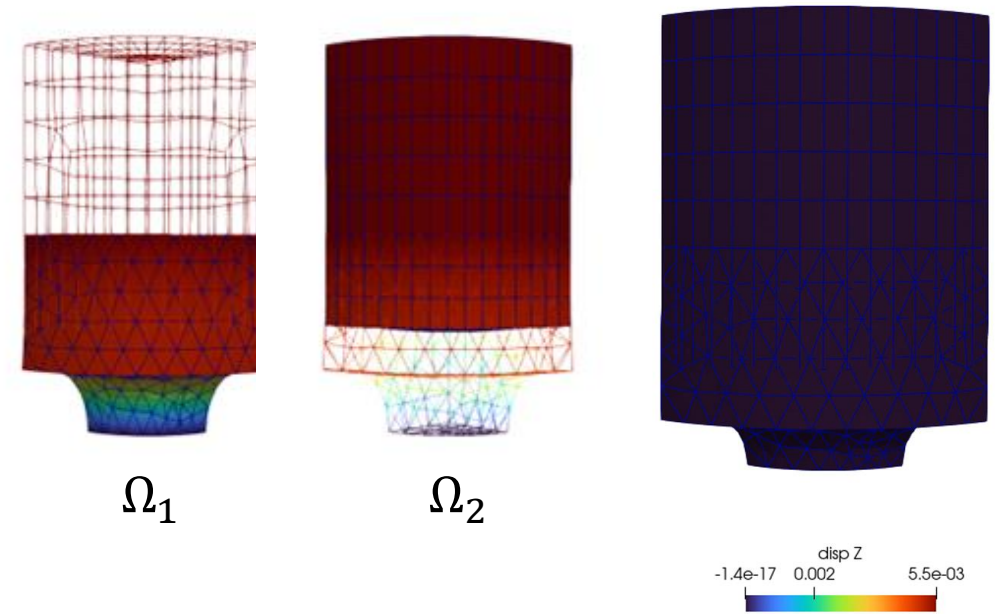
- Methodology
- Numerical Examples

3. Non-overlapping SAM for OpInf ROM Coupling

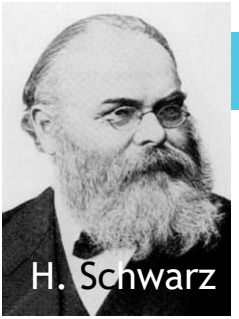
- Methodology
- Numerical Example

4. Summary

5. Ongoing & Future Work



Schwarz Alternating Method (SAM)



- Proposed in 1870 by H. Schwarz for solving Laplace PDE on irregular domains.

Crux of Method: if the solution is known in regularly shaped domains, use those as pieces to iteratively build a solution for the more complex domain.

Basic Schwarz Algorithm

Initialize:

- Solve PDE by any method on Ω_1 w/ initial guess for transmission boundary conditions (BCs) on Γ_1 .

Iterate until convergence:

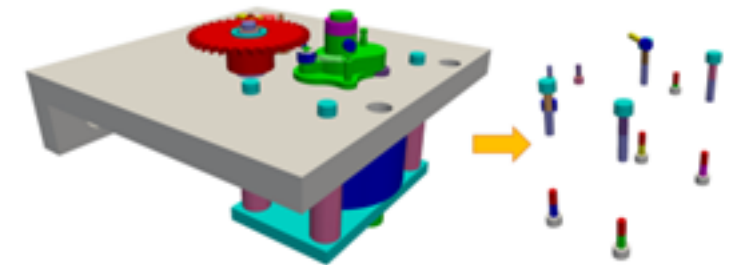
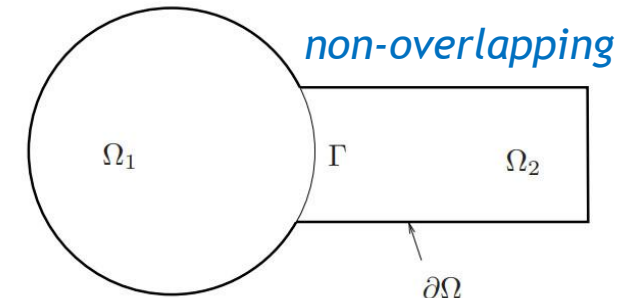
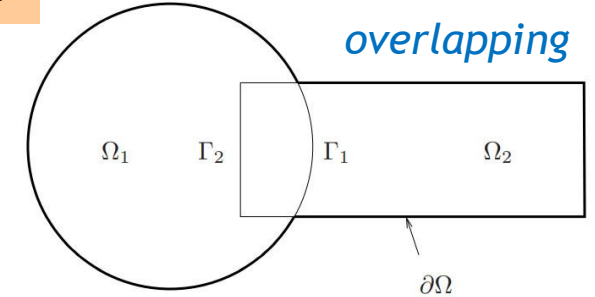
- Solve PDE by any method in Ω_2 w/ BCs on Γ_2 from just-obtained Ω_1 solution.
- Solve PDE by any method in Ω_1 w/ BCs on Γ_1 from just-obtained Ω_2 solution.

- SAM most commonly used as a **preconditioner** for linear solvers.

Idea behind this work: using SAM as a **discretization/ coupling method** for solving multiscale PDEs.

Original driving application: simplifying meshing in solid mechanics.

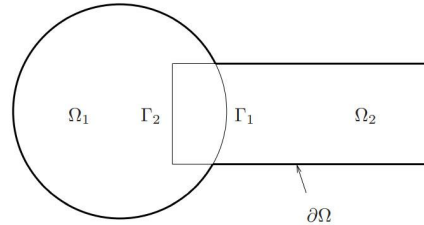
- Enables coupling* of subdomains with **different non-conformal meshes, element types, levels of refinement, time-steppers, solvers and models**



Overlapping Domain Decomposition

$$\begin{cases} \text{Div } \mathbf{P}_1^{(n+1)} + \rho \mathbf{B}(t_i) = \mathbf{0}, & \text{in } \Omega_1 \\ \boldsymbol{\varphi}_1^{(n+1)} = \boldsymbol{\chi}, & \text{on } \partial\Omega_1 \setminus \Gamma_1 \\ \boldsymbol{\varphi}_1^{(n+1)} = \boldsymbol{\varphi}_2^{(n)} & \text{on } \Gamma_2 \end{cases}$$

$$\begin{cases} \text{Div } \mathbf{P}_2^{(n+1)} + \rho \mathbf{B}(t_i) = \mathbf{0}, & \text{in } \Omega_2 \\ \boldsymbol{\varphi}_2^{(n+1)} = \boldsymbol{\chi}, & \text{on } \partial\Omega_2 \setminus \Gamma_2 \\ \boldsymbol{\varphi}_2^{(n+1)} = \boldsymbol{\varphi}_1^{(n+1)} & \text{on } \Gamma_2 \end{cases}$$



*Easier implementation
and faster convergence*

Model PDE:

$$\begin{cases} \text{Div } \mathbf{P} + \rho \mathbf{B} = \mathbf{0}, & \text{in } \Omega \\ \boldsymbol{\varphi} = \boldsymbol{\chi}, & \text{on } \partial\Omega \end{cases}$$

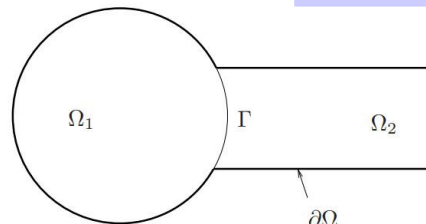
- Dirichlet-Dirichlet transmission BCs [Schwarz, 1870; Lions, 1988]

Non-overlapping Domain Decomposition

$$\begin{cases} \text{Div } \mathbf{P}_1^{(n+1)} + \rho \mathbf{B}(t_i) = \mathbf{0}, & \text{in } \Omega_1 \\ \boldsymbol{\varphi}_1^{(n+1)} = \boldsymbol{\chi}, & \text{on } \partial\Omega_1 \setminus \Gamma \\ \boldsymbol{\varphi}_1^{(n+1)} = \boldsymbol{\lambda}_{n+1} & \text{on } \Gamma \end{cases}$$

$$\begin{cases} \text{Div } \mathbf{P}_2^{(n+1)} + \rho \mathbf{B}(t_i) = \mathbf{0}, & \text{in } \Omega_2 \\ \boldsymbol{\varphi}_2^{(n+1)} = \boldsymbol{\chi}, & \text{on } \partial\Omega_2 \setminus \Gamma \\ \mathbf{P}_2^{(n+1)} \mathbf{n} = \mathbf{P}_1^{(n+1)} \mathbf{n}, & \text{on } \Gamma \end{cases}$$

$$\boldsymbol{\lambda}_{n+1} = \theta \boldsymbol{\varphi}_2^{(n)} + (1 - \theta) \boldsymbol{\lambda}_n, \text{ on } \Gamma, \text{ for } n \geq 1$$

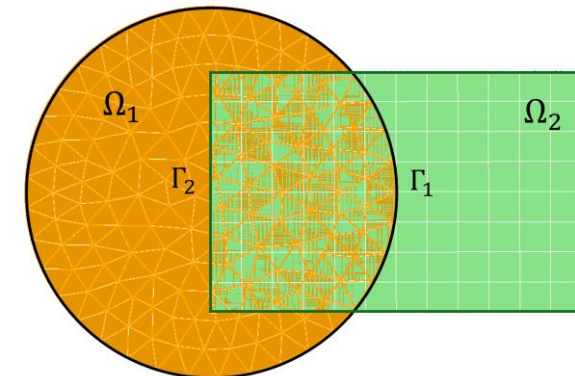
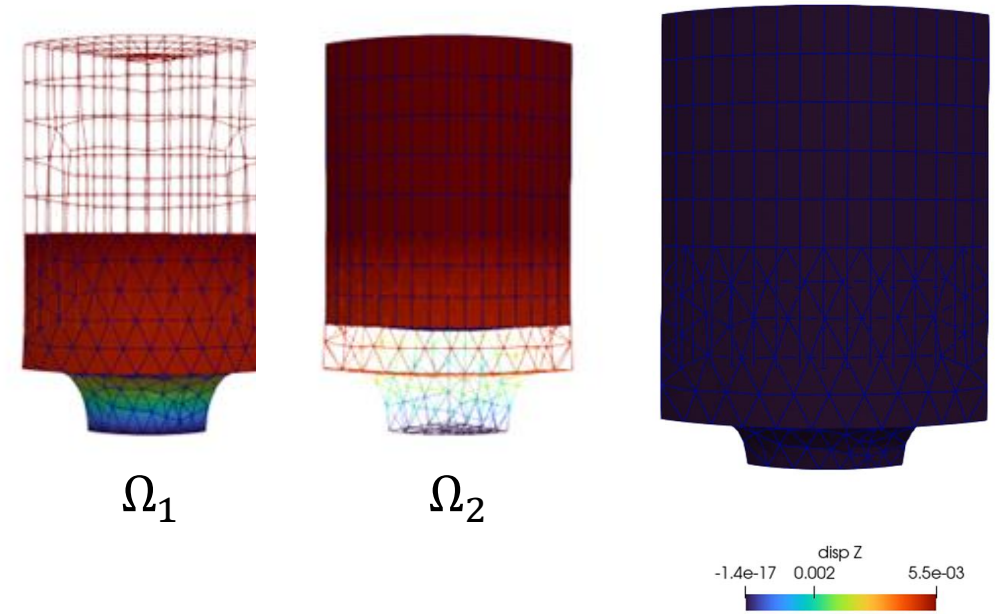


*More flexible but
slower to converge*

- Relevant for multi-material and multiphysics coupling
- Alternating Dirichlet-Neumann transmission BCs [Zanolli *et al.*, 1987]
- Robin-Robin transmission BCs also lead to convergence [Lions, 1990]
- $\theta \in [0,1]$: relaxation parameter (can help convergence)

Outline

1. **Preliminaries**
 - Motivation
 - The Schwarz Alternating Method (SAM) for Multi-Scale Coupling
 - **Non-Intrusive Operator Inference (OpInf)**
2. Overlapping SAM for OpInf Reduced Order Model (ROM) Coupling
 - Methodology
 - Numerical Examples
3. Non-overlapping SAM for OpInf ROM Coupling
 - Methodology
 - Numerical Example
4. Summary
5. Ongoing & Future Work

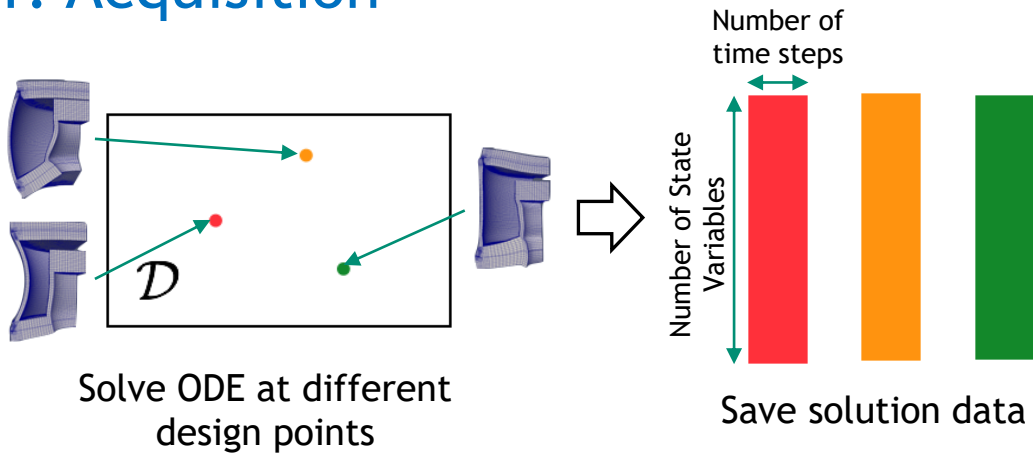


Projection-Based Model Order Reduction via the POD/Galerkin Method



$$\text{Full Order Model (FOM): } M \frac{d^2 \mathbf{u}}{dt^2} + \mathbf{f}_{\text{int}}(\mathbf{u}) = \mathbf{f}_{\text{ext}}$$

1. Acquisition



2. Learning

Proper Orthogonal Decomposition (POD):

$$\mathbf{X} = \begin{bmatrix} \text{red} & \text{orange} & \text{green} \end{bmatrix} = \begin{bmatrix} \text{brown} & \text{light blue} \end{bmatrix} \mathbf{U} \quad \Sigma \quad \begin{bmatrix} \text{light blue} \end{bmatrix} \mathbf{V}^T$$

ROM = projection-based Reduced Order Model

3. Projection-Based Reduction

Reduce the number of unknowns

$$\mathbf{u}(t) \approx \tilde{\mathbf{u}}(t) = \Phi \hat{\mathbf{u}}(t)$$



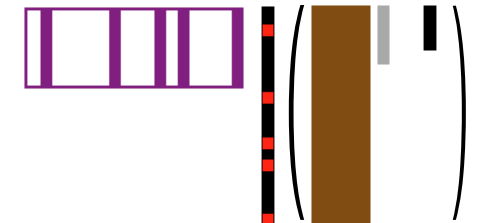
Perform Galerkin projection

$$\Phi^T M \Phi \frac{d^2 \hat{\mathbf{u}}}{dt^2} + \Phi^T \mathbf{f}_{\text{int}}(\Phi \hat{\mathbf{u}}) = \Phi^T \mathbf{f}_{\text{ext}}$$

Disadvantage: intrusive!

Hyper-reduce nonlinear terms

$$\mathbf{f}_{\text{int}}(\Phi \hat{\mathbf{u}}) \approx \mathbf{A} \mathbf{f}_{\text{int}}(\Phi \hat{\mathbf{u}})$$



Hyper-reduction/sample mesh

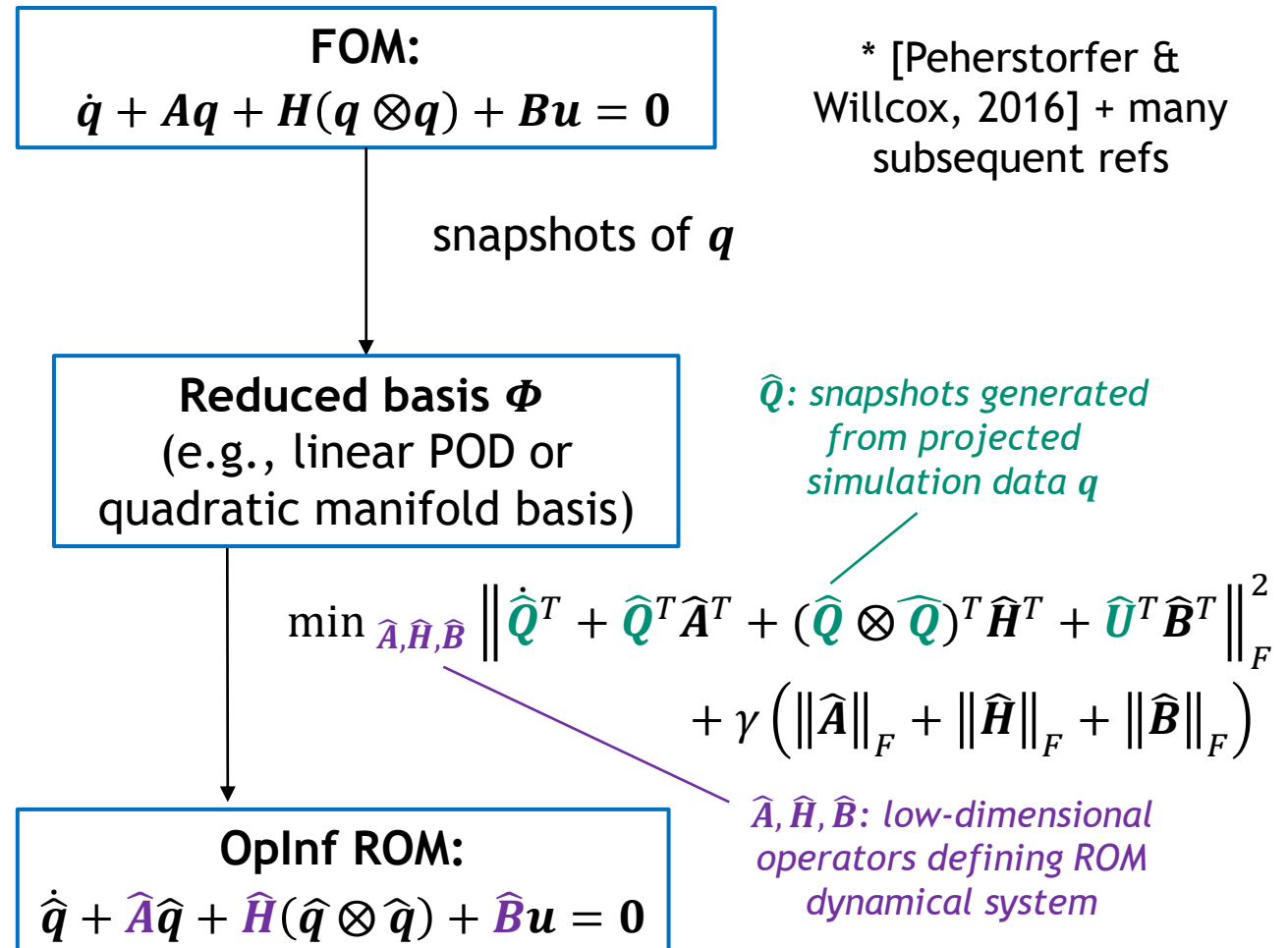
HROM = Hyper-reduced ROM



Key Idea Behind OpInf: circumvent the burden of implementing intrusive ROMs in HPC codes by **combining projection-based ROM and machine learning (ML)**.

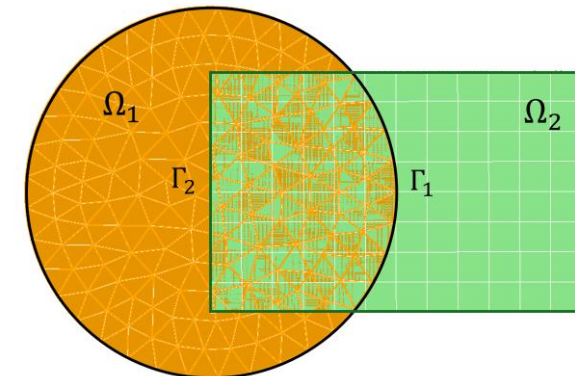
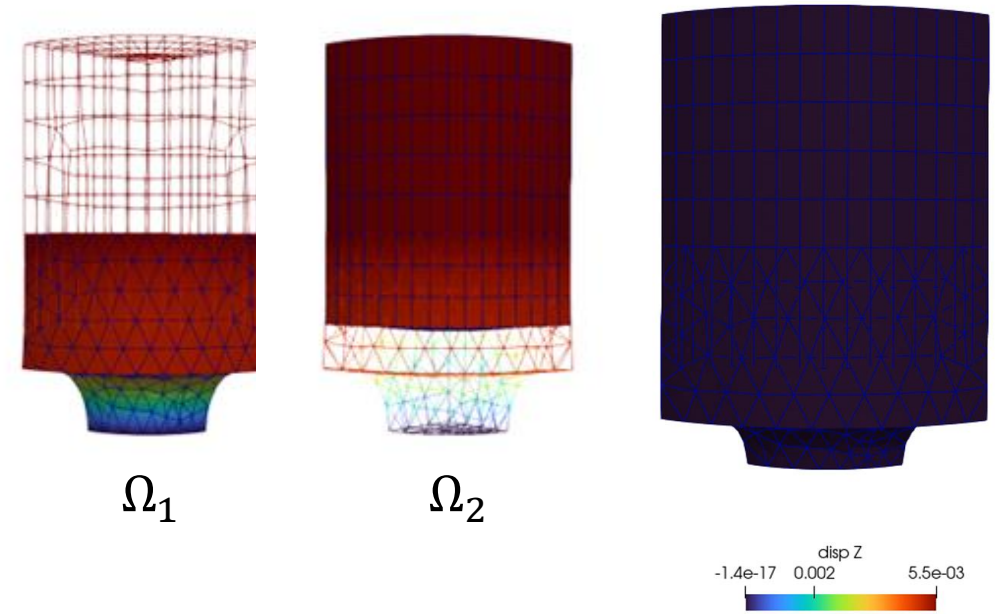
Nuances:

- OpInf can be applied to **nonlinear problems** by transforming the nonlinear PDEs into PDEs with a polynomial functional form (“**lifting**” [Qian *et al.*, 2019]) or assuming a **polynomial functional form** for the ROM
- The OpInf least-squares (LS) minimization problem often requires **regularization** to be solvable, e.g., Tikhonov regularization
- **Structure preservation** (e.g., symmetry constraints) can be incorporated into the OpInf LS minimization problem



Outline

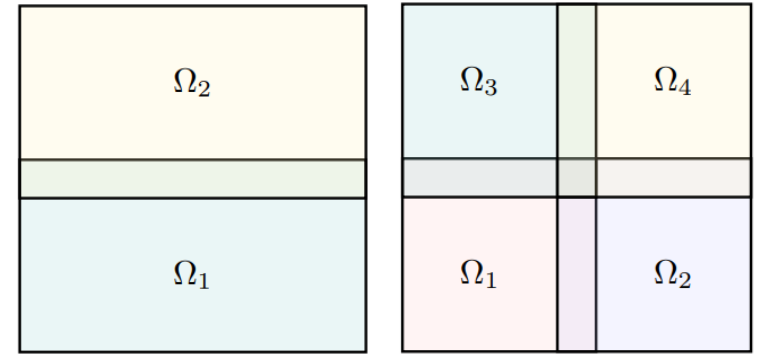
1. Preliminaries
 - Motivation
 - The Schwarz Alternating Method (SAM) for Multi-Scale Coupling
 - Non-Intrusive Operator Inference (OpInf)
2. Overlapping SAM for OpInf Reduced Order Model (ROM) Coupling
 - Methodology
 - Numerical Examples
3. Non-overlapping SAM for OpInf ROM Coupling
 - Methodology
 - Numerical Example
4. Summary
5. Ongoing & Future Work





Offline stage:

- Create **DD** of Ω into d **overlapping subdomains** Ω_i
- Perform a SAM-coupled **all-FOM simulation** on $\cup_i \Omega_i$
- Compute **POD basis** Φ_i on each Ω_i
- Assume a **functional form** for your ROM in Ω_i , informed by the functional form of the corresponding FOM
 - *Key question: how to impose Schwarz BCs in OpInf ROMs?*

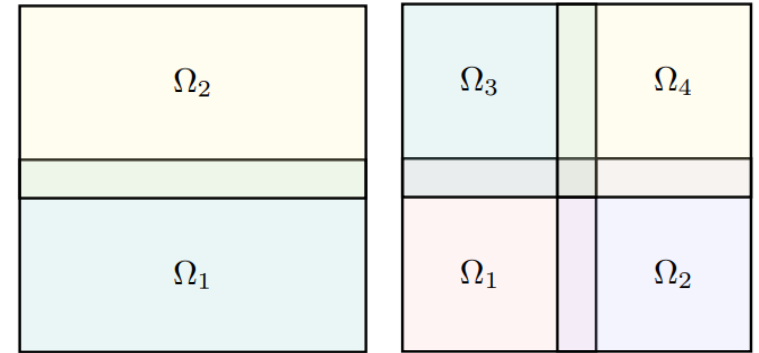


OpInf ROM in Ω_i :

$$\hat{\mathbf{q}}_i + \hat{\mathbf{A}}_i \hat{\mathbf{q}}_i + \hat{\mathbf{H}}_i(\hat{\mathbf{q}}_i \otimes \hat{\mathbf{q}}_i) = \mathbf{0}$$

Offline stage:

- Create **DD** of Ω into d **overlapping subdomains** Ω_i
- Perform a SAM-coupled **all-FOM simulation** on $\cup_i \Omega_i$
- Compute **POD basis** Φ_i on each Ω_i
- Assume a **functional form** for your ROM in Ω_i , informed by the functional form of the corresponding FOM
 - **Key question: how to impose Schwarz BCs in OpInf ROMs?**
 - ❖ **Boundary transmission enters through learned source term $\hat{B}_i g_i$ added to OpInf ROM dynamical system**



OpInf ROM + Schwarz BCs in Ω_i :

$$\hat{q}_i + \hat{A}_i \hat{q}_i + \hat{H}_i (\hat{q}_i \otimes \hat{q}_i) + \underbrace{\hat{B}_i g_i}_{\text{Schwarz Dirichlet BC term}} = \mathbf{0}$$

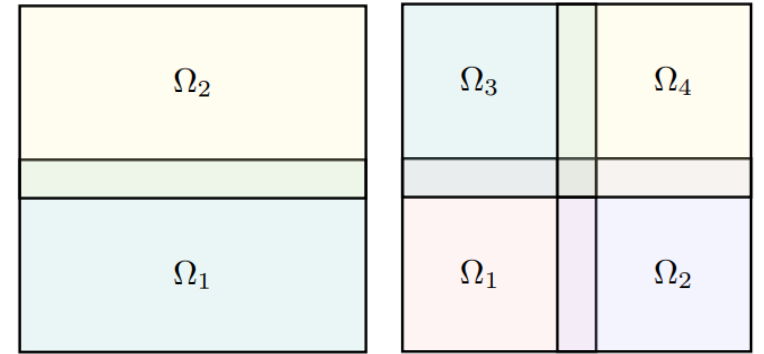
Motivated by
implementation of
Dirichlet BCs in FEM

Schwarz
Dirichlet BC
term



Offline stage:

- Create **DD** of Ω into d **overlapping subdomains** Ω_i
- Perform a SAM-coupled **all-FOM simulation** on $\cup_i \Omega_i$
- Compute **POD basis** Φ_i on each Ω_i
- Assume a **functional form** for your ROM in Ω_i , informed by the functional form of the corresponding FOM
 - **Key question: how to impose Schwarz BCs in OpInf ROMs?**
 - ❖ **Boundary transmission enters through learned source term** $\hat{\mathbf{B}}_i \mathbf{g}_i$ added to OpInf ROM dynamical system
 - ❖ **Further reduction achieved by expanding** \mathbf{g}_i in its own POD basis Φ_i^g and approximating $\hat{\mathbf{B}}_i \mathbf{g}_i \approx \hat{\mathbf{B}}_i \hat{\mathbf{g}}_i = \tilde{\mathbf{B}}_i \mathbf{g}_i$ where $\hat{\mathbf{g}}_i = \Phi_i^g \mathbf{g}_i$



OpInf ROM + Schwarz BCs in Ω_i :

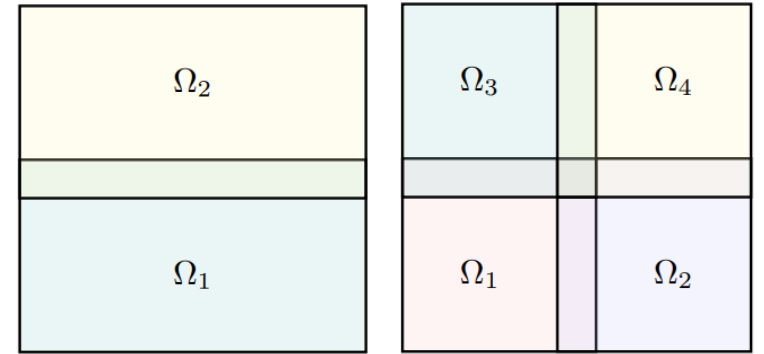
$$\hat{\mathbf{q}}_i + \hat{\mathbf{A}}_i \hat{\mathbf{q}}_i + \hat{\mathbf{H}}_i (\hat{\mathbf{q}}_i \otimes \hat{\mathbf{q}}_i) + \underbrace{\tilde{\mathbf{B}}_i \mathbf{g}_i}_{\text{Schwarz Dirichlet BC term}} = \mathbf{0}$$

Motivated by
implementation of
Dirichlet BCs in FEM

Schwarz
Dirichlet BC
term

Offline stage:

- Create DD of Ω into d overlapping subdomains Ω_i
- Perform a SAM-coupled all-FOM simulation on $\cup_i \Omega_i$
- Compute POD basis Φ_i on each Ω_i
- Assume a functional form for your ROM in Ω_i , informed by the functional form of the corresponding FOM
 - *Key question: how to impose Schwarz BCs in OpInf ROMs?*
 - ❖ *Boundary transmission enters through learned source term $\hat{\mathbf{B}}_i \mathbf{g}_i$ added to OpInf ROM dynamical system*
 - ❖ *Further reduction achieved by expanding \mathbf{g}_i in its own POD basis Φ_i^g and approximating $\hat{\mathbf{B}}_i \mathbf{g}_i \approx \hat{\mathbf{B}}_i \hat{\mathbf{g}}_i = \tilde{\mathbf{B}}_i \mathbf{g}_i$ where $\hat{\mathbf{g}}_i = \Phi_i^g \mathbf{g}_i$*
- Compute OpInf operators $\hat{\mathbf{A}}_i, \hat{\mathbf{H}}_i$ and $\tilde{\mathbf{B}}_i$ in each subdomain Ω_i by solving regularized OpInf LS minimization problem



OpInf ROM + Schwarz BCs in Ω_i :

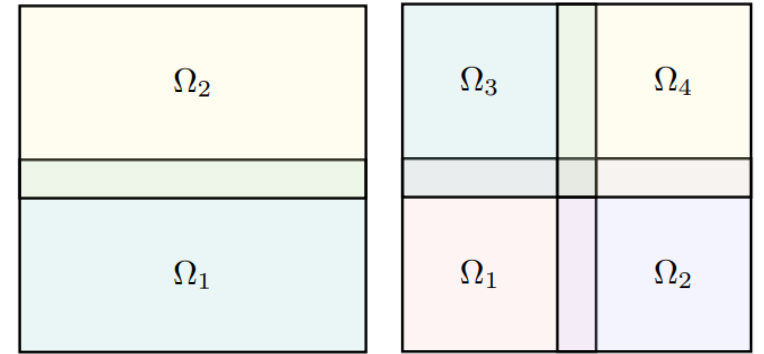
$$\hat{\mathbf{q}}_i + \hat{\mathbf{A}}_i \hat{\mathbf{q}}_i + \hat{\mathbf{H}}_i (\hat{\mathbf{q}}_i \otimes \hat{\mathbf{q}}_i) + \underbrace{\tilde{\mathbf{B}}_i \mathbf{g}_i}_{\text{Schwarz Dirichlet BC term}} = \mathbf{0}$$

Motivated by
implementation of
Dirichlet BCs in FEM

Schwarz
Dirichlet BC
term

Offline stage:

- Create DD of Ω into d overlapping subdomains Ω_i
- Perform a SAM-coupled all-FOM simulation on $\cup_i \Omega_i$
- Compute POD basis Φ_i on each Ω_i
- Assume a functional form for your ROM in Ω_i , informed by the functional form of the corresponding FOM
 - *Key question: how to impose Schwarz BCs in OpInf ROMs?*
 - ❖ *Boundary transmission enters through learned source term $\tilde{\mathbf{B}}_i \mathbf{g}_i$ added to OpInf ROM dynamical system*
 - ❖ *Further reduction achieved by expanding \mathbf{g}_i in its own POD basis Φ_i^g and approximating $\tilde{\mathbf{B}}_i \mathbf{g}_i \approx \hat{\mathbf{B}}_i \hat{\mathbf{g}}_i = \tilde{\tilde{\mathbf{B}}}_i \mathbf{g}_i$ where $\hat{\mathbf{g}}_i = \Phi_i^g \mathbf{g}_i$*
- Compute OpInf operators $\hat{\mathbf{A}}_i, \hat{\mathbf{H}}_i$ and $\tilde{\mathbf{B}}_i$ in each subdomain Ω_i by solving regularized OpInf LS minimization problem



OpInf ROM + Schwarz BCs in Ω_i :

$$\hat{\mathbf{q}}_i + \hat{\mathbf{A}}_i \hat{\mathbf{q}}_i + \hat{\mathbf{H}}_i (\hat{\mathbf{q}}_i \otimes \hat{\mathbf{q}}_i) + \underbrace{\tilde{\mathbf{B}}_i \mathbf{g}_i}_{\text{Schwarz Dirichlet BC term}} = \mathbf{0}$$

Motivated by implementation of Dirichlet BCs in FEM

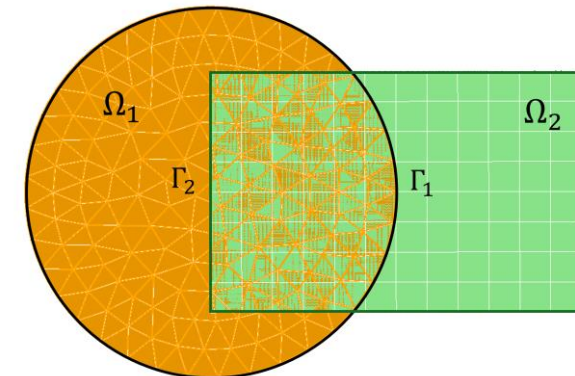
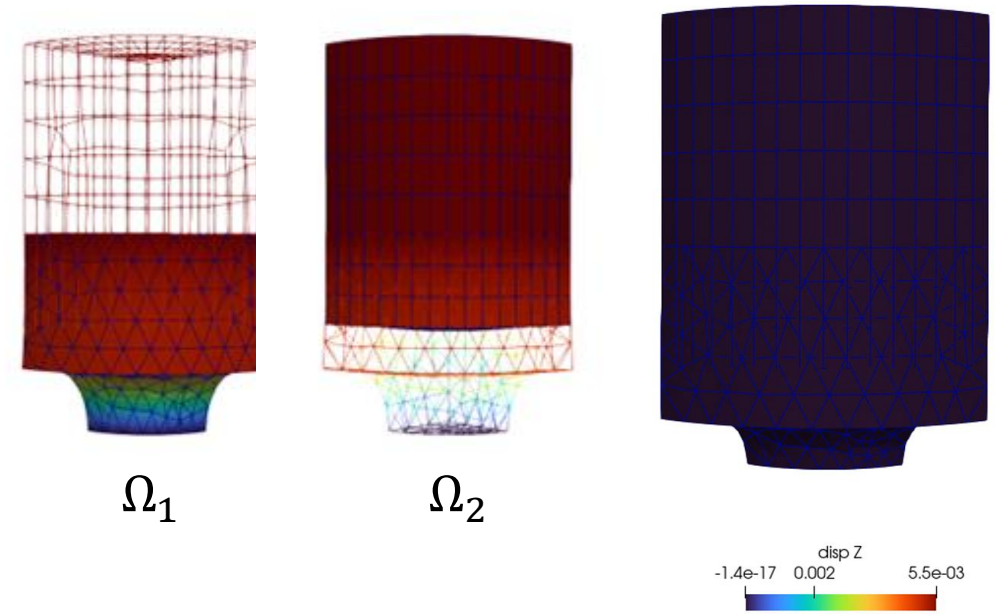
Schwarz Dirichlet BC term

Online stage:

- Apply Schwarz iteration procedure, with Schwarz BC transfer via pre-learned boundary contributions $\tilde{\mathbf{B}}_i \mathbf{g}_i$

Outline

1. Preliminaries
 - Motivation
 - The Schwarz Alternating Method (SAM) for Multi-Scale Coupling
 - Non-Intrusive Operator Inference (OpInf)
2. **Overlapping SAM for OpInf Reduced Order Model (ROM) Coupling**
 - Methodology
 - **Numerical Examples**
3. Non-overlapping SAM for OpInf ROM Coupling
 - Methodology
 - Numerical Example
4. Summary
5. Ongoing & Future Work

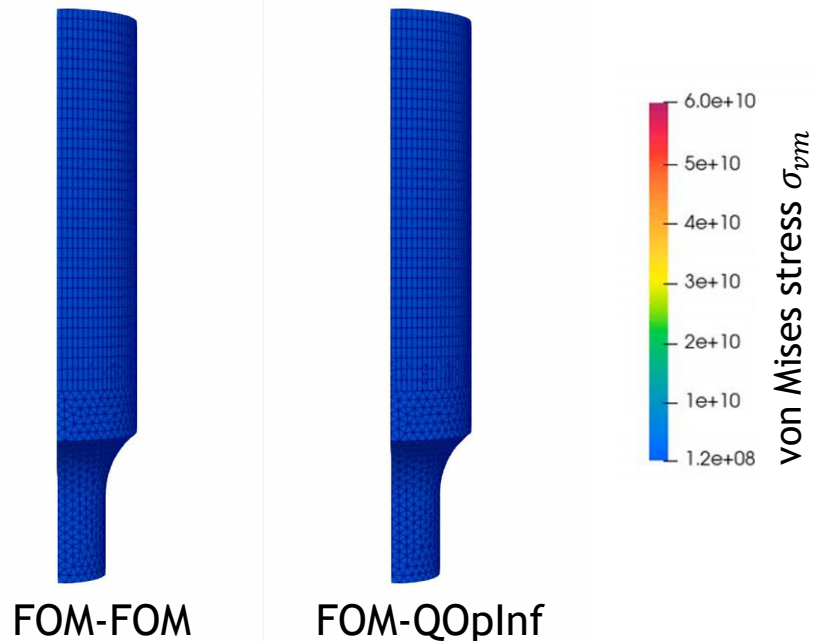


Tension Specimen (Overlapping SAM, Predictive)

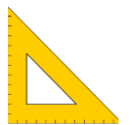


- Hyperelastic (NeoHookean) tension specimen pulled from top
- TET10 - HEX8 overlapping coupling with implicit Newmark with same Δt
- Quadratic OpInf (QOpInf) models with $M=2$ POD modes, capturing 99.9999% snapshot energy
- All results are predictive w.r.t. DBC applied at top of holder

		FOM-FOM	FOM-QOpInf	QOpInf-QOpInf
Ω_1 rel errs	displacement	—	3.44e-4	5.73e-4
	velocity	—	1.72e-2	1.83e-2
	σ_{vm} stress	—	3.41e-4	8.53e-4
Ω_2 rel errs	displacement	—	2.50e-4	4.41e-4
	velocity	—	1.86e-2	1.96e-2
	σ_{vm} stress	—	2.40e-3	6.00e-3
CPU time	—	8h 19m 29.5s	1h 21m 25.9s	4m 42.1s
Mean/max # Schwarz iters	—	32.0/32	7.03/8	7.74/8



QOpInf = Quadratic OpInf

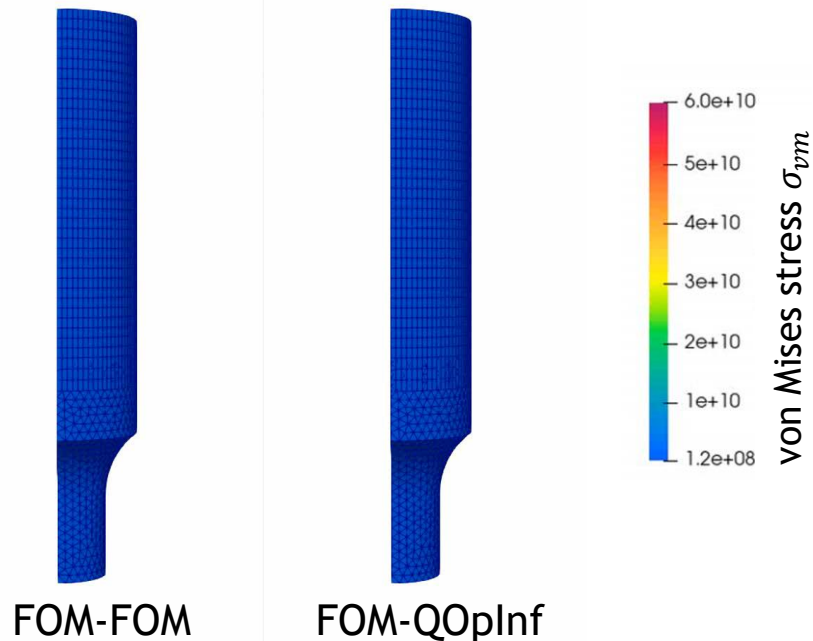


Tension Specimen (Overlapping SAM, Predictive)



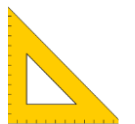
- Hyperelastic (NeoHookean) tension specimen pulled from top
- TET10 - HEX8 overlapping coupling with implicit Newmark with same Δt
- Quadratic OpInf (QOpInf) models with $M=2$ POD modes, capturing 99.9999% snapshot energy
- All results are predictive w.r.t. DBC applied at top of holder

		FOM-FOM	FOM-QOpInf	QOpInf-QOpInf
Ω_1 rel errs	displacement	—	3.44e-4	5.73e-4
	velocity	—	1.72e-2	1.83e-2
	σ_{vm} stress	—	3.41e-4	8.53e-4
Ω_2 rel errs	displacement	—	2.50e-4	4.41e-4
	velocity	—	1.86e-2	1.96e-2
	σ_{vm} stress	—	2.40e-3	6.00e-3
CPU time	—	8h 19m 29.5s	1h 21m 25.9s	4m 42.1s
Mean/max # Schwarz iters	—	32.0/32	7.03/8	7.74/8



- Relative errors of $O(1e-4)$ - $O(1e-3)$ are achieved for the displacement and von Mises stress (σ_{vm})

QOpInf = Quadratic OpInf

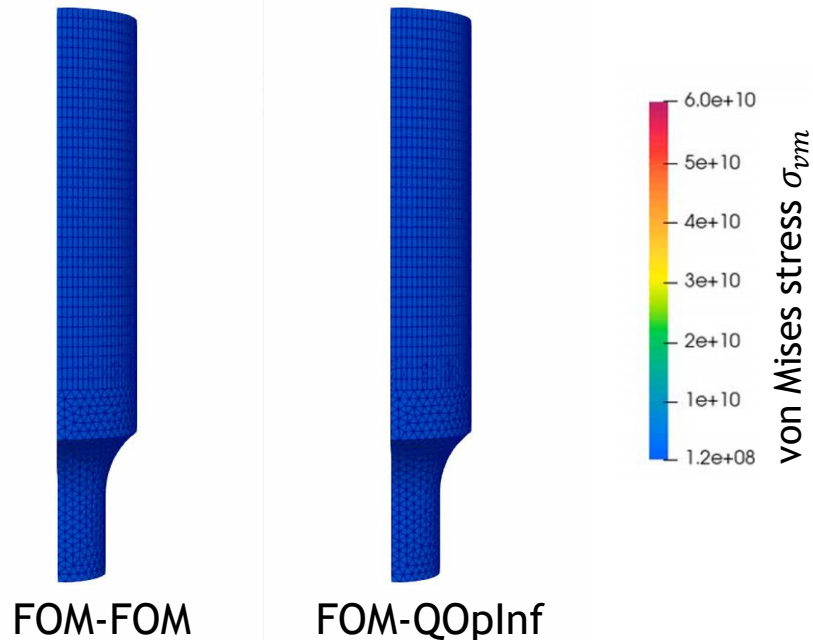


Tension Specimen (Overlapping SAM, Predictive)



- Hyperelastic (Neo-Hookean) tension specimen pulled from top
- TET10 - HEX8 overlapping coupling with implicit Newmark with same Δt
- Quadratic Oplnf (QOplnf) models with $M=2$ POD modes, capturing 99.9999% snapshot energy
- All results are predictive w.r.t. DBC applied at top of holder

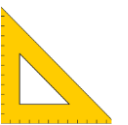
		FOM-FOM	FOM-QOplnf	QOplnf-QOplnf
Ω_1 rel errs	displacement	—	3.44e-4	5.73e-4
	velocity	—	1.72e-2	1.83e-2
	σ_{vm} stress	—	3.41e-4	8.53e-4
Ω_2 rel errs	displacement	—	2.50e-4	4.41e-4
	velocity	—	1.86e-2	1.96e-2
	σ_{vm} stress	—	2.40e-3	6.00e-3
CPU time	—	8h 19m 29.5s	1h 21m 25.9s	4m 42.1s
Mean/max # Schwarz iters	—	32.0/32	7.03/8	7.74/8



- Relative errors of $O(1e-4)$ - $O(1e-3)$ are achieved for the displacement and von Mises stress (σ_{vm})

Impressive $6.13\times$ and $106\times$ speedups are achieved via FOM-QOplnf and QOplnf-QOplnf couplings, respectively!

QOplnf = Quadratic Oplnf

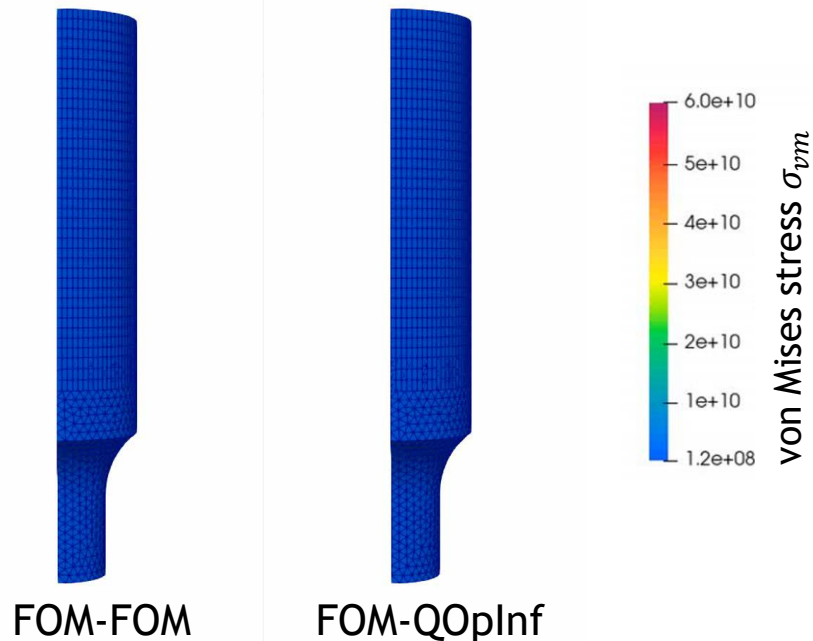


Tension Specimen (Overlapping SAM, Predictive)



- Hyperelastic (NeoHookean) tension specimen pulled from top
- TET10 - HEX8 overlapping coupling with implicit Newmark with same Δt
- Quadratic Oplnf (QOplnf) models with $M=2$ POD modes, capturing 99.9999% snapshot energy
- All results are predictive w.r.t. DBC applied at top of holder

		FOM-FOM	FOM-QOplnf	QOplnf-QOplnf
Ω_1 rel errs	displacement	—	3.44e-4	5.73e-4
	velocity	—	1.72e-2	1.83e-2
	σ_{vm} stress	—	3.41e-4	8.53e-4
Ω_2 rel errs	displacement	—	2.50e-4	4.41e-4
	velocity	—	1.86e-2	1.96e-2
	σ_{vm} stress	—	2.40e-3	6.00e-3
CPU time	—	8h 19m 29.5s	1h 21m 25.9s	4m 42.1s
Mean/max # Schwarz iters	—	32.0/32	7.03/8	7.74/8

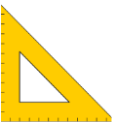


- Relative errors of $O(1e-4)$ - $O(1e-3)$ are achieved for the displacement and von Mises stress (σ_{vm})

Impressive $6.13\times$ and $106\times$ speedups are achieved via FOM-QOplnf and QOplnf-QOplnf couplings, respectively!

- Speedup largely due to huge reduction in # Schwarz iterations

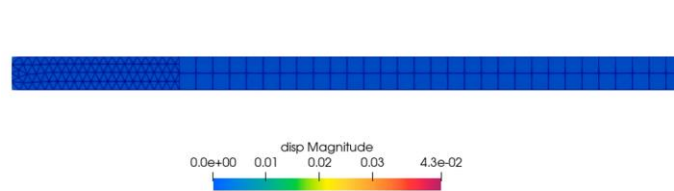
QOplnf = Quadratic Oplnf



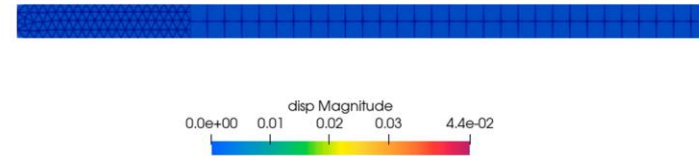
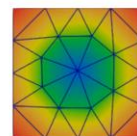
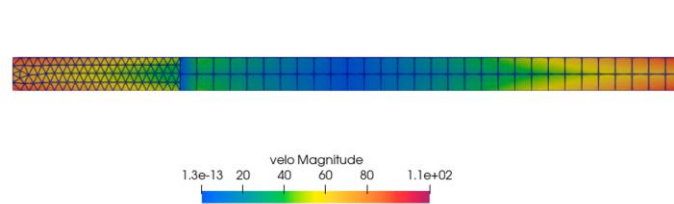
Torsion (Overlapping SAM, Reproductive & Predictive)

- **Neohookean material model**
- **TET4 - HEX8 overlapping coupling with implicit-explicit Newmark having different Δt**
- **QOpInf-FOM coupled models with $M=27$ and $M=30$ POD modes, capturing 99.9999% snapshot energy**
- **Prediction w.r.t. initial velocity (rotation speed/direction)**
- **(Linear) OpInf-FOM coupling insufficient**

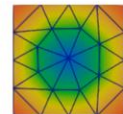
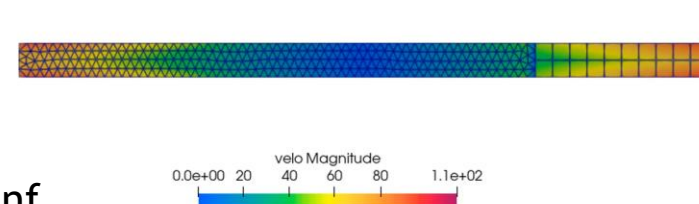
		FOM-FOM	QOpInf-FOM reproductive	QOpInf-FOM predictive
Ω_1 rel errs	displacement	—	2.67e-3	4.32e-2
	velocity	—	3.56e-2	1.49e-1
Ω_2 rel errs	displacement	—	1.13e-3	2.44e-2
	velocity	—	1.12e-2	9.52e-2
CPU time	—	39m 11.8s	1m 40.2s	1m 39.5s
Mean/max # Schwarz iters	—	3.0/3	2.0/2	2.0/2



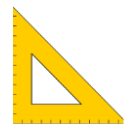
FOM-FOM



QOpInf-FOM



QOpInf = Quadratic OpInf

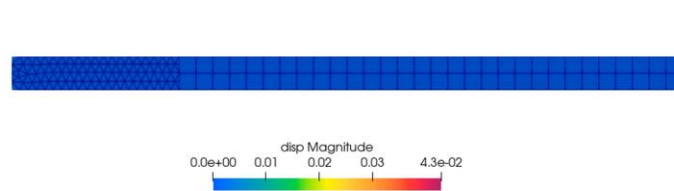


Torsion (Overlapping SAM, Reproductive & Predictive)

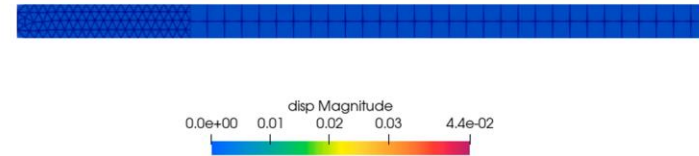
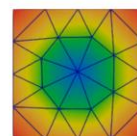
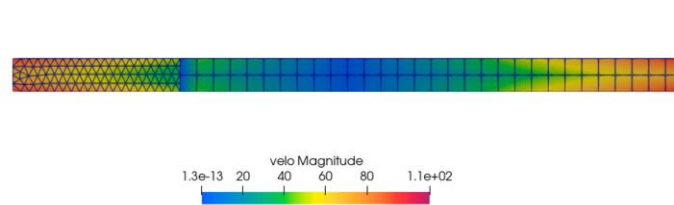
- **Neohookean material model**
- **TET4 - HEX8 overlapping coupling with implicit-explicit Newmark having different Δt**
- **QOpInf-FOM coupled models with $M=27$ and $M=30$ POD modes, capturing 99.9999% snapshot energy**
- **Prediction w.r.t. initial velocity (rotation speed/direction)**
- **(Linear) OpInf-FOM coupling insufficient**

		FOM-FOM	QOpInf-FOM reproductive	QOpInf-FOM predictive
Ω_1 rel errs	displacement	—	2.67e-3	4.32e-2
	velocity	—	3.56e-2	1.49e-1
Ω_2 rel errs	displacement	—	1.13e-3	2.44e-2
	velocity	—	1.12e-2	9.52e-2
CPU time	—	39m 11.8s	1m 40.2s	1m 39.5s
Mean/max # Schwarz iters	—	3.0/3	2.0/2	2.0/2

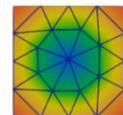
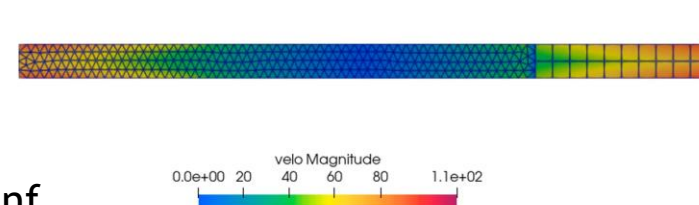
Relative errors are of $O(1e-3)$ - $O(1e-2)$ for displacement and velocity!



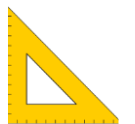
FOM-FOM



QOpInf-FOM

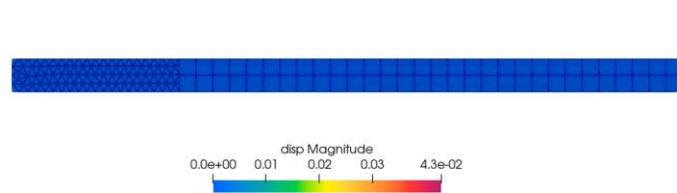


QOpInf = Quadratic OpInf

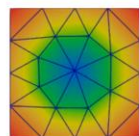
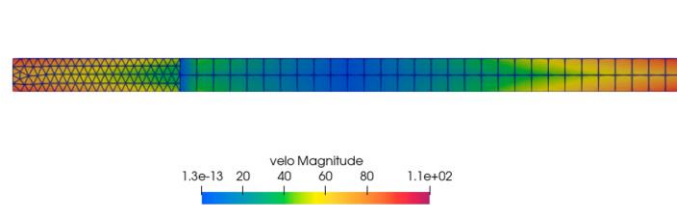


Torsion (Overlapping SAM, Reproductive & Predictive)

- Neohookean material model
- TET4 - HEX8 overlapping coupling with implicit-explicit Newmark having different Δt
- QOpInf-FOM coupled models with $M=27$ and $M=30$ POD modes, capturing 99.9999% snapshot energy
- Prediction w.r.t. initial velocity (rotation speed/direction)
- (Linear) OpInf-FOM coupling insufficient



FOM-FOM

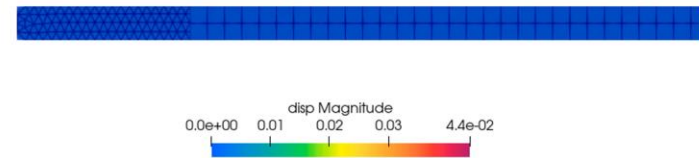


QOpInf = Quadratic OpInf

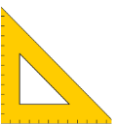
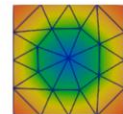
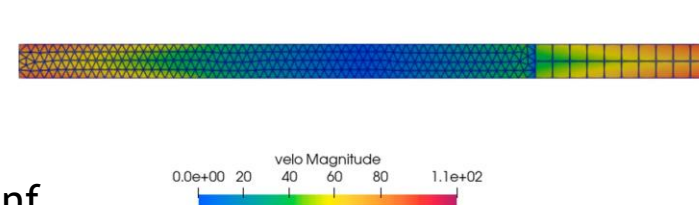
		FOM-FOM	QOpInf-FOM reproductive	QOpInf-FOM predictive
Ω_1 rel errs	displacement	—	2.67e-3	4.32e-2
	velocity	—	3.56e-2	1.49e-1
Ω_2 rel errs	displacement	—	1.13e-3	2.44e-2
	velocity	—	1.12e-2	9.52e-2
CPU time	—	39m 11.8s	1m 40.2s	1m 39.5s
Mean/max # Schwarz iters	—	3.0/3	2.0/2	2.0/2

Relative errors are of $O(1e-3)$ - $O(1e-2)$ for displacement and velocity!

~23.5× speedups are achieved via QOpInf-FOM couplings



QOpInf-FOM



Bolted Joint (Overlapping SAM, Reproductive)



- Hyper-elastic (Saint-Venant Kirchhoff) problem with TET10 - HEX8 meshes
- Loading is applied to top part of bolted joint
- Cubic OpInf (COpInf) coupled models
- Hybrid couplings require fewer Schwarz iterations to converge
- Convergence w.r.t. basis size is observed for reproductive FOM-QOpInf couplings (right)

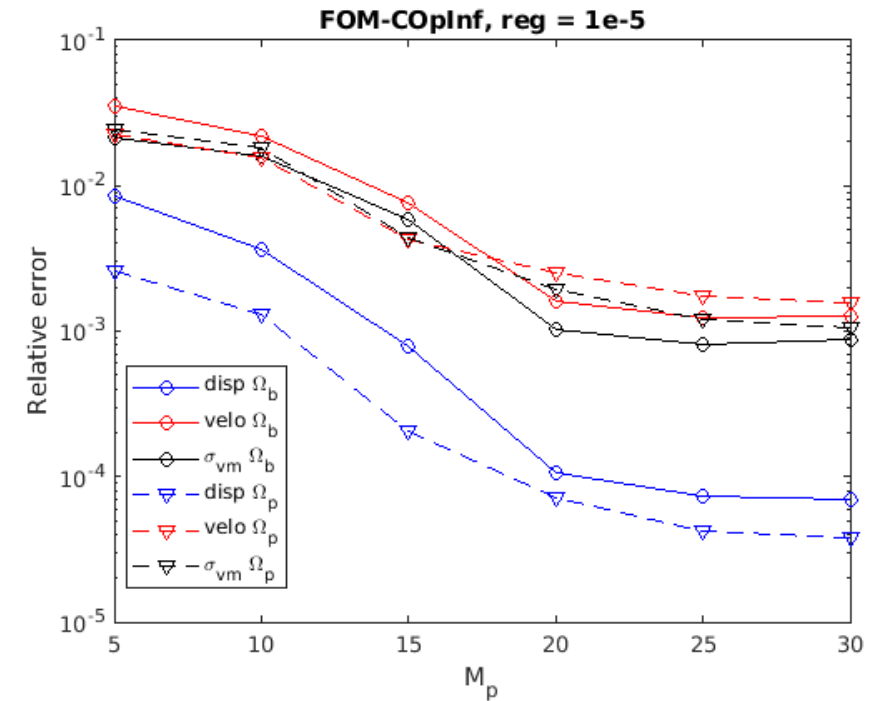
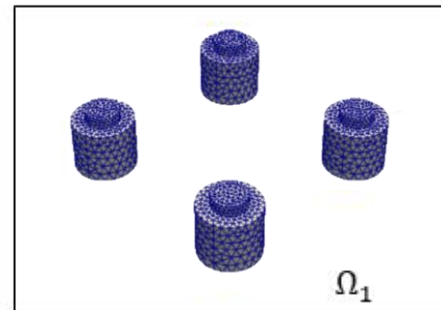
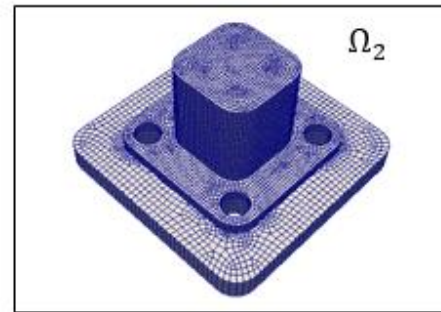
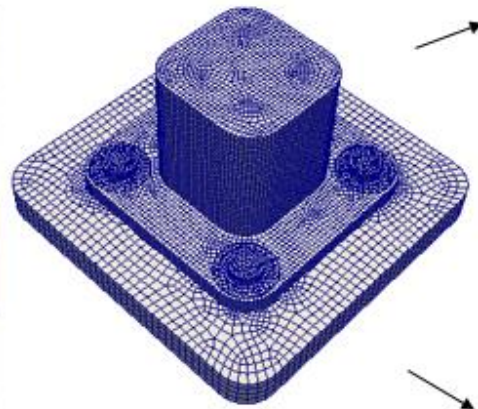
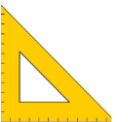


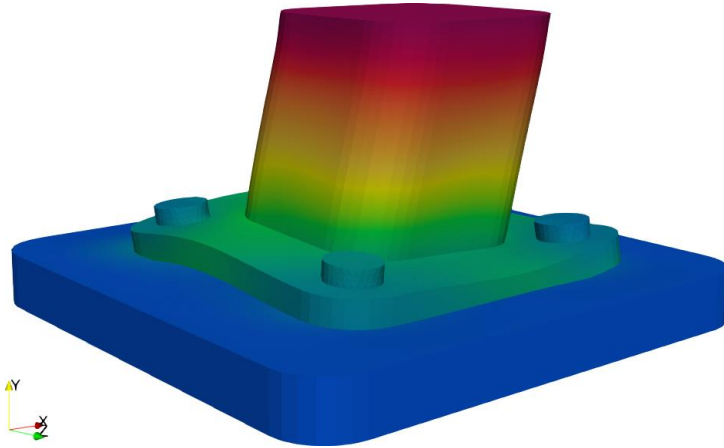
Figure above: convergence w.r.t. basis size for reproductive FOM-COpInf coupling



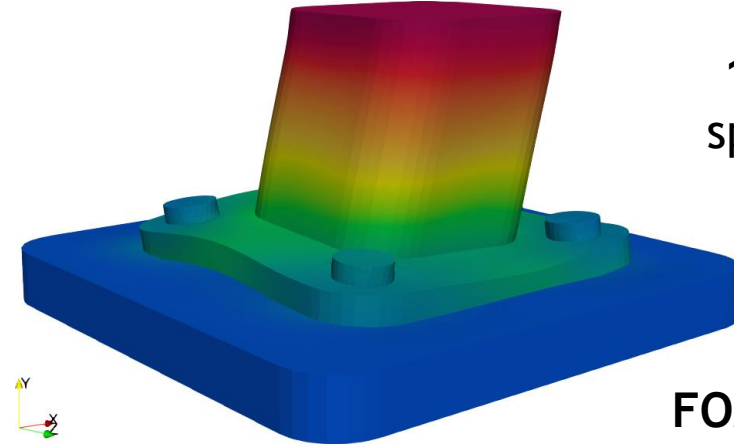
Bolted Joint (Overlapping SAM, Predictive): Displacements



COplnf = Cubic Oplnf



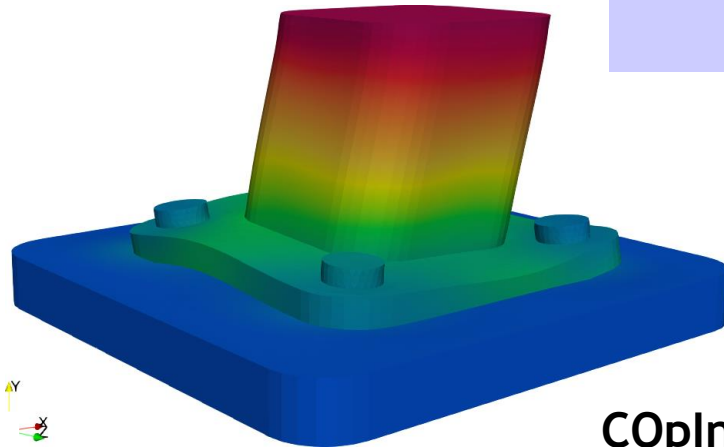
FOM-FOM



1.65×
speedup

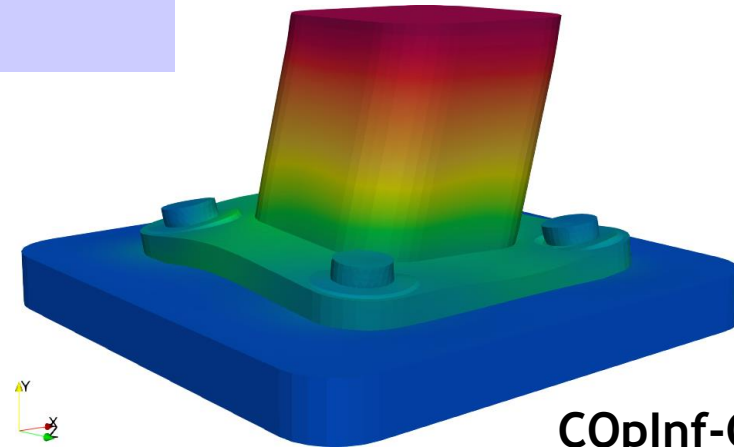
FOM-COplnf
0.69% rel err (parts)
3.51% rel err (bolts)

Models generally achieve
relative errors of $O(1\%)$ in
displacement.



6.12×
speedup

COplnf-COplnf (best)
0.98% rel err (parts)
4.41% rel err (bolts)

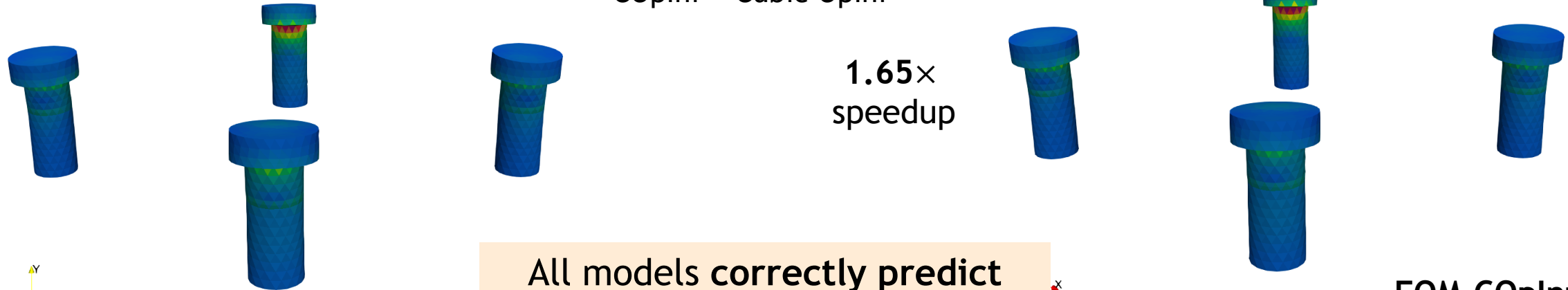


COplnf-COplnf (worst)
12.9% rel err (parts)
12.5% rel err (bolts)

Bolted Joint (Overlapping SAM, Predictive): von Mises Stresses



COplnf = Cubic Oplnf



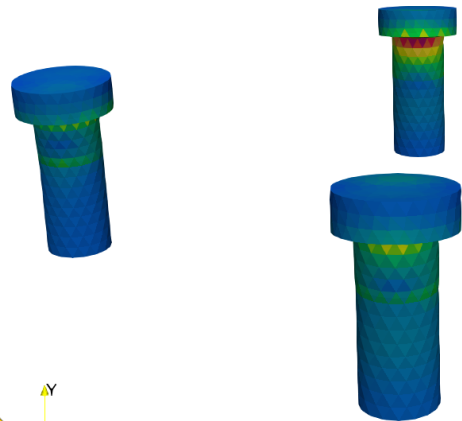
1.65×
speedup



FOM-FOM

All models correctly predict
locations of maximum von
Mises stress (failure).

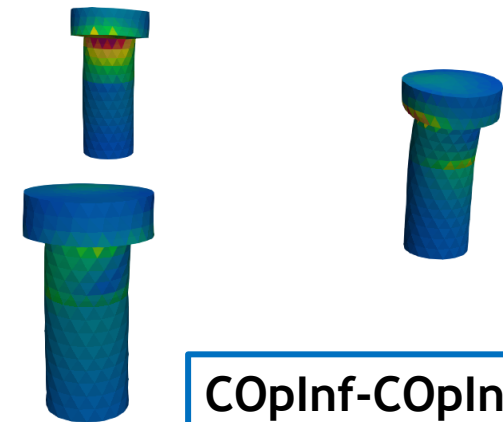
FOM-COplnf
7.74% rel err



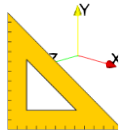
6.12×
speedup

COplnf-COplnf (best)
12.4% rel error

*High errors do not necessarily
mean result cannot be
informative.*

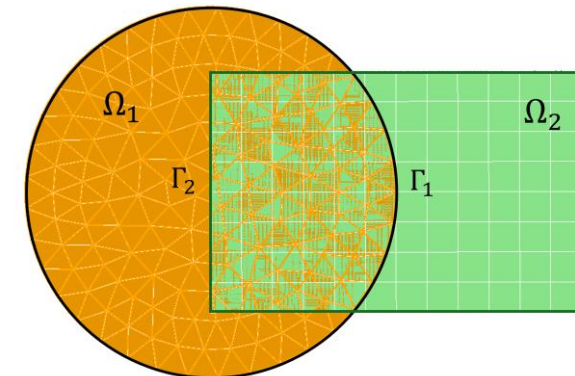
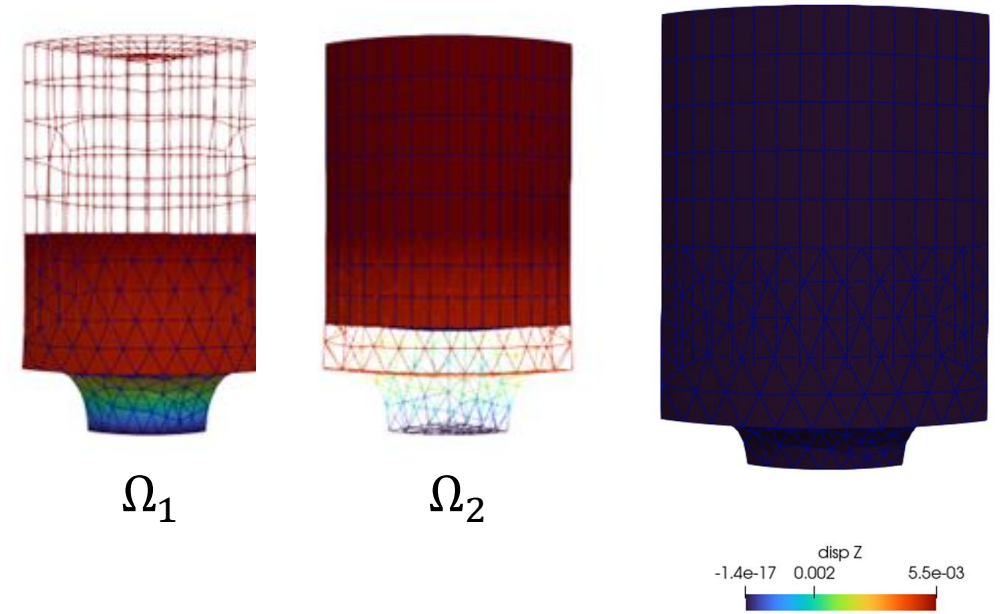


COplnf-COplnf (worst)
30.9% rel error



Outline

1. Preliminaries
 - Motivation
 - The Schwarz Alternating Method (SAM) for Multi-Scale Coupling
 - Non-Intrusive Operator Inference (OpInf)
2. Overlapping SAM for OpInf Reduced Order Model (ROM) Coupling
 - Methodology
 - Numerical Examples
3. Non-overlapping SAM for OpInf ROM Coupling
 - Methodology
 - Numerical Example
4. Summary
5. Ongoing & Future Work



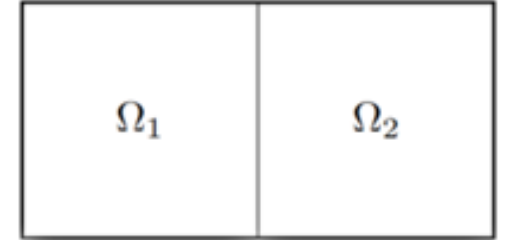
Non-overlapping SAM-based Coupling for Non-Intrusive OpInf ROMs



Alternating Dirichlet-Neumann non-overlapping SAM (dynamic linear elastic problem)

$$\begin{cases} \text{Div } \mathbf{P}_1^{(n+1)} = \rho \dot{\boldsymbol{\varphi}}_1^{(n+1)}, & \text{in } \Omega_1 \\ \boldsymbol{\varphi}_1^{(n+1)} = \boldsymbol{\chi}, & \text{on } \partial\Omega_1 \setminus \Gamma \\ \boldsymbol{\varphi}_1^{(n+1)} = \boldsymbol{\varphi}_2^{(n)}, & \text{on } \Gamma \end{cases}$$

$$\begin{cases} \text{Div } \mathbf{P}_2^{(n+1)} = \rho \dot{\boldsymbol{\varphi}}_2^{(n+1)}, & \text{in } \Omega_2 \\ \boldsymbol{\varphi}_2^{(n+1)} = \boldsymbol{\chi}, & \text{on } \partial\Omega_2 \setminus \Gamma \\ \mathbf{P}_2^{(n+1)} \mathbf{n} = \mathbf{P}_1^{(n+1)} \mathbf{n}, & \text{on } \Gamma \end{cases}$$

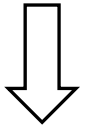


Non-overlapping SAM-based Coupling for Non-Intrusive OpInf ROMs



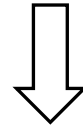
Alternating Dirichlet-Neumann non-overlapping SAM (dynamic linear elastic problem)

$$\begin{cases} \text{Div } \mathbf{P}_1^{(n+1)} = \rho \ddot{\boldsymbol{\varphi}}_1^{(n+1)}, & \text{in } \Omega_1 \\ \boldsymbol{\varphi}_1^{(n+1)} = \boldsymbol{\chi}, & \text{on } \partial\Omega_1 \setminus \Gamma \\ \boldsymbol{\varphi}_1^{(n+1)} = \boldsymbol{\varphi}_2^{(n)}, & \text{on } \Gamma \end{cases}$$

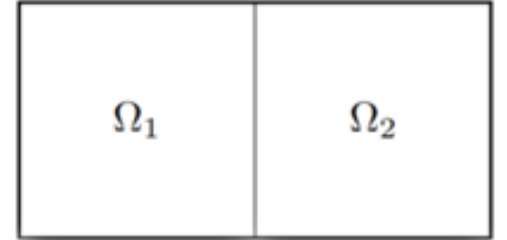


$$\int_I \left[\int_{\Omega_1} (\rho \ddot{\boldsymbol{\varphi}}_1^{(n+1)} \cdot \boldsymbol{\xi} + \mathbf{P}_1^{(n+1)} : \nabla \boldsymbol{\xi}) d\Omega \right] dt = 0$$

$$\begin{cases} \text{Div } \mathbf{P}_2^{(n+1)} = \rho \ddot{\boldsymbol{\varphi}}_2^{(n+1)}, & \text{in } \Omega_2 \\ \boldsymbol{\varphi}_2^{(n+1)} = \boldsymbol{\chi}, & \text{on } \partial\Omega_2 \setminus \Gamma \\ \mathbf{P}_2^{(n+1)} \mathbf{n} = \mathbf{P}_1^{(n+1)} \mathbf{n}, & \text{on } \Gamma \end{cases}$$



$$\int_I \left[\int_{\Omega_2} (\rho \ddot{\boldsymbol{\varphi}}_2^{(n+1)} \cdot \boldsymbol{\xi} + \mathbf{P}_2^{(n+1)} : \nabla \boldsymbol{\xi}) d\Omega - \int_{\Gamma} (\mathbf{P}_1^{(n+1)} \mathbf{n}) \cdot \boldsymbol{\xi} dS \right] dt = 0$$



Non-overlapping SAM-based Coupling for Non-Intrusive OpInf ROMs



Alternating Dirichlet-Neumann non-overlapping SAM (dynamic linear elastic problem)

$$\begin{cases} \text{Div } \mathbf{P}_1^{(n+1)} = \rho \ddot{\boldsymbol{\varphi}}_1^{(n+1)}, & \text{in } \Omega_1 \\ \boldsymbol{\varphi}_1^{(n+1)} = \boldsymbol{\chi}, & \text{on } \partial\Omega_1 \setminus \Gamma \\ \boldsymbol{\varphi}_1^{(n+1)} = \boldsymbol{\varphi}_2^{(n)}, & \text{on } \Gamma \end{cases}$$

↓

$$\int_I \left[\int_{\Omega_1} (\rho \ddot{\boldsymbol{\varphi}}_1^{(n+1)} \cdot \boldsymbol{\xi} + \mathbf{P}_1^{(n+1)} : \nabla \boldsymbol{\xi}) d\Omega \right] dt = 0$$

↓

$$\hat{\mathbf{M}}_1 \ddot{\hat{\mathbf{q}}}_1 + \hat{\mathbf{K}}_1 \hat{\mathbf{q}}_1 + \hat{\mathbf{B}}_1 \mathbf{g}_1 = 0$$

Dirichlet problem: learn $\hat{\mathbf{M}}_1, \hat{\mathbf{K}}_1, \hat{\mathbf{B}}_1$

- Use snapshots of displacement, acceleration and Dirichlet data to train ROM

$$\begin{cases} \text{Div } \mathbf{P}_2^{(n+1)} = \rho \ddot{\boldsymbol{\varphi}}_2^{(n+1)}, & \text{in } \Omega_2 \\ \boldsymbol{\varphi}_2^{(n+1)} = \boldsymbol{\chi}, & \text{on } \partial\Omega_2 \setminus \Gamma \\ \mathbf{P}_2^{(n+1)} \mathbf{n} = \mathbf{P}_1^{(n+1)} \mathbf{n}, & \text{on } \Gamma \end{cases}$$

↓

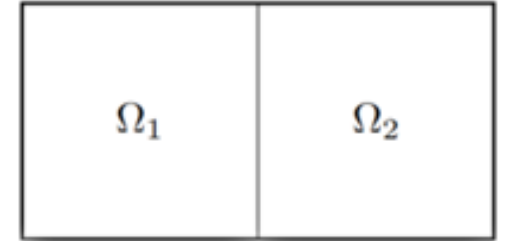
$$\int_I \left[\int_{\Omega_2} (\rho \ddot{\boldsymbol{\varphi}}_2^{(n+1)} \cdot \boldsymbol{\xi} + \mathbf{P}_2^{(n+1)} : \nabla \boldsymbol{\xi}) d\Omega - \int_{\Gamma} (\mathbf{P}_1^{(n+1)} \mathbf{n}) \cdot \boldsymbol{\xi} dS \right] dt = 0$$

↓

$$\hat{\mathbf{M}}_2 \ddot{\hat{\mathbf{q}}}_2 + \hat{\mathbf{K}}_2 \hat{\mathbf{q}}_2 + \hat{\mathbf{B}}_2 \mathbf{g}_2 + \hat{\mathbf{H}}_2 \mathbf{t}_2 = 0$$

Neumann problem: learn $\hat{\mathbf{M}}_2, \hat{\mathbf{K}}_2, \hat{\mathbf{B}}_2, \hat{\mathbf{H}}_2$

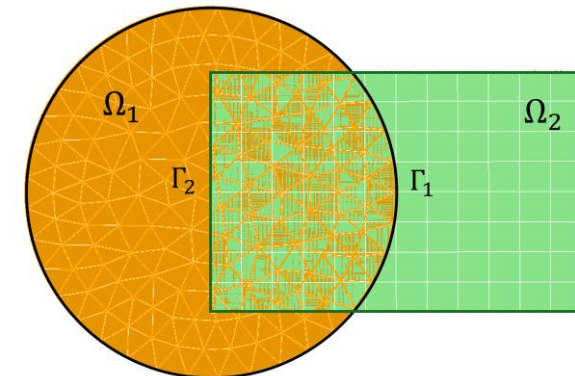
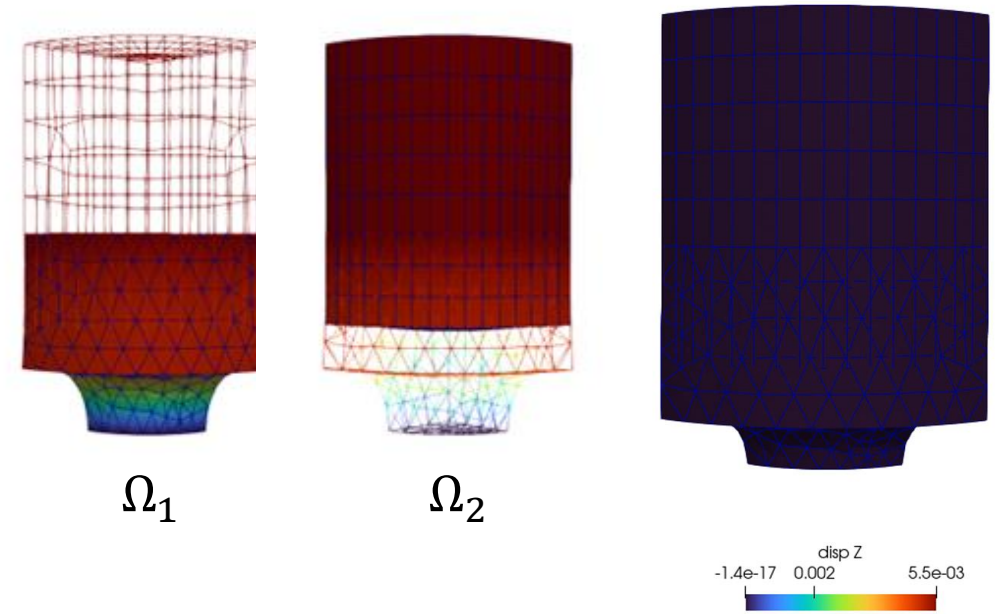
- Use snapshots of displacement, acceleration, Dirichlet data and tractions to train ROM



OpInf ROMs

Outline

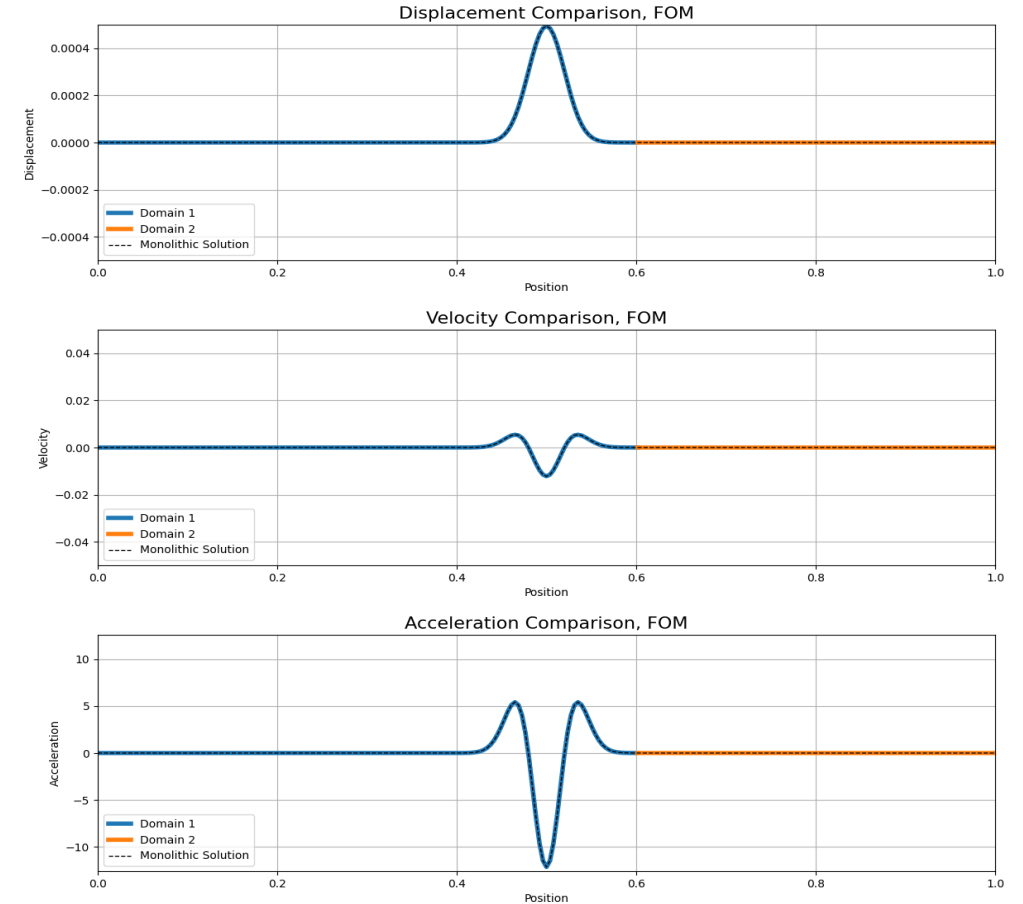
1. Preliminaries
 - Motivation
 - The Schwarz Alternating Method (SAM) for Multi-Scale Coupling
 - Non-Intrusive Operator Inference (OpInf)
2. Overlapping SAM for OpInf Reduced Order Model (ROM) Coupling
 - Methodology
 - Numerical Examples
3. Non-overlapping SAM for OpInf ROM Coupling
 - Methodology
 - **Numerical Example**
4. Summary
5. Ongoing & Future Work



Linear Elastic Wave Propagation (Non-Overlapping SAM, Reproductive)

- 1D linear elastic *clamped beam* with Gaussian initial condition for the displacement.
- Simple problem with analytical exact solution but very *stringent test* for discretization methods.
- Test non-overlapping SAM w/ **2 subdomains**:
 $\Omega_1 = (0,0.6), \Omega_2 = (0.6,1)$.

Transmission Type	Model	M_1 / M_2	Error	Iterations	CPU time (s)
Dirichlet-Neumann	FOM-FOM	- / -	3.43×10^{-4}	3.73	52
Dirichlet-Neumann	OpInf-FOM	20 / -	7.37×10^{-4}	6.08	64
Dirichlet-Neumann	FOM-OpInf	- / 17	7.31×10^{-4}	4.10	47
Dirichlet-Neumann	OpInf-OpInf	20 / 17	9.63×10^{-4}	4.12	37
Dirichlet-Neumann	OpInf-FOM	34 / -	1.29×10^{-4}	5.45	60
Dirichlet-Neumann	FOM-OpInf	- / 29	1.53×10^{-4}	4.19	51
Dirichlet-Neumann	OpInf-OpInf	34 / 29	2.03×10^{-4}	4.10	39



Above: representative OpInf-FOM coupling result

Good accuracy and moderate speedups over FOM-FOM coupling are possible. Larger speedups expected in *multi-D*.

Work in Progress: Accelerating Non-Overlapping SAM via Transmission Condition Design



C. Rodriguez
(Columbia U)

- Risk:** non-overlapping Schwarz can be slow to converge w/ Dirichlet-Neumann TCs.
- Mitigation:** explore optimized Robin-Robin transmission conditions (TCs).

$$\begin{cases} M_1 \ddot{u}_1^{(s+1)} + K_1 u_1^{(s+1)} = F_1^{(s+1)} & \text{in } \Omega_1 \\ u_1^{(s+1)} = u_D & \text{on } \partial_\Psi \Omega_1 \setminus \Gamma \\ \alpha_{12} T_1^{(s+1)} + \beta_{12} u_1^{(s+1)} = \lambda_1^{(s+1)} & \text{on } \Gamma \end{cases}$$

$$\begin{cases} M_2 \ddot{u}_2^{(s+1)} + K_2 u_2^{(s+1)} = F_2^{(s+1)} & \text{in } \Omega_2 \\ u_2^{(s+1)} = u_D & \text{on } \partial_\Psi \Omega_2 \setminus \Gamma \\ \alpha_{21} T_2^{(s+1)} + \beta_{21} u_2^{(s+1)} = \lambda_2^{(s+1)} & \text{on } \Gamma \end{cases}$$

$$\lambda_1^{(s+1)} = \alpha_{12} T_2^{(s)} + \beta_{12} u_2^{(s)}$$

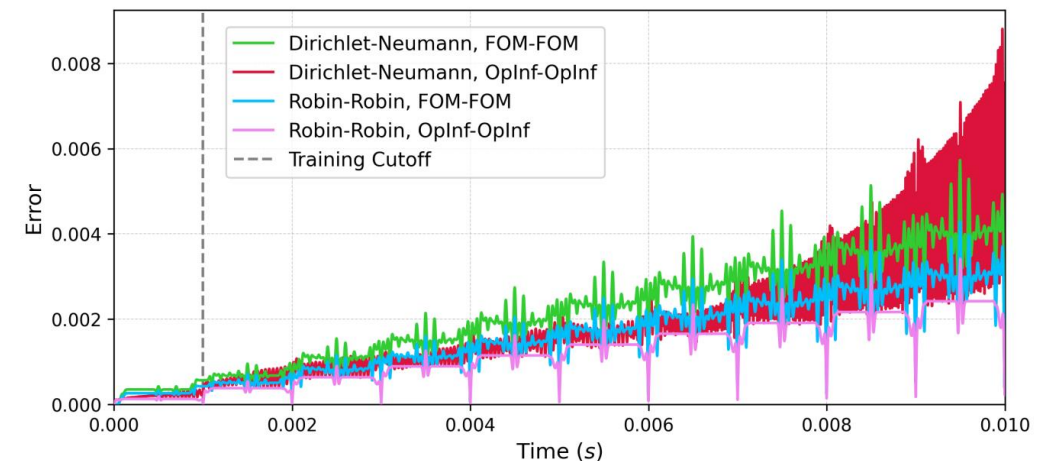
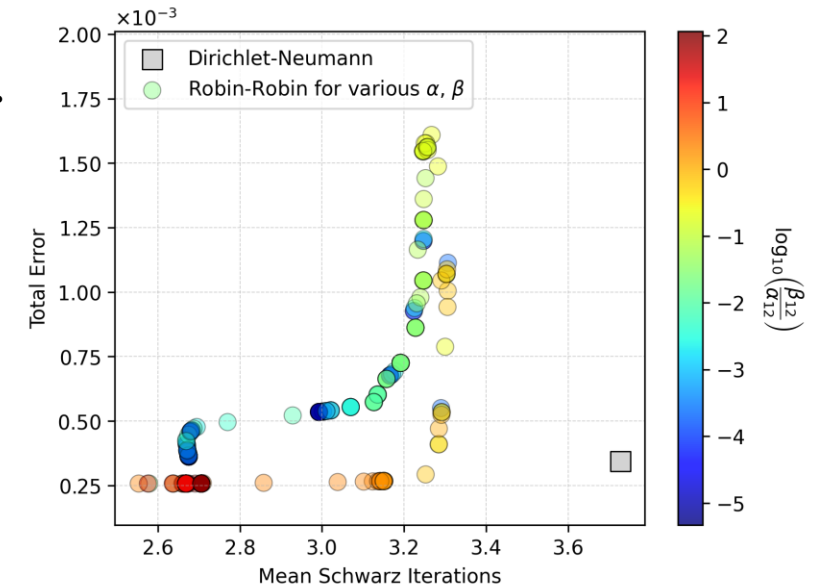
$$\lambda_2^{(s+1)} = \alpha_{21} T_1^{(s+1)} + \beta_{21} u_1^{(s+1)}$$

α_{ij}, β_{ij} : tuning parameters

Automatic tuning of α_{ij}, β_{ij} possible using *Bayesian optimization* via *GPTune*.

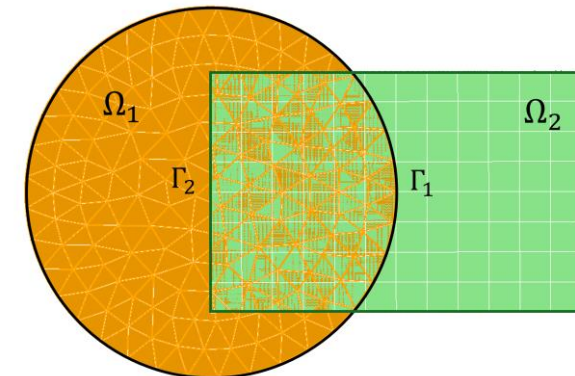
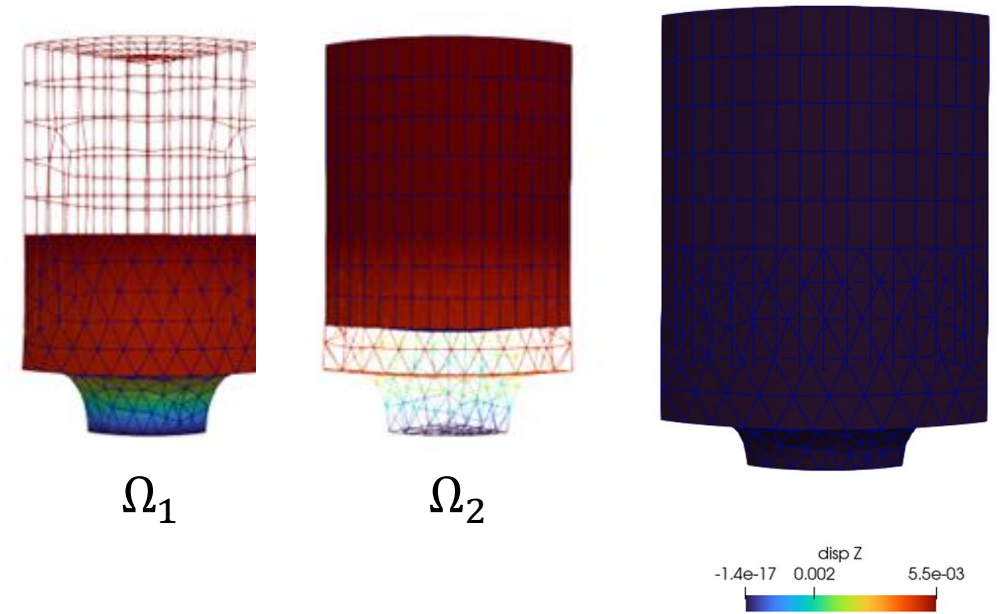
Non-overlapping SAM with optimized Robin-Robin TCs can give to faster convergence (29% less Schwarz iterations), lower errors (by up to 25%), and more stable/accurate time-predictive ROMs than non-overlapping SAM with Dirichlet-Neumann TCs.

Total Error vs. Mean Schwarz Iterations



Outline

1. Preliminaries
 - Motivation
 - The Schwarz Alternating Method (SAM) for Multi-Scale Coupling
 - Non-Intrusive Operator Inference (OpInf)
2. Overlapping SAM for OpInf Reduced Order Model (ROM) Coupling
 - Methodology
 - Numerical Examples
3. Non-overlapping SAM for OpInf ROM Coupling
 - Methodology
 - Numerical Example
4. Summary
5. Ongoing & Future Work



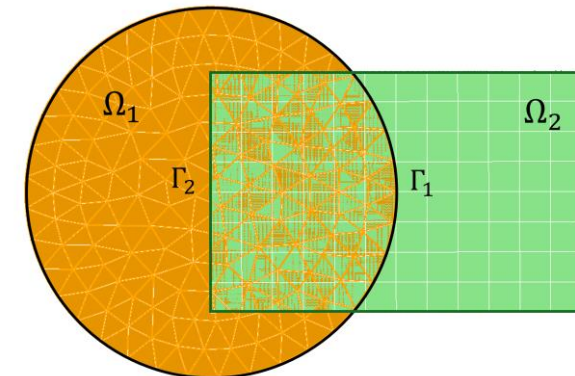
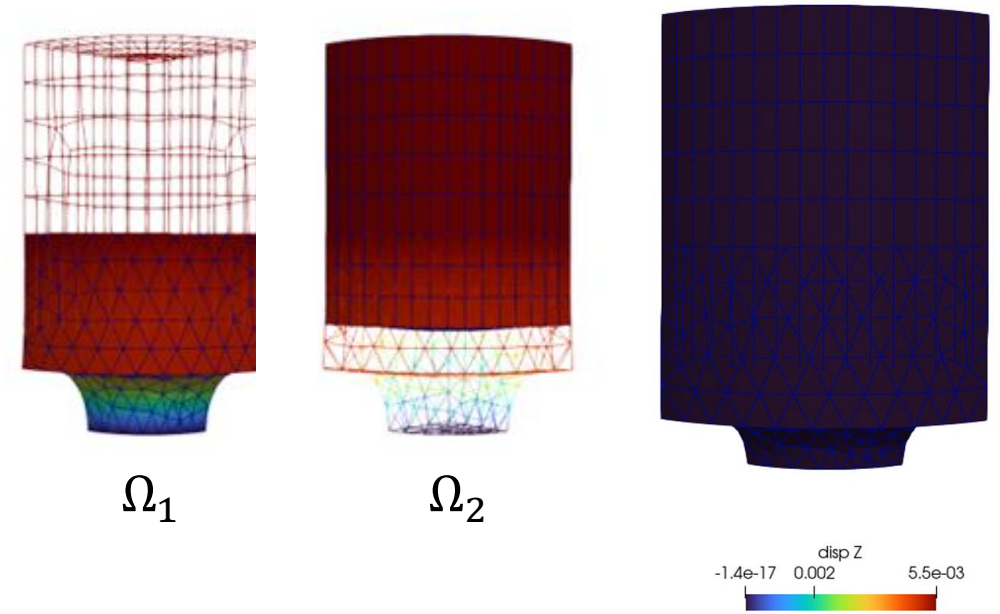


The **Schwarz alternating method** has been developed for concurrent multiscale coupling of **conventional** and **data-driven models**.

- ☺ Coupling is *concurrent* (two-way).
- ☺ *Ease of implementation* into existing massively-parallel HPC codes.
- ☺ “*Plug-and-play*” *framework*: simplifies task of meshing complex geometries!
 - ☺ Ability to couple regions with *different non-conformal meshes*, *different element types* and *different levels of refinement*.
 - ☺ Ability to use *different solvers (including ROM/FOM)* and *time-integrators* in different regions.
- ☺ *Scalable, fast, robust* on *real* engineering problems
- ☺ Coupling does not introduce *nonphysical artifacts*.
- ☺ *Theoretical* convergence properties/guarantees.

Outline

1. Preliminaries
 - Motivation
 - The Schwarz Alternating Method (SAM) for Multi-Scale Coupling
 - Non-Intrusive Operator Inference (OpInf)
2. Overlapping SAM for OpInf Reduced Order Model (ROM) Coupling
 - Methodology
 - Numerical Examples
3. Non-overlapping SAM for OpInf ROM Coupling
 - Methodology
 - Numerical Example
4. Summary
5. Ongoing & Future Work



Ongoing & Future Work

Performance Improvements

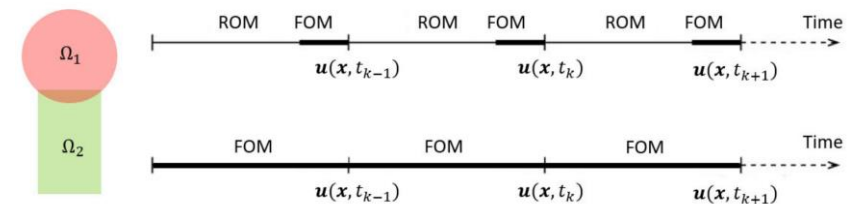
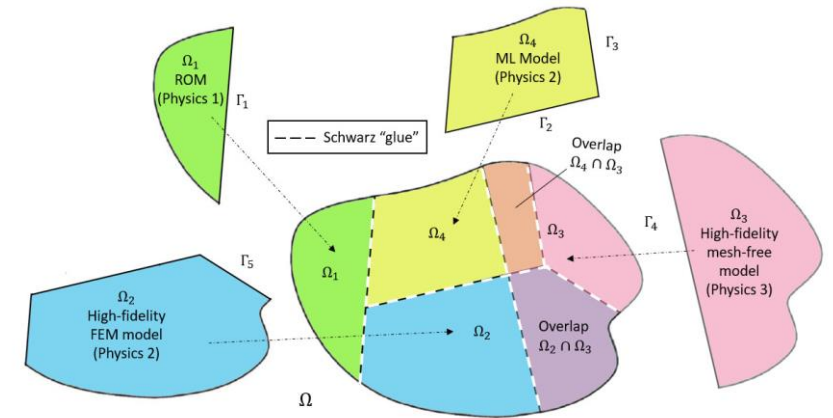
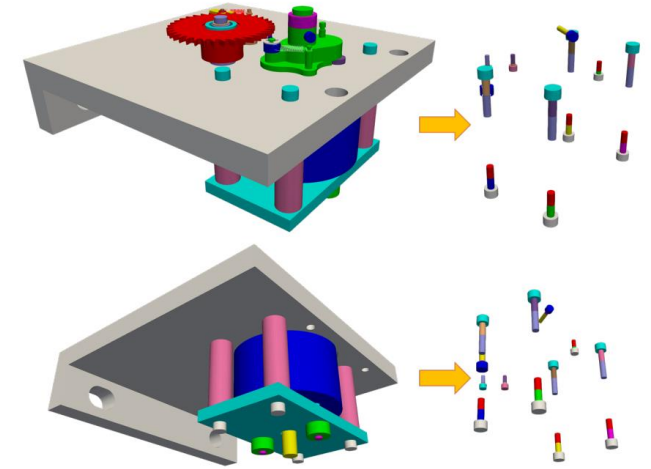
- Acceleration of Schwarz via optimized Robin-Robin TCs
- Acceleration of Schwarz via Aitken and Anderson Acceleration
- Asynchronous additive Schwarz on GPUs

Automated & Adaptive Schwarz

- Automated optimization of meshes/DD with multiple constraints
- Automated criteria to determine appropriate use of less refined or reduced-order models w/o sacrificing accuracy

Schwarz for ROM/Data-Driven Model Coupling

- Non-overlapping Schwarz + OpInf
- Schwarz + Deep NN-OpInf ROMs
- Schwarz + kernel-based ROMs (w/ Ionut Farcas, Virginia Tech)
- Fully non-intrusive adaptive ROM-FOM coupling (w/ K. Willcox & N. Aretz, UT Austin)
- On-the-fly switching between ROMs and FOMs
- Implementation in Sandia's production code, SIERRA/SM
- Schwarz + multiphysics coupling



Thank you! Questions?



Schwarz Couplings Involving Non-Intrusive Oplnf ROMs:

- I. Tezaur, E. Parish, A. Gruber, I. Moore, C. Wentland, A. Mota. “Hybrid coupling with operator inference and the overlapping Schwarz alternating method”. ArXiv pre-print, 2025. <https://arxiv.org/abs/2511.20687>
 - **Implementation:** Norma.jl Julia code (<https://github.com/sandiaabs/Norma.jl>)
- C. Rodriguez, I. Tezaur, A. Mota, A. Gruber, E. Parish, C. Wentland. “Transmission Conditions for the Non-Overlapping Schwarz Coupling of Full Order and Operator Inference Models”, CSRI Summer Proceedings 2025, Sandia National Laboratories. <https://arxiv.org/abs/2509.12228>
 - **First application of non-overlapping Schwarz to Oplnf-FOM and Oplnf-Oplnf coupling that we are aware of**



NORMA.JL

Contact: Irina Tezaur (ikalash@sandia.gov)



I. Tezaur

J. Barnett

I. Moore

E. Parish

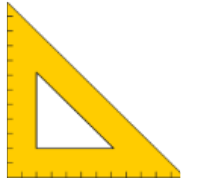
C. Wentland

A. Gruber

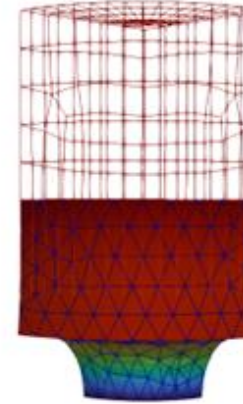
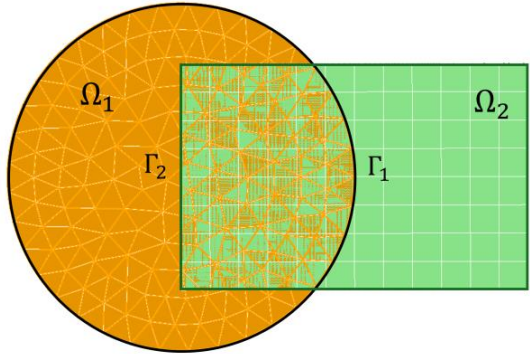
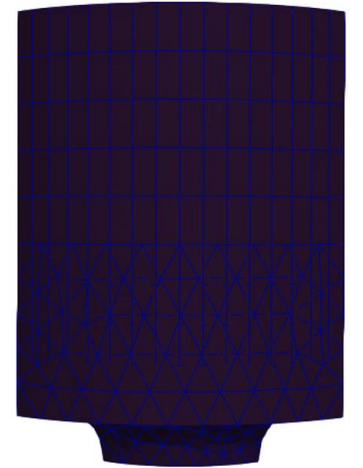
C. Rodriguez

W. Snyder

G. Sambataro



NORMA.JL

 Ω_1  Ω_2 

ikalash@sandia.gov
www.sandia.gov/~ikalash

Schwarz Couplings Involving Intrusive Projection-Based ROMs:

- J. Barnett, I. Tezaur, A. Mota. “The Schwarz alternating method for the seamless coupling of nonlinear reduced order models and full order models”, CSRI Summer Proceedings 2023, Sandia National Laboratories. <https://arxiv.org/abs/2210.12551>
- C. Wentland, F. Rizzi, J. Barnett, I. Tezaur. “The role of interface boundary conditions and sampling strategies for Schwarz-based coupling of projection-based reduced order models”, *J. Comput. Appl. Math.*, 465 116584, 2025

Schwarz Couplings Involving Physics-Informed Neural Networks (PINNs):

- W. Snyder, I. Tezaur, C. Wentland. “Domain decomposition-based coupling of PINNs via the Schwarz alternating method”, CSRI Summer Proceedings 2023, Sandia National Laboratories. <https://arxiv.org/abs/2311.00224>



I. Tezaur

J. Barnett

I. Moore

E. Parish

C. Wentland

A. Gruber

C. Rodriguez

W. Snyder

G. Sambataro

Start of Backup Slides

Requirements for Multiscale Coupling Method



- Coupling is *concurrent* (two-way)
- “*Plug-and-play*” *framework*: simplifies task of meshing complex geometries
 - Ability to couple regions with *different non-conformal meshes*, *different element types* and *different levels of refinement*
 - Ability to use *different solvers/time-integrators* in different regions
 - Ability to mix-and-match *conventional* and *data-driven models* in different regions
- **Ease of implementation** into existing massively-parallel HPC codes
- *Scalable, fast, robust* (we target *real* engineering problems, e.g., analyses involving failure of bolted components!)
- Coupling does not introduce *nonphysical artifacts*
- *Theoretical* convergence properties/ guarantees

A great method theoretically may not make it if it is too difficult to implement in production codes.

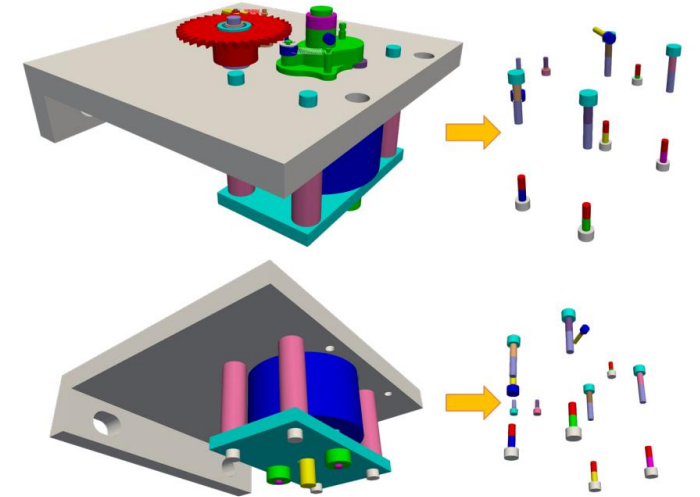


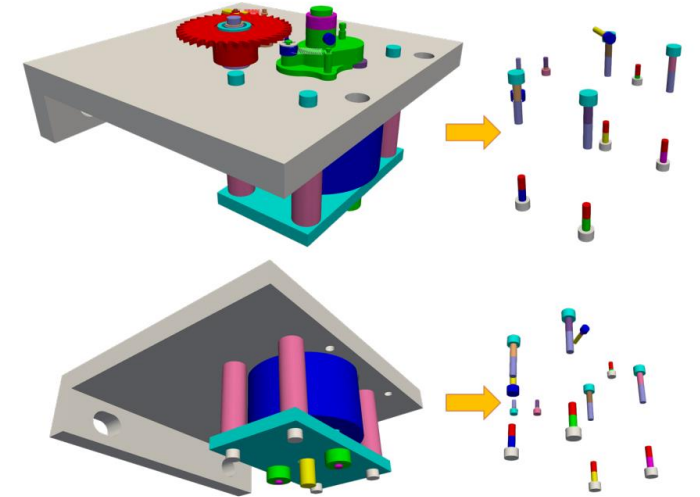
Figure above: schematic of difficult-to-mesh ratcheting mechanism with multiple threaded fasteners. From Parish *et al.*, 2024.

Requirements for Multiscale Coupling Method



- Coupling is *concurrent* (two-way)
- **“Plug-and-play” framework**: simplifies task of meshing complex geometries
 - Ability to couple regions with *different non-conformal meshes*, *different element types* and *different levels of refinement*
 - Ability to use *different solvers/time-integrators* in different regions
 - Ability to mix-and-match *conventional* and *data-driven models* in different regions
- *Ease of implementation* into existing massively-parallel HPC codes
- *Scalable, fast, robust* (we target *real* engineering problems, e.g., analyses involving failure of bolted components!)
- Coupling does not introduce *nonphysical artifacts*
- *Theoretical* convergence properties/ guarantees

Creating a high-quality mesh can take weeks or longer, making it “the single biggest bottleneck in [mod/sim] analyses” [Sandia Lab News, 2020]



Above: schematic of difficult-to-mesh ratcheting mechanism with multiple threaded fasteners.
From Parish *et al.*, 2024.

Projects on Coupling for Predictive Hybrid Models



$$\int \mathcal{M}^2 dt$$

Three projects:

- **FHNM:** Flexible Heterogeneous Numerical Methods [LDRD, FY22-FY24]
- **M2dt:** Multi-faceted Mathematics for Predictive Digital Twins [ASCR, FY23-FY27]
- **AHEAD:** Adaptive Hybrid modELs via domAin Decomposition [LDRD, FY25-FY27]



Principal research objective:

- Develop rigorous methods to enable the “**plug-and-play**” coupling of **standard and data-driven models** from the following classes
 - *Class A:* intrusive projection-based ROMs
 - *Class B:* machine-learned models
 - *Class C:* flow map approximation models, i.e., dynamic model decomposition (DMD)
 - *Class D:* non-intrusive operator inference (OpInf) ROMs



Three classes of coupling methods:

- Alternating Schwarz-based coupling [FHNM, M2dt, AHEAD]
- Optimization-based coupling [FHNM, M2dt]
- Coupling via **generalized mortar methods** [FHNM, M2dt]

Projects on Coupling for Predictive Hybrid Models



$$\int \mathcal{M}^2 dt$$

Three projects:

- **FHNM**: Flexible Heterogeneous Numerical Methods [LDRD, FY22-FY24]
- **M2dt**: Multi-faceted Mathematics for Predictive Digital Twins [ASCR, FY23-FY27]
- **AHEAD**: Adaptive Hybrid modELs via domAin Decomposition [LDRD, FY25-FY27]



Principal research objective:

- Develop rigorous methods to enable the “**plug-and-play**” coupling of standard and data-driven models from the following classes
 - *Class A*: intrusive projection-based ROMs
 - *Class B*: machine-learned models
 - *Class C*: flow map approximation models, i.e., dynamic model decomposition (DMD)
 - *Class D*: non-intrusive operator inference (OpInf) ROMs → this talk

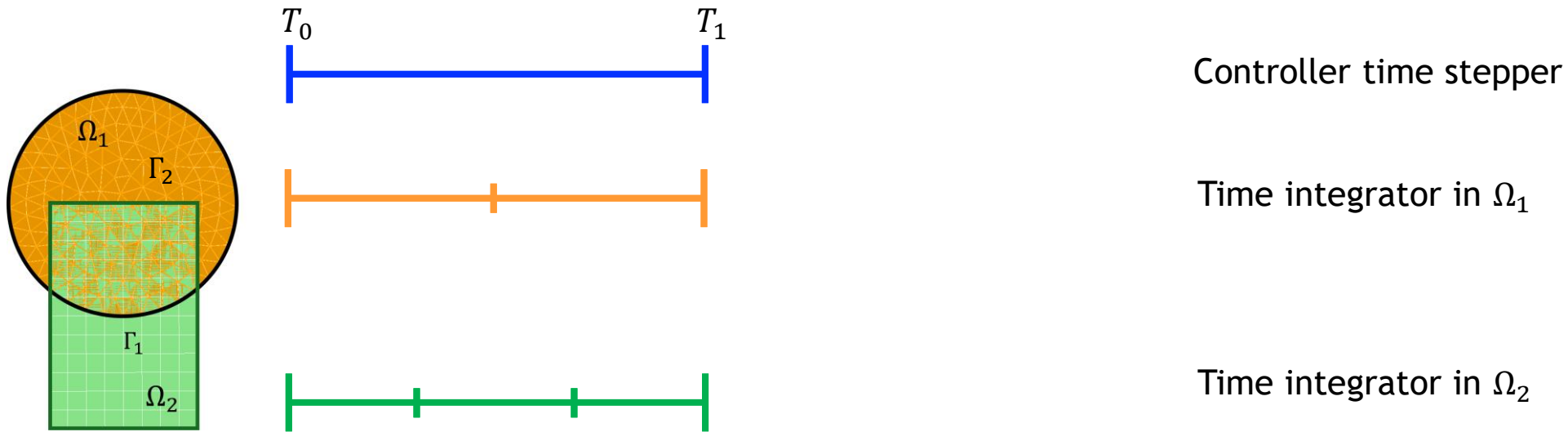


Three classes of coupling methods:

- Alternating Schwarz-based coupling [FHNM, M2dt, AHEAD] → this talk
- Optimization-based coupling [FHNM, M2dt]
- Coupling via generalized mortar methods [FHNM, M2dt]

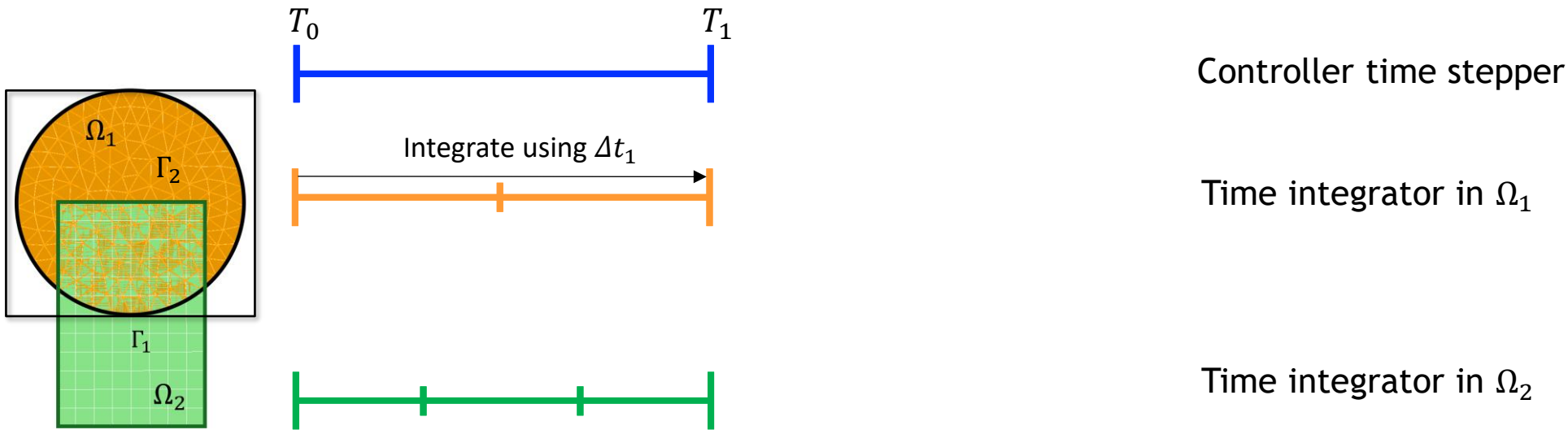
Why? Less intrusive to integrate into production codes.

Time-Advancement within the Schwarz Framework



Step 0: Initialize $i = 0$ (controller time index).

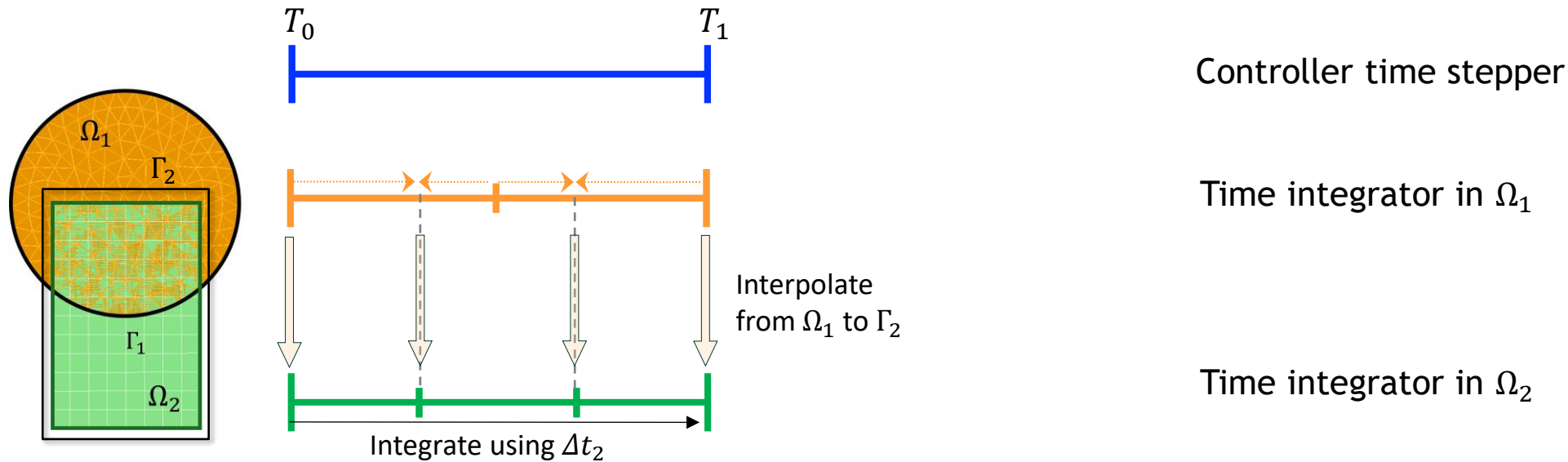
$$\text{Model PDE: } \begin{cases} M\ddot{\mathbf{u}} + \mathbf{f}_{\text{int}}(\mathbf{u}, \dot{\mathbf{u}}) = \mathbf{f}_{\text{ext}} \\ \mathbf{u}(\mathbf{x}, 0) = \mathbf{u}_0 \end{cases}$$



Step 0: Initialize $i = 0$ (controller time index).

Step 1: Advance Ω_1 solution from time T_i to time T_{i+1} using time-stepper in Ω_1 with time-step Δt_1 , using solution in Ω_2 interpolated to Γ_1 at times $T_i + n\Delta t_1$.

$$\text{Model PDE: } \begin{cases} M\ddot{\mathbf{u}} + \mathbf{f}_{\text{int}}(\mathbf{u}, \dot{\mathbf{u}}) = \mathbf{f}_{\text{ext}} \\ \mathbf{u}(\mathbf{x}, 0) = \mathbf{u}_0 \end{cases}$$



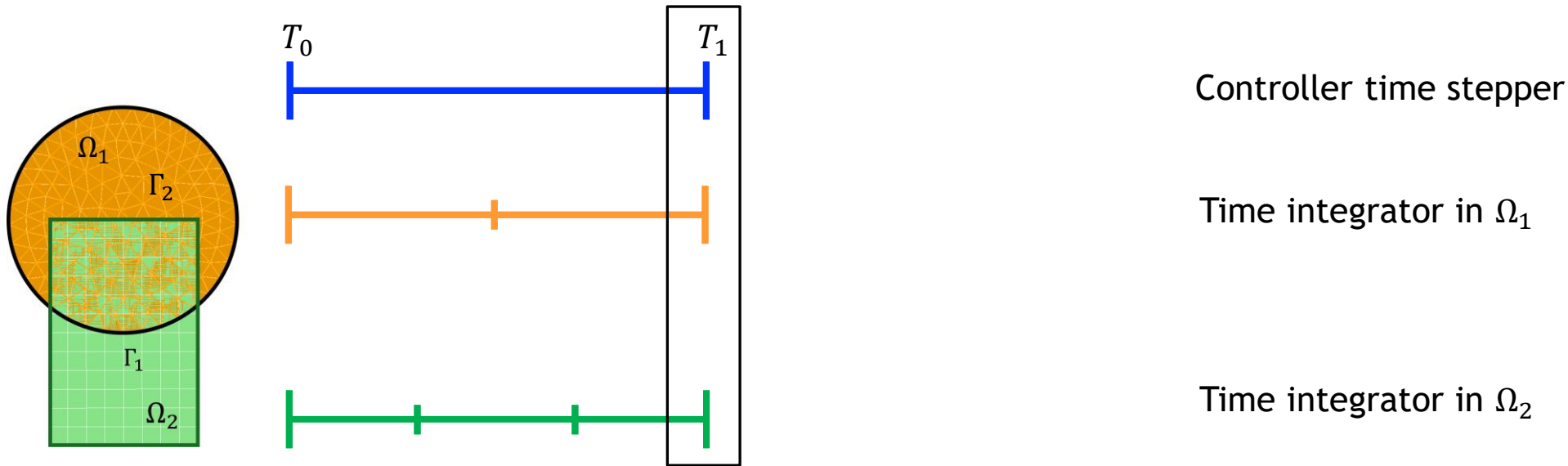
Step 0: Initialize $i = 0$ (controller time index).

Step 1: Advance Ω_1 solution from time T_i to time T_{i+1} using time-stepper in Ω_1 with time-step Δt_1 , using solution in Ω_2 interpolated to Γ_1 at times $T_i + n\Delta t_1$.

Step 2: Advance Ω_2 solution from time T_i to time T_{i+1} using time-stepper in Ω_2 with time-step Δt_2 , using solution in Ω_1 interpolated to Γ_2 at times $T_i + n\Delta t_2$.

.

$$\text{Model PDE: } \begin{cases} M\ddot{\mathbf{u}} + \mathbf{f}_{\text{int}}(\mathbf{u}, \dot{\mathbf{u}}) = \mathbf{f}_{\text{ext}} \\ \mathbf{u}(\mathbf{x}, 0) = \mathbf{u}_0 \end{cases}$$



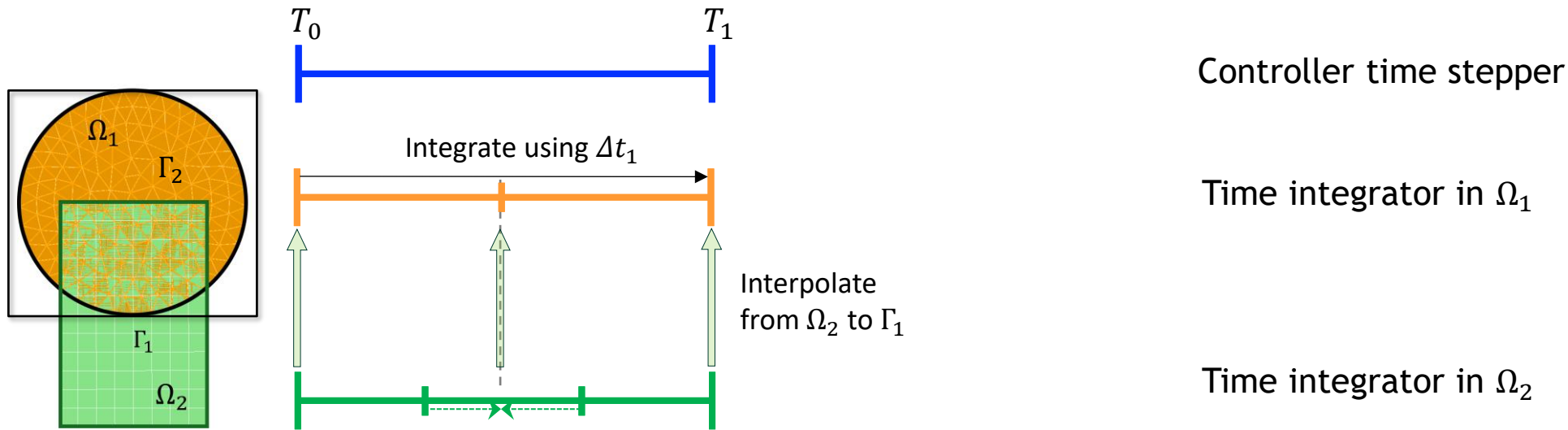
Step 0: Initialize $i = 0$ (controller time index).

Step 1: Advance Ω_1 solution from time T_i to time T_{i+1} using time-stepper in Ω_1 with time-step Δt_1 , using solution in Ω_2 interpolated to Γ_1 at times $T_i + n\Delta t_1$.

Step 2: Advance Ω_2 solution from time T_i to time T_{i+1} using time-stepper in Ω_2 with time-step Δt_2 , using solution in Ω_1 interpolated to Γ_2 at times $T_i + n\Delta t_2$.

Step 3: Check for convergence at time T_{i+1} .

$$\text{Model PDE: } \begin{cases} M\ddot{\mathbf{u}} + \mathbf{f}_{\text{int}}(\mathbf{u}, \dot{\mathbf{u}}) = \mathbf{f}_{\text{ext}} \\ \mathbf{u}(\mathbf{x}, 0) = \mathbf{u}_0 \end{cases}$$



Step 0: Initialize $i = 0$ (controller time index).

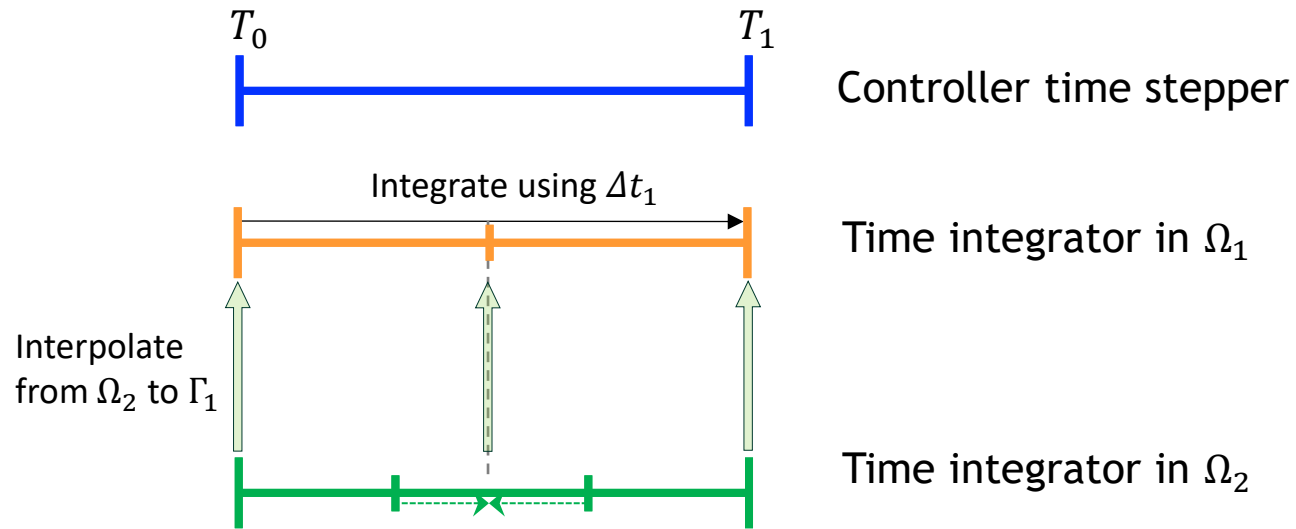
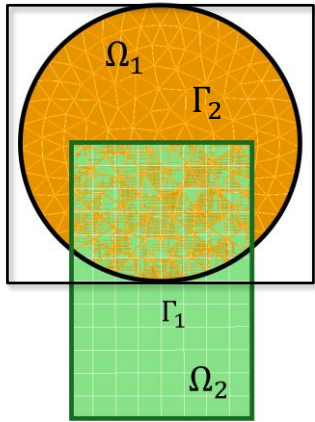
Step 1: Advance Ω_1 solution from time T_i to time T_{i+1} using time-stepper in Ω_1 with time-step Δt_1 , using solution in Ω_2 interpolated to Γ_1 at times $T_i + n\Delta t_1$.

Step 2: Advance Ω_2 solution from time T_i to time T_{i+1} using time-stepper in Ω_2 with time-step Δt_2 , using solution in Ω_1 interpolated to Γ_2 at times $T_i + n\Delta t_2$.

Step 3: Check for convergence at time T_{i+1} .

- If unconverged, return to Step 1.

$$\text{Model PDE: } \begin{cases} M\ddot{\mathbf{u}} + \mathbf{f}_{\text{int}}(\mathbf{u}, \dot{\mathbf{u}}) = \mathbf{f}_{\text{ext}} \\ \mathbf{u}(\mathbf{x}, 0) = \mathbf{u}_0 \end{cases}$$



Can use *different integrators* with *different time steps* within each domain!

Time-stepping procedure is *equivalent* to doing Schwarz on *space-time domain* [Mota, IT, et al. 2022].

Step 0: Initialize $i = 0$ (controller time index).

Step 1: Advance Ω_1 solution from time T_i to time T_{i+1} using time-stepper in Ω_1 with time-step Δt_1 , using solution in Ω_2 interpolated to Γ_1 at times $T_i + n\Delta t_1$.

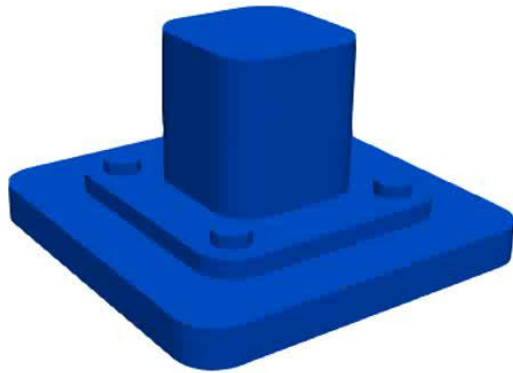
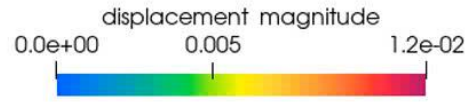
Step 2: Advance Ω_2 solution from time T_i to time T_{i+1} using time-stepper in Ω_2 with time-step Δt_2 , using solution in Ω_1 interpolated to Γ_2 at times $T_i + n\Delta t_2$.

Step 3: Check for convergence at time T_{i+1} .

- If unconverged, return to Step 1.
- If converged, set $i = i + 1$ and return to Step 1.

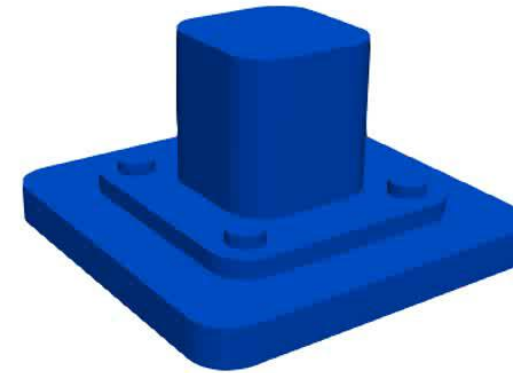
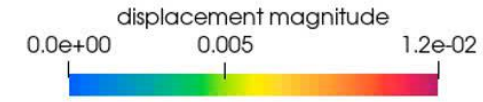
$$\text{Model PDE: } \begin{cases} M\ddot{\mathbf{u}} + \mathbf{f}_{\text{int}}(\mathbf{u}, \dot{\mathbf{u}}) = \mathbf{f}_{\text{ext}} \\ \mathbf{u}(\mathbf{x}, 0) = \mathbf{u}_0 \end{cases}$$

Bolted Joint (Overlapping SAM, Predictive): Animations

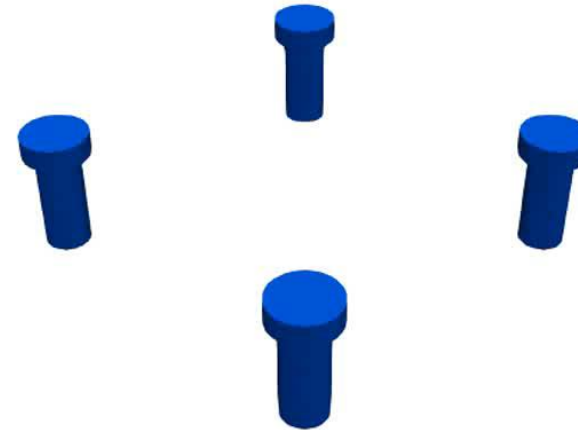
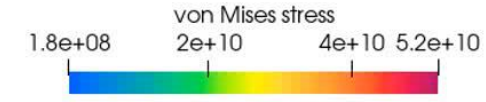
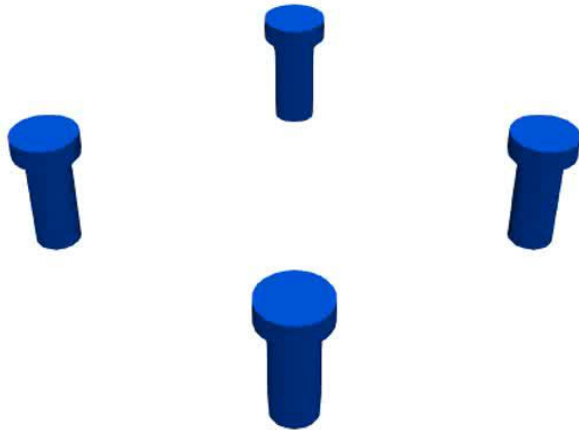
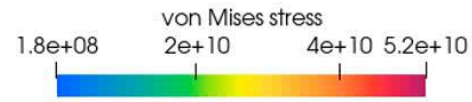


FOM-FOM
~53m

COplnf = Cubic OpInf



COplnf-COplnf
~8.5m



Schwarz Couplings Involving Intrusive Projection-Based ROMs:

- J. Barnett, I. Tezaur, A. Mota. “The Schwarz alternating method for the seamless coupling of nonlinear reduced order models and full order models”, CSRI Summer Proceedings 2023, Sandia National Laboratories. <https://arxiv.org/abs/2210.12551>
- C. Wentland, F. Rizzi, J. Barnett, I. Tezaur. “The role of interface boundary conditions and sampling strategies for Schwarz-based coupling of projection-based reduced order models”, *J. Comput. Appl. Math.*, 465 116584, 2025

Schwarz Couplings Involving Physics-Informed Neural Networks (PINNs):

- W. Snyder, I. Tezaur, C. Wentland. “Domain decomposition-based coupling of PINNs via the Schwarz alternating method”, CSRI Summer Proceedings 2023, Sandia National Laboratories. <https://arxiv.org/abs/2311.00224>



I. Tezaur

J. Barnett

I. Moore

E. Parish

C. Wentland

A. Gruber

C. Rodriguez

W. Snyder

G. Sambataro

Current Research Directions

Production Applications

- 4-way multiscale coupling in salt caverns for Strategic Petroleum Reserve (SPR)
- Schwarz coupling for J-integral around crack front on pressure vessel
- Multiscale coupling for stronglinks
- Schwarz multiphysics coupling for electronics package survivability

Performance Improvements

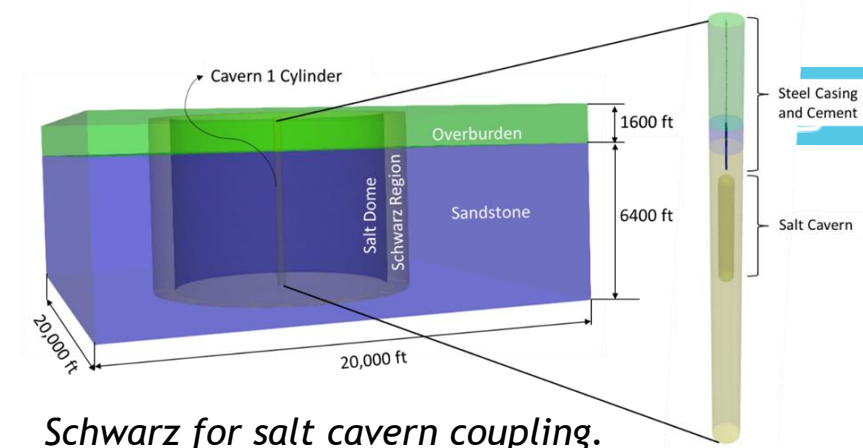
- Acceleration of Schwarz
- Asynchronous additive Schwarz on GPUs

Automated & Adaptive Schwarz

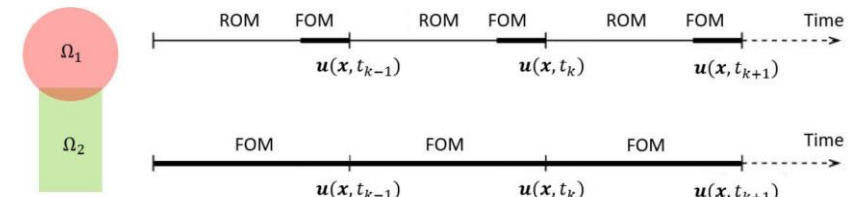
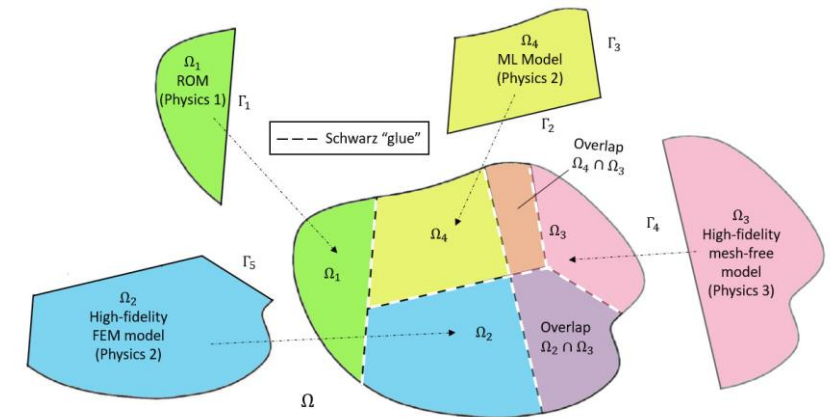
- Automated optimization of meshes/DD with multiple constraints
- Automated criteria to determine appropriate use of less refined or reduced-order models w/o sacrificing accuracy

Schwarz for ROM/Data-Driven Model Coupling

- Non-overlapping Schwarz + Oplnf
- Schwarz + Deep NN-based ROMs
- Schwarz + kernel-based ROMs
- Fully non-intrusive ROM-FOM coupling (w/ K. Willcox & N. Aretz, UT Austin)
- On-the-fly switching between ROMs and FOMs
- Implementation in SIERRA/SM

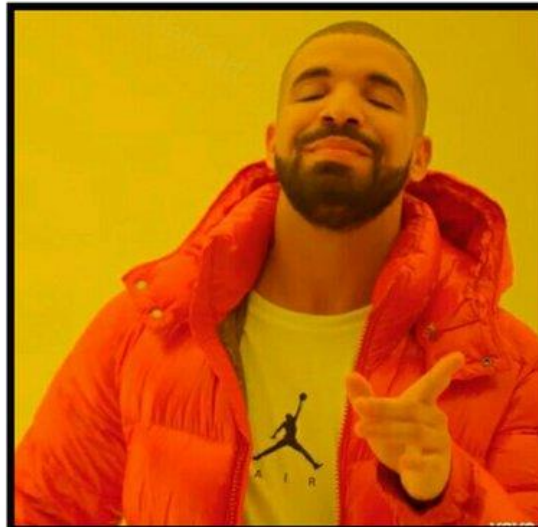


*Schwarz for salt cavern coupling.
Courtesy of T. Ross.*





AS A *PRECONDITIONER*
FOR THE LINEARIZED
SYSTEM



AS A *SOLVER* FOR THE
COUPLED
FULLY NONLINEAR
PROBLEM

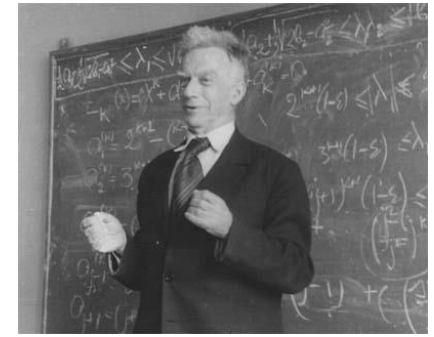
Theoretical Foundation

Using the Schwarz alternating as a *discretization method* for PDEs is natural idea with a sound *theoretical foundation*.

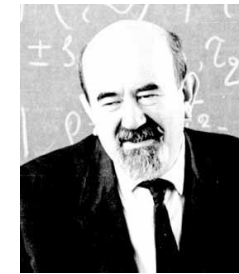
- [S.L. Sobolev \(1936\)](#): posed Schwarz method for *linear elasticity* in variational form and *proved method's convergence* by proposing a convergent sequence of energy functionals.
- [S.G. Mikhlin \(1951\)](#): *proved convergence* of Schwarz method for general linear elliptic PDEs.
- [P.-L. Lions \(1988\)](#): studied convergence of Schwarz for *nonlinear monotone elliptic problems* using max principle.
- [A. Mota, I. Tezaur, C. Alleman \(2017\)](#): proved *convergence* of the alternating Schwarz method for *finite deformation quasi-static nonlinear PDEs* (with energy functional $\Phi[\varphi]$) with a *geometric convergence rate*.

$$\Phi[\varphi] = \int_B A(\mathbf{F}, \mathbf{Z}) dV - \int_B \mathbf{B} \cdot \boldsymbol{\varphi} dV$$

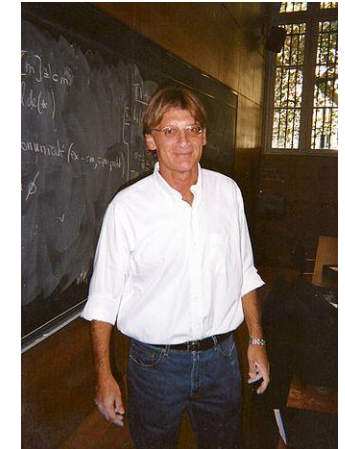
$$\nabla \cdot \mathbf{P} + \mathbf{B} = \mathbf{0}$$



S.L. Sobolev (1908 - 1989)



S.G. Mikhlin
(1908 - 1990)



P.- L. Lions (1956-)



A. Mota, I. Tezaur, C. Alleman

Theory: Overlapping SAM for Quasistatic Multiscale Coupling*



2 Formulation of the Schwarz Alternating Method

We start by defining the standard finite deformation variational formulation to establish notation before presenting the formulation of the coupling method.

2.1 Variational Formulation on a Single Domain

Consider a body as the open set $\Omega \subset \mathbb{R}^d$ undergoing a motion described by the mapping $\varphi = \varphi(X; t) : \Omega \times \mathbb{R} \rightarrow \mathbb{R}^d$. Assume that the boundary of the body is $\partial\Omega = \partial\Omega_D \cup \partial\Omega_N \cup \partial\Omega_S$, where $\partial\Omega_D$ is a displacement boundary, $\partial\Omega_N$ is a traction boundary, and $\partial\Omega_S \cap \partial\Omega_D = \emptyset$. The prescribed boundary displacements or Dirichlet boundary conditions are $\varphi_D = \varphi_D^0 \in \mathbb{R}^d$. The prescribed boundary tractions or Neumann boundary conditions are $T \cdot \nu_D = T_D \in \mathbb{R}^d$. Let $F = \text{Grad} \varphi$ be the deformation gradient. Let also $\rho_0 : \Omega \rightarrow \mathbb{R}^+$ be the body mass, with $\bar{\rho}$ the mass density in the reference configuration. Furthermore, introduce the energy functional

$$\Phi[\varphi] = \int_{\Omega} A(F; Z) dV - \int_{\Omega} BB \cdot \varphi dV - \int_{\partial\Omega_D} T_D \cdot \varphi dS, \quad (1)$$

in which $A(F; Z)$ is the Helmholtz free energy density and Z is a collection of internal variables. The weak form of the problem is obtained by minimizing the energy functional $\Phi[\varphi]$ over the Sobolev space $H^1(\Omega)$ that is comprised of all functions that are square-integrable and have square-integrable first derivatives. Define

$$S := \{ \varphi \in H^1(\Omega) : \varphi = \chi \text{ on } \partial\Omega_D \}$$

and

$$V := \{ \xi \in H^1(\Omega) : \xi = 0 \text{ on } \partial\Omega_D \}$$

where $\xi \in V$ is a test function. The potential energy is minimized if and only if $\Phi[\varphi] \leq \Phi[\varphi + \xi]$ for all $\xi \in V$ and $\xi \in V$. It is straightforward to show that the minimum of $\Phi[\varphi]$ is the mapping $\varphi \in S$ that satisfies

$$D\Phi[\varphi](\xi) = \int_{\Omega} P : \text{Grad} \xi dV - \int_{\partial\Omega_N} BB \cdot \xi dV - \int_{\partial\Omega_S} T \cdot \xi dS = 0, \quad (4)$$

where $P = P(F; Z)$ denotes the first Piola-Kirchhoff stress. The Euler-Lagrange equation corresponding to the variational statement (4) is



Figure 1: Two subdomains Ω_1 and Ω_2 and the corresponding boundary Γ , and Γ_+ , used by the Schwarz alternating method.

that is $i \in \{1, 2\}$ and $j \in \{1, 2\}$ is odd, and $i = 2$ and $j = 1$ if i is even. Introduce the following definitions for each subdomain i :

- Closure $\bar{\Omega}_i = \Omega_i \cup \partial\Omega_i$
- Dirichlet boundary $\partial\Omega_i^D = \partial\Omega_i \cap \partial\Omega_D$
- Neumann boundary $\partial\Omega_i^N = \partial\Omega_i \cap \partial\Omega_N$
- Schwarz boundary $\Gamma_i = \partial\Omega_i \cap \Omega_j$

Note that with these definitions we guarantee that $\partial\Omega_1 \cap \partial\Omega_2 = \Gamma$, $\partial\Omega_1 \cap \Gamma_+ = \emptyset$ and $\partial\Omega_2 \cap \Gamma_+ = \Gamma$. Now define the spaces

$$S_i := \{ \varphi \in H^1(\bar{\Omega}_i) : \varphi = \chi \text{ on } \partial\Omega_i^D \}, \quad (7)$$

and

$$V_i := \{ \xi \in H^1(\bar{\Omega}_i) : \xi = 0 \text{ on } \partial\Omega_i^D \}, \quad (8)$$

where the symbol $P_{\Omega_i, \Gamma_i}[\cdot]$ denotes the projection from the subdomain $\bar{\Omega}_i$ onto the Schwarz boundary Γ_i . This projection operator plays a central role in the Schwarz alternating method. Its form and implementation are discussed in subsequent sections. For the moment it is sufficient to assume that the operator is able to project a field φ from one subdomain to the Schwarz boundary of the other subdomain.

The Schwarz alternating method solves a sequence of problems on Ω_1 and Ω_2 . The solution $\varphi^{(n)}$ for the

1. $\varphi_i^{(n)} \in X_i^{(n)}$ with $X_i^{(n)} = X_i^{(n-1)} \cup \varphi_j^{(n-1)}$	= iterate for Ω_i
2. $\varphi_j^{(n)} \in X_j^{(n)}$ with $X_j^{(n)} = X_j^{(n-1)} \cup \varphi_i^{(n)}$	= iterate for Ω_j
3. $\varphi_i^{(n)} \in X_i^{(n)}$ with $X_i^{(n)} = X_i^{(n-1)} \cup \varphi_j^{(n)}$	= iterate for Ω_i
4. $\varphi_j^{(n)} \in X_j^{(n)}$ with $X_j^{(n)} = X_j^{(n-1)} \cup \varphi_i^{(n)}$	= iterate for Ω_j
5. $\varphi_i^{(n)} \in X_i^{(n)}$ with $X_i^{(n)} = X_i^{(n-1)} \cup \varphi_j^{(n)}$	= iterate for Ω_i
6. $\varphi_j^{(n)} \in X_j^{(n)}$ with $X_j^{(n)} = X_j^{(n-1)} \cup \varphi_i^{(n)}$	= iterate for Ω_j
7. $\varphi_i^{(n)} \in X_i^{(n)}$ with $X_i^{(n)} = X_i^{(n-1)} \cup \varphi_j^{(n)}$	= iterate for Ω_i
8. $\varphi_j^{(n)} \in X_j^{(n)}$ with $X_j^{(n)} = X_j^{(n-1)} \cup \varphi_i^{(n)}$	= iterate for Ω_j
9. $\varphi_i^{(n)} \in X_i^{(n)}$ with $X_i^{(n)} = X_i^{(n-1)} \cup \varphi_j^{(n)}$	= iterate for Ω_i
10. $\varphi_j^{(n)} \in X_j^{(n)}$ with $X_j^{(n)} = X_j^{(n-1)} \cup \varphi_i^{(n)}$	= iterate for Ω_j

[15, 34, 41]. Although we do not provide here formal convergence proofs for the remaining variants of the Schwarz method, we offer some numerical results illustrating their convergence in Section 4.

Consider the energy functional $\Phi[\varphi]$ defined in (1). We will denote by φ^* the usual L^2 inner product over Ω , that is,

$$(\varphi, \psi) = \int_{\Omega} \varphi \cdot \psi dV, \quad (9)$$

for $\varphi, \psi \in H^1(\Omega)$, with corresponding norm $\|\cdot\|$. The proof of the convergence of the Schwarz alternating method requires that the functional $\Phi[\varphi]$ satisfy the following properties over the space S defined in (2):

1. $\Phi[\varphi]$ is convex.
2. $\Phi[\varphi]$ is Fréchet differentiable, with $\Phi'[\varphi]$ denoting its Fréchet derivative.
3. $\Phi[\varphi]$ is strictly convex.
4. $\Phi[\varphi]$ is lower semi-continuous.
5. $\Phi'[\varphi]$ is uniformly continuous on K_{in} , where

$$K_{\text{in}} := \{ \varphi \in S : \Phi[\varphi] \leq B, B \in \mathbb{R}, B < \infty \}. \quad (10)$$

It can be shown that the energy functional $\Phi[\varphi]$ defined in (1) is strictly convex in S . Property 1) provided that the bilinearity form (φ, ψ) is a non-degenerate bilinear form. The last example is true

Remark that [15]

$$\delta_{\varphi} := \varphi^{(n+1)} - \varphi, \quad \text{for } \varphi^{(n+1)} \in \delta_{\varphi}, \quad \varphi^{(n+1)} \in \delta_{\varphi}. \quad (10)$$

Theorem 1. Assume that the energy functional $\Phi[\varphi]$ satisfies properties 1–5 above. Consider the Schwarz alternating method of Section 2, defined by (9)–(13) and its equivalent form (39). Then:

- (a) $\Phi[\varphi^{(n)}] \geq \Phi[\varphi^{(n+1)}] \geq \dots \geq \Phi[\varphi^{(n-1)}] \geq \Phi[\varphi^{(n)}] \geq \dots \geq \Phi[\varphi]$, where φ is the minimizer of $\Phi[\varphi]$ over S .
- (b) the sequence $\{\varphi^{(n)}\}$ defined in (39) converges to the minimizer φ of $\Phi[\varphi]$ in S .
- (c) the Schwarz minimum value $\Phi[\varphi^{(n)}]$ converges monotonically to the minimum value $\Phi[\varphi]$ in S starting from any initial guess $\varphi^{(0)}$.
- (d) if $\Phi'[\varphi]$ is Lipschitz continuous in a neighborhood of φ , then the sequence $\{\varphi^{(n)}\}$ converges geometrically to the minimizer φ .

Proof. See Appendix 5. \square

Finally, while most of works cited above present their analysis for the specific case of two subdomains, extension to multiple subdomains is in general straightforward. The case of multiple subdomains is considered specifically in Loos [15], Babel [1], and Li-Shan and Fran [34].

4 Numerical Examples

In this section, we present numerical examples of the behavior of the Schwarz alternating method for two different implementations. First, we briefly describe the two implementations, one in MATLAB and the other in the open-source ABAQUS finite element code [1]. Next, we discuss the error measures used throughout the numerical examples. Then, we continue with four examples that demonstrate different features of the Schwarz alternating method and our implementation. The first example, a one-dimensional singular bar, is used to demonstrate the behavior of the four Schwarz variants of Section 2. The second example, a cuboid body of square base, aims to study the effect of the size of the overlap region on the convergence of the method. The objective of the third example, a matched cylinder, is to analyze the numerical error in the results and to demonstrate the ability of the method to compute different boundary conditions. The last example is a

Theorem 1. Assume that the energy functional $\Phi[\varphi]$ satisfies properties 1–5 above. Consider the Schwarz alternating method of Section 2 defined by (9)–(13) and its equivalent form (39). Then

- (a) $\Phi[\varphi^{(0)}] \geq \Phi[\varphi^{(1)}] \geq \dots \geq \Phi[\varphi^{(n-1)}] \geq \Phi[\varphi^{(n)}] \geq \dots \geq \Phi[\varphi]$, where φ is the minimizer of $\Phi[\varphi]$ over S .
- (b) The sequence $\{\varphi^{(n)}\}$ defined in (39) converges to the minimizer φ of $\Phi[\varphi]$ in S .
- (c) The Schwarz minimum values $\Phi[\varphi^{(n)}]$ converge monotonically to the minimum value $\Phi[\varphi]$ in S starting from any initial guess $\varphi^{(0)}$.



Remark 1. The convexity of $\Phi[\varphi]$ follows from the Lax-Milgram theorem that a unique minimizer to this functional over S exists, i.e., the minimization of $\Phi[\varphi]$ is well-posed.

Remark 2. By the Stampacchia theorem, the minimization of $\Phi[\varphi]$ in S is equivalent to finding $\varphi \in S$ such that

$$(\Phi'[\varphi], \xi) = 0, \quad \forall \xi \in S. \quad (11)$$

Recall that the strict convexity property of $\Phi[\varphi]$ can be written as

$$\Phi[\varphi] - \Phi[\psi] - (\Phi'[\psi], \varphi - \psi) \geq 0, \quad \forall \varphi, \psi \in S. \quad (12)$$

From (11), remark that if $\Phi[\varphi]$ is strictly convex over S for $B \in \mathbb{R}$ such that $B < \infty$, we can find $\alpha > 0$ such that $\Phi[\varphi] - \Phi[\psi] \geq \alpha \|\varphi - \psi\|$.

Remark 3. Recall that the uniform continuity of $\Phi'[\varphi]$ is a sufficient condition of continuity $\varphi \rightarrow 0$, with $\varphi : K_{\text{in}} \rightarrow K_{\text{in}}$, such that

$$\|\Phi'[\varphi] - \Phi'[\psi]\| \leq c \|\varphi - \psi\|, \quad \forall \varphi, \psi \in K_{\text{in}}. \quad (13)$$

By definition, $c(\cdot) = 0 \rightarrow c(\cdot) = 0$.

Remark 4. It was shown in [15] that in the case $\Omega_1 \cap \Omega_2 \neq \emptyset$, there exist $C_1 \in S_1$ and $C_2 \in S_2$ such that

$$\varphi = C_1 + C_2. \quad (14)$$

and

$$\|\varphi\| \leq C_3 \|\varphi\|, \quad (15)$$

for some $C_3 > 0$ independent of φ .

Remark 5. Note that (15) can be written as

$$(\Phi'[\varphi^{(n)}], \varphi^{(n)}) \leq 0, \quad \text{for } \varphi^{(n)} \in S_n, \quad (16)$$

for $n \in \{1, 2, 3, \dots\}$ (recall from (9) the selection between 1 and 2). This is due to the uniqueness of the solution to each minimization problem over S_n , and the definition of $\varphi^{(n)}$ as the minimizer of $\Phi[\varphi]$ over S_n .

Remark 6. Let $\varphi^{(n)} \in S_n$, and let $\xi \in S$. By Remark 5, there exist $C_1 \in S_1$ and $C_2 \in S_2$ such that

$$(\Phi'[\varphi^{(n)}], \xi) = (\Phi'[\varphi^{(n)}], C_1 + C_2). \quad (17)$$

Again using (7) and also (8) in (16) leads to

$$(\Phi'[\varphi^{(n)}], \varphi^{(n)} - \varphi) = (\Phi'[\varphi^{(n)}], \xi) \leq \|(\Phi'[\varphi^{(n)}], \varphi^{(n)} - \varphi)\| \|C_3\|, \quad (18)$$

and substituting (18) into (16) we finally obtain that

$$(\Phi'[\varphi^{(n)}], \xi) \leq C_3 \|(\Phi'[\varphi^{(n)}], \varphi^{(n)} - \varphi)\| \|C_3\|, \quad (19)$$

$\forall \xi \in S$.

Remark 7. For part (a) of Theorem 1, recall the definition of geometric convexity:

$$K_{\text{in}} \subseteq C K_{\text{in}}, \quad (20)$$

for $n \in \{1, 2, 3, \dots\}$ for some $C > 0$, where

$$K_{\text{in}} := \{\varphi \in S : \Phi[\varphi] \leq B\}. \quad (21)$$

Remark 8. Recall from the definition of continuity that if $\Phi'[\varphi]$ is Lipschitz continuous at $\varphi^{(n)}$ near φ , then there exists a constant $K > 0$ such that

$$\frac{\|(\Phi'[\varphi^{(n)}], \varphi^{(n)} - \varphi)\|}{\|\varphi^{(n)} - \varphi\|} \leq K. \quad (22)$$

Considering that $\Phi'[\varphi] = 0$ since φ is the minimizer of $\Phi[\varphi]$, (22) is equivalent to

$$\|(\Phi'[\varphi^{(n)}], \varphi)\| \leq K \|\varphi^{(n)} - \varphi\|. \quad (23)$$

Proof of Theorem 1.

Proof of (a). Let $\varphi^{(n)} = \arg \min_{\varphi \in S_n} \Phi[\varphi]$. By (20), $\varphi^{(n)} \in S_n$. Let φ^* be the minimizer of $\Phi[\varphi]$ over S , and suppose $\varphi^{(n)} \neq \varphi^*$. But this is a contradiction, since we can take $\varphi^* \in S_n$. Hence, it cannot be that $\varphi^{(n)} \neq \varphi^*$, where $\varphi^{(n)} = \arg \min_{\varphi \in S_n} \Phi[\varphi]$. It follows by induction that

$$\varphi^{(n)} \leq \Phi[\varphi^{(n+1)}] \leq \Phi[\varphi^*] \quad (24)$$

for $n \in \{1, 2, 3, \dots\}$. Now let φ be the minimizer of $\Phi[\varphi]$ over S . Since the problem is well-posed and is unique, hence $\Phi[\varphi] \leq \Phi[\varphi^{(n)}]$ for all $n \in \{1, 2, 3, \dots\}$. \square

$$\lim_{n \rightarrow \infty} \|\varphi^{(n)} - \varphi^{(n+1)}\| = 0. \quad (25)$$

From which we can conclude that $\varphi^{(n)} = \varphi^{(n+1)} = \varphi$ as $n \rightarrow \infty$. We must now show that $\varphi^{(n)}$ converges to φ , the minimizer of $\Phi[\varphi]$ on S . By (15) with $\varphi_1 = \varphi$ and $\varphi_2 = \varphi^{(n)}$, we have

$$\|\varphi - \varphi^{(n)}\| \leq \frac{1}{\alpha} \left((\Phi'[\varphi], \varphi - \varphi^{(n)}) - (\Phi'[\varphi^{(n)}], \varphi - \varphi^{(n)}) \right). \quad (26)$$

Since φ is the minimum of $\Phi[\varphi]$, by (11) we have that $\Phi[\varphi] \leq \Phi[\varphi^{(n)}]$. It follows that

$$\Phi[\varphi] - \Phi[\varphi^{(n)}] - (\Phi'[\varphi^{(n)}], \varphi - \varphi^{(n)}) \leq - \left((\Phi'[\varphi^{(n)}], \varphi - \varphi^{(n)}) - (\Phi'[\varphi^{(n)}], \varphi^{(n)} - \varphi) \right). \quad (27)$$

Using (27) into (26) we have

$$\|\varphi - \varphi^{(n)}\| \leq \frac{1}{\alpha} \left((\Phi'[\varphi^{(n)}], \varphi^{(n)} - \varphi) \right). \quad (28)$$

Now by (22) (Remark 7),

$$\left((\Phi'[\varphi^{(n)}], \varphi^{(n)} - \varphi) \right) \leq C_3 \|(\Phi'[\varphi^{(n)}], \varphi^{(n)} - \varphi)\| \|C_3\|. \quad (29)$$

Substituting (29) into (28) leads to

$$\|\varphi - \varphi^{(n)}\| \leq \frac{C_3}{\alpha} \|(\Phi'[\varphi^{(n)}], \varphi^{(n)} - \varphi)\| \|C_3\|. \quad (30)$$

Applying the uniform continuity assumption (13), we obtain

$$\|\varphi - \varphi^{(n)}\| \leq \frac{C_3}{\alpha} \|C_3\| \|\varphi^{(n)} - \varphi\|. \quad (31)$$

By (29), $\|\varphi^{(n)} - \varphi^{(n+1)}\| \rightarrow 0$ as $n \rightarrow \infty$. From this we obtain the result, namely that $\varphi^{(n)} \rightarrow \varphi$ as $n \rightarrow \infty$. \square

Proof of (b). This follows immediately from (a) and (b).

Proof of (c). For large enough n , there exists some $C_1 > 0$ independent of n such that

$$\|\varphi^{(n)} - \varphi\| \leq C_1 \|\varphi^{(n+1)} - \varphi^{(n)}\|. \quad (32)$$

Let us choose C_1 such that $C_1 > \alpha_2/K$, where K is the Lipschitz continuity constant in (16). Combining (32) with (23) leads to

$$\frac{1}{\alpha} \left((\Phi'[\varphi^{(n)}], \varphi - \varphi^{(n)}) \right) \geq \|\varphi^{(n+1)} - \varphi^{(n)}\| \geq \frac{\alpha_2}{C_1} \|\varphi^{(n)} - \varphi\|. \quad (33)$$

$$\|(\Phi'[\varphi^{(n)}], \varphi - \varphi^{(n)})\| \leq \|(\Phi'[\varphi^{(n+1)}], \varphi^{(n+1)} - \varphi^{(n)})\| + \alpha_2 \|\varphi^{(n)} - \varphi^{(n+1)}\| \leq \Phi[\varphi^{(n)}] - \Phi[\varphi^{(n+1)}] \quad (34)$$

since $\alpha_2 \geq 0$. Now, by the Cauchy-Schwarz inequality followed by the application of the Lipschitz continuity of $\Phi'[\varphi]$ (16) we can write

$$\|(\Phi'[\varphi^{(n)}], \varphi - \varphi^{(n)})\| \leq \|(\Phi'[\varphi^{(n)}], \varphi - \varphi^{(n)})\| \|C_1\| \leq K \|(\varphi^{(n)} - \varphi)\| \|C_1\|. \quad (35)$$

Hence, from (34),

$$\Phi[\varphi^{(n)}] - \Phi[\varphi^{(n+1)}] \leq K \|\varphi^{(n)} - \varphi\|^2. \quad (36)$$

Moreover, by (15) since $\Phi'[\varphi] = 0$,

$$\Phi[\varphi^{(n)}] - \Phi[\varphi] \leq \alpha_1 \|\varphi^{(n)} - \varphi\|. \quad (37)$$

Using (36) and (37) we obtain

$$\left(\Phi[\varphi^{(n)}] - \Phi[\varphi] \right) - \left(\Phi[\varphi^{(n+1)}] - \Phi[\varphi] \right) \leq K \|\varphi^{(n)} - \varphi\|^2 - \alpha_1 \|\varphi^{(n+1)} - \varphi\|. \quad (38)$$

Combining (36) and (37) leads to

$$\frac{\alpha_2}{C_1} \|\varphi^{(n)} - \varphi\| \leq \left(\Phi[\varphi^{(n)}] - \Phi[\varphi] \right) - \left(\Phi[\varphi^{(n+1)}] - \Phi[\varphi] \right) \leq K \|\varphi^{(n)} - \varphi\|^2 - \alpha_1 \|\varphi^{(n+1)} - \varphi\|. \quad (39)$$

or

$$\|\varphi^{(n+1)} - \varphi\| \leq B \|\varphi^{(n)} - \varphi\| \quad (40)$$

with

$$B := \frac{1}{\alpha_2} \left(\frac{K}{C_1} - \alpha_1 \right), \quad (41)$$

and $B \in \mathbb{R}$ as we chose $C_1 > \alpha_2/K$. Furthermore, since the sequence $\{\varphi^{(n)}\}$ converges monotonically to the minimizer φ of $\Phi[\varphi]$ by (a) and (b), it follows that $B \in (0, 1)$. Define C as $1 - B \in (0, 1)$, then (40) can be recast as

$$\|\varphi^{(n+1)} - \varphi\| \leq C \|\varphi^{(n)} - \varphi\| \quad (42)$$

whereupon the claim is proven. \square

B Analytic Solution for Linear-Elastic Singular Bar

As reference, herein we provide the solution of the singular bar of Section 4.3 for linear elasticity. The equilibrium equation is

$$P = \sigma(X)A(X) = \text{const.}, \quad \sigma(X) = B\sigma(X), \quad \sigma(X) = \sigma(X), \quad A(X) = A_0 \left(\frac{X}{L} \right)^2. \quad (43)$$

Theory: Overlapping SAM for Dynamic Multiscale Coupling*



- Like for quasistatics, dynamic alternating Schwarz method converges provided each single-domain problem is **well-posed** and **overlap region** is **non-empty**, under some **conditions** on Δt .
- **Well-posedness** for the dynamic problem requires that action functional $S[\boldsymbol{\varphi}] := \int_I \int_{\Omega} L(\boldsymbol{\varphi}, \dot{\boldsymbol{\varphi}}) dV dt$ be **strictly convex** or **strictly concave**, where $L(\boldsymbol{\varphi}, \dot{\boldsymbol{\varphi}}) := T(\dot{\boldsymbol{\varphi}}) + V(\boldsymbol{\varphi})$ is the Lagrangian.
 - This is studied by looking at its second variation $\delta^2 S[\boldsymbol{\varphi}_h]$
- We can show assuming a **Newmark** time-integration scheme that for the **fully-discrete** problem:

$$\delta^2 S[\boldsymbol{\varphi}_h] = \mathbf{x}^T \left[\frac{\gamma^2}{(\beta \Delta t)^2} \mathbf{M} - \mathbf{K} \right] \mathbf{x}$$

- $\delta^2 S[\boldsymbol{\varphi}_h]$ can always be made positive by choosing a **sufficiently small** Δt
- Numerical experiments reveal that Δt requirements for **stability/accuracy** typically lead to automatic satisfaction of this bound.



* Mota, IT, et al., 2022.

This talk

Multiplicative Overlapping Schwarz

$$\begin{cases} \text{Div } \mathbf{P}_1^{(n+1)} + \rho \mathbf{B}(t_i) = \mathbf{0}, & \text{in } \Omega_1 \\ \boldsymbol{\varphi}_1^{(n+1)} = \boldsymbol{\chi}, & \text{on } \partial\Omega_1 \setminus \Gamma_1 \\ \boldsymbol{\varphi}_1^{(n+1)} = \boldsymbol{\varphi}_2^{(n)} & \text{on } \Gamma_2 \end{cases}$$

$$\begin{cases} \text{Div } \mathbf{P}_2^{(n+1)} + \rho \mathbf{B}(t_i) = \mathbf{0}, & \text{in } \Omega_2 \\ \boldsymbol{\varphi}_2^{(n+1)} = \boldsymbol{\chi}, & \text{on } \partial\Omega_2 \setminus \Gamma_2 \\ \boldsymbol{\varphi}_2^{(n+1)} = \boldsymbol{\varphi}_1^{(n+1)} & \text{on } \Gamma_2 \end{cases}$$

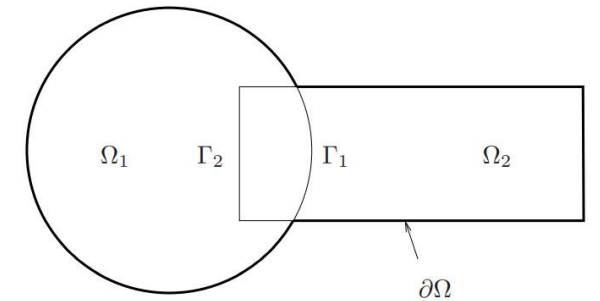
Additive Overlapping Schwarz

$$\begin{cases} \text{Div } \mathbf{P}_1^{(n+1)} + \rho \mathbf{B}(t_i) = \mathbf{0}, & \text{in } \Omega_1 \\ \boldsymbol{\varphi}_1^{(n+1)} = \boldsymbol{\chi}, & \text{on } \partial\Omega_1 \setminus \Gamma_1 \\ \boldsymbol{\varphi}_1^{(n+1)} = \boldsymbol{\varphi}_2^{(n)} & \text{on } \Gamma_2 \end{cases}$$

$$\begin{cases} \text{Div } \mathbf{P}_2^{(n+1)} + \rho \mathbf{B}(t_i) = \mathbf{0}, & \text{in } \Omega_2 \\ \boldsymbol{\varphi}_2^{(n+1)} = \boldsymbol{\chi}, & \text{on } \partial\Omega_2 \setminus \Gamma_2 \\ \boldsymbol{\varphi}_2^{(n+1)} = \boldsymbol{\varphi}_1^{(n+1)} & \text{on } \Gamma_2 \end{cases}$$

Model PDE:

$$\begin{cases} \text{Div } \mathbf{P} + \rho \mathbf{B} = \mathbf{0}, & \text{in } \Omega \\ \boldsymbol{\varphi} = \boldsymbol{\chi}, & \text{on } \partial\Omega \end{cases}$$



- **Multiplicative Schwarz:** solves subdomain problems **sequentially** (in serial)
- **Additive Schwarz:** advance subdomains in **parallel**, communicate boundary condition data later
 - Typically requires a few more **Schwarz iterations**, but does not degrade **accuracy**
 - **Parallelism** helps balance additional **cost** due to Schwarz iterations
 - Applicable to both **overlapping** and **non-overlapping** Schwarz

How to Apply Schwarz to Dynamics?

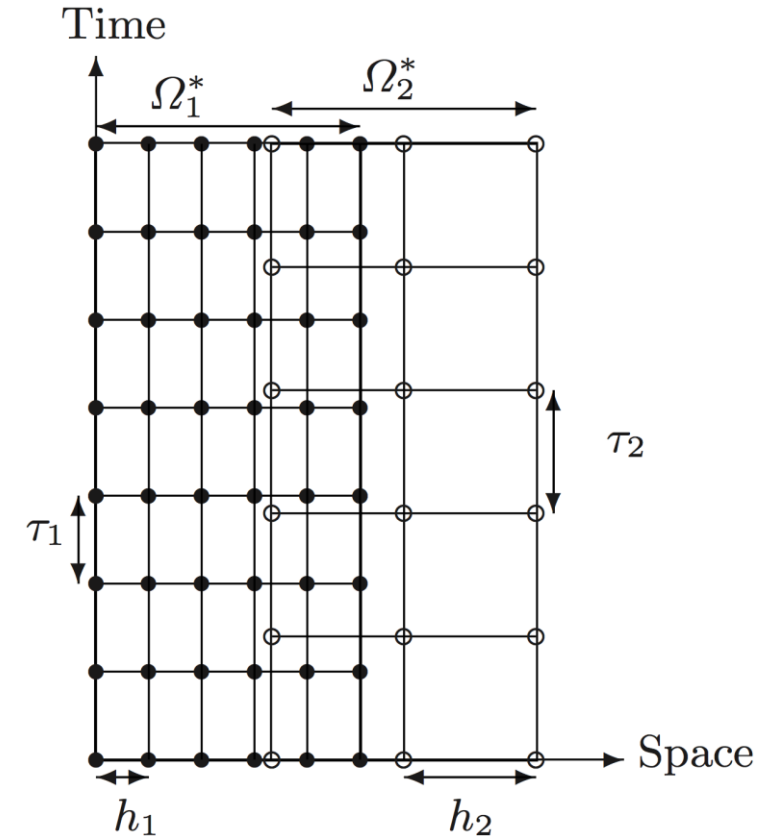
- In the literature the Schwarz method is applied to dynamics by using *space-time discretizations*.

Pro 😊: Can use *non-matching* meshes and time-steps (see right figure).

Con 😞: *Unfeasible* given the design of our current codes and size of simulations.

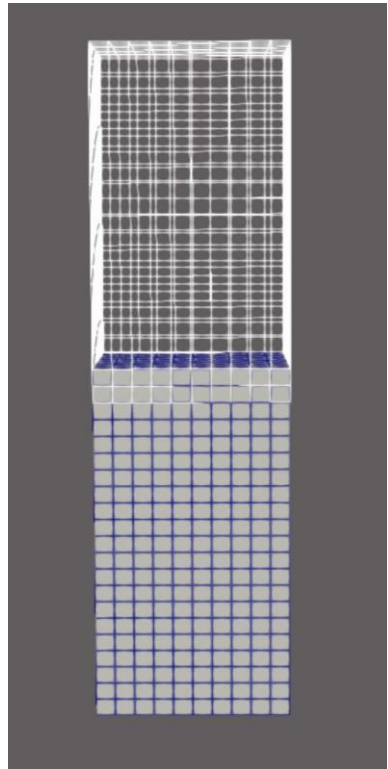


Ease of implementation is a very important requirement!

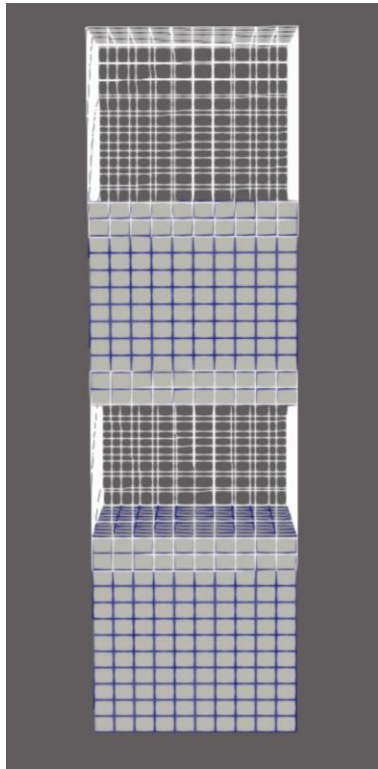


Overlapping non-matching meshes and time steps in dynamics.

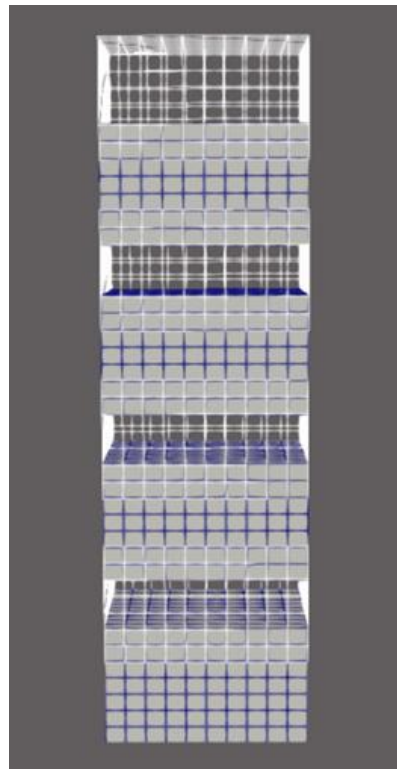
Scaling with Respect to the Number of Subdomains



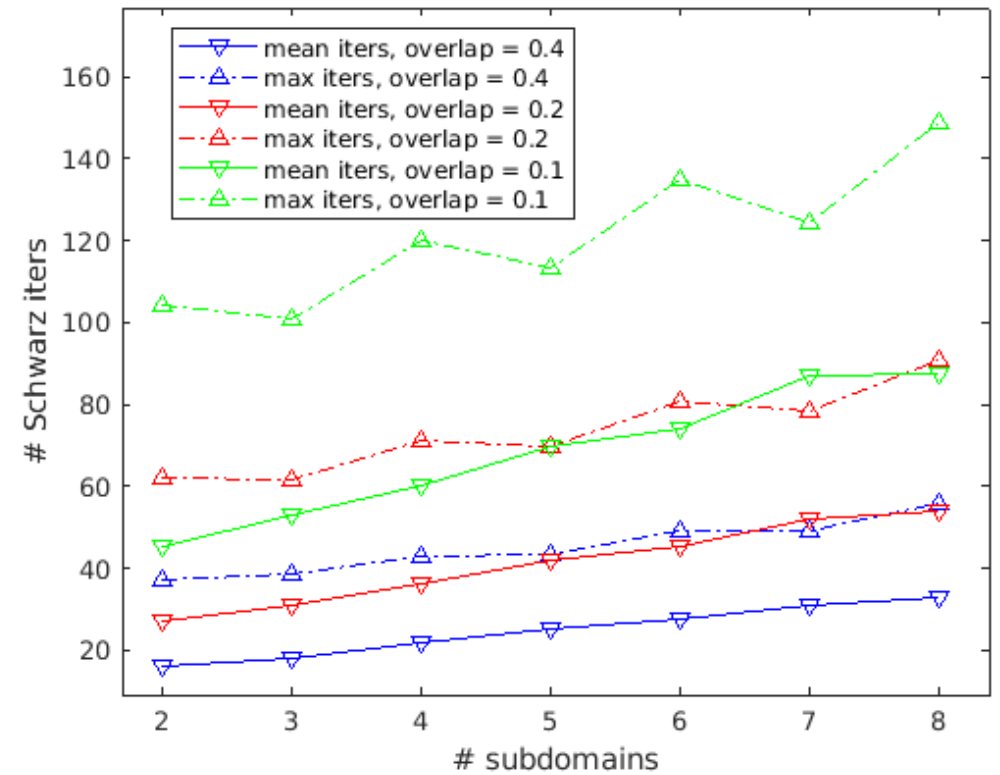
2 subdomains



4 subdomains



8 subdomains



- Overlapping SAM scaling study from 2 to 8 subdomains
- Linear elastic cuboid problem, pulled from top at rate of $0.5 - 0.5 \cos(\pi t)$
- Overlap size varied: 0.4, 0.2 (above) and 0.1
- Same mesh resolution of 0.1 in all subdomains
- Linear convergence observed w.r.t. # subdomains



Generally, we do not target cases with >5-6 subdomains

Choice of domain decomposition

- **Overlapping vs. non-overlapping** domain decomposition?
 - Non-overlapping more flexible but typically requires more Schwarz iterations
- **FOM vs. ROM** subdomain assignment?
 - Do not assign ROM to subdomains where they have no hope of approximating solution

Snapshot collection and reduced basis construction

- Are subdomains **simulated independently** in each subdomains or together?

Enforcement of boundary conditions (BCs) in ROM at Schwarz boundaries

- **Strong vs. weak** BC enforcement?
 - Strong BC enforcement difficult for some models (e.g., cell-centered finite volume, PINNs)
- **Optimizing parameters** in Schwarz BCs for non-overlapping Schwarz?

Choice of hyper-reduction

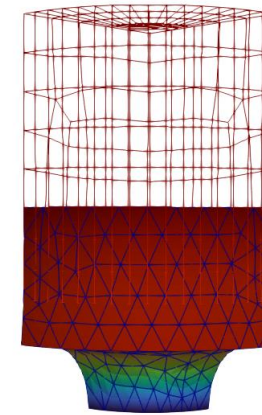
- What **hyper-reduction** method to use?
 - Application may require particular method (e.g., ECSW for solid mechanics problems)
- How to **sample Schwarz boundaries** in applying hyper-reduction?
 - Need to have enough sample mesh points at Schwarz boundaries to apply Schwarz

3D Linear Elastic Notched Cylinder Problem

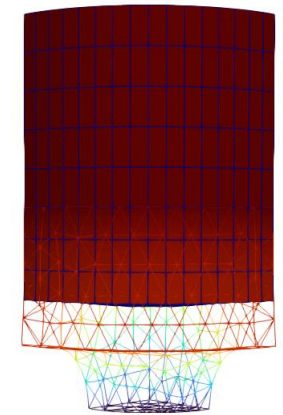
- Geometry is *linear elastic notched cylinder* pulled from top *dynamically* to time $T_{max} = 1.5$ at rate of $0.0064t$ with $\Delta t = 0.005$
- Demonstration of SAM's ability to *couple disparate meshes, element types* and *models*: TET10 + FOM (notched region) and HEX8 + Linear Oplnf with $M = 30$ modes (top region)
- *Linear Oplnf* trained on 301 snapshots in time
- *Reproductive* problem for now

Key result: regularization parameter γ influences accuracy & convergence. Coupled models are remarkably accurate! Schwarz is *not* introducing coupling error/artifacts.

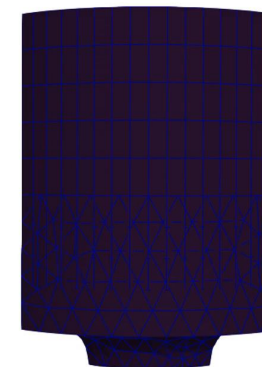
	Mean/max # Schwarz iters	Max z-disp rel error Ω_1	Max z-disp rel error Ω_2
FOM-FOM	5.83/9	—	—
FOM-Oplnf ($\gamma = 1 \times 10^{-6}$)	5.09/8	2.9e-3	4.2e-3
FOM-Oplnf ($\gamma = 1 \times 10^{-7}$)	5.48/9	3.8e-4	4.3e-4
FOM-Oplnf ($\gamma = 1 \times 10^{-8}$)	5.54/9	1.3e-4	2.2e-4
FOM-Oplnf ($\gamma = 1 \times 10^{-9}$)	5.52/9	3.1e-5	3.6e-5



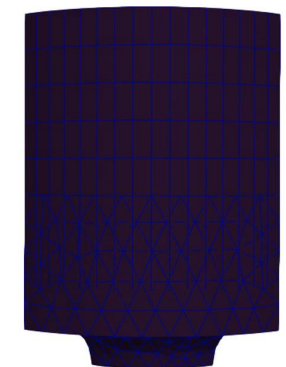
Ω_1 (TET10 + FOM)



Ω_2 (HEX8 + Oplnf)



FOM-FOM

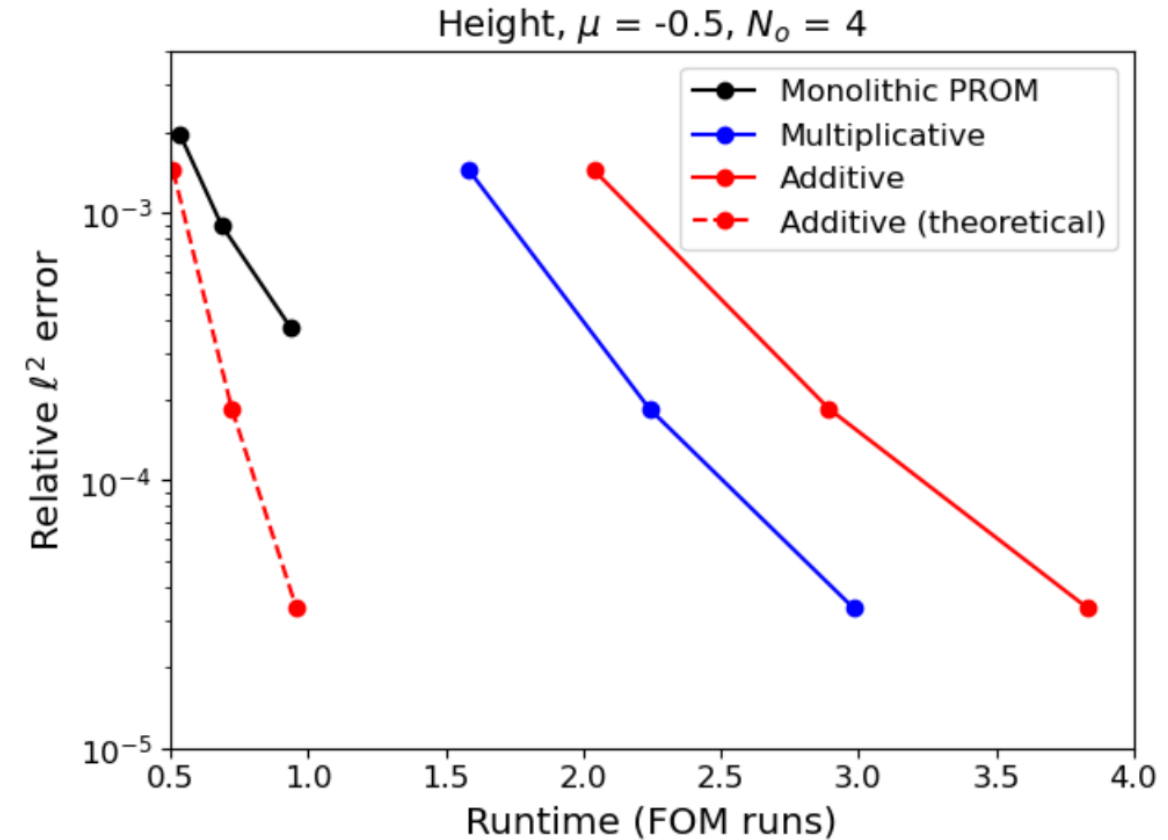


FOM-Oplnf

Movies above: z-displacement solutions for FOM-FOM and FOM-Oplnf ($M = 30$, $\gamma = 1 \times 10^{-6}$)

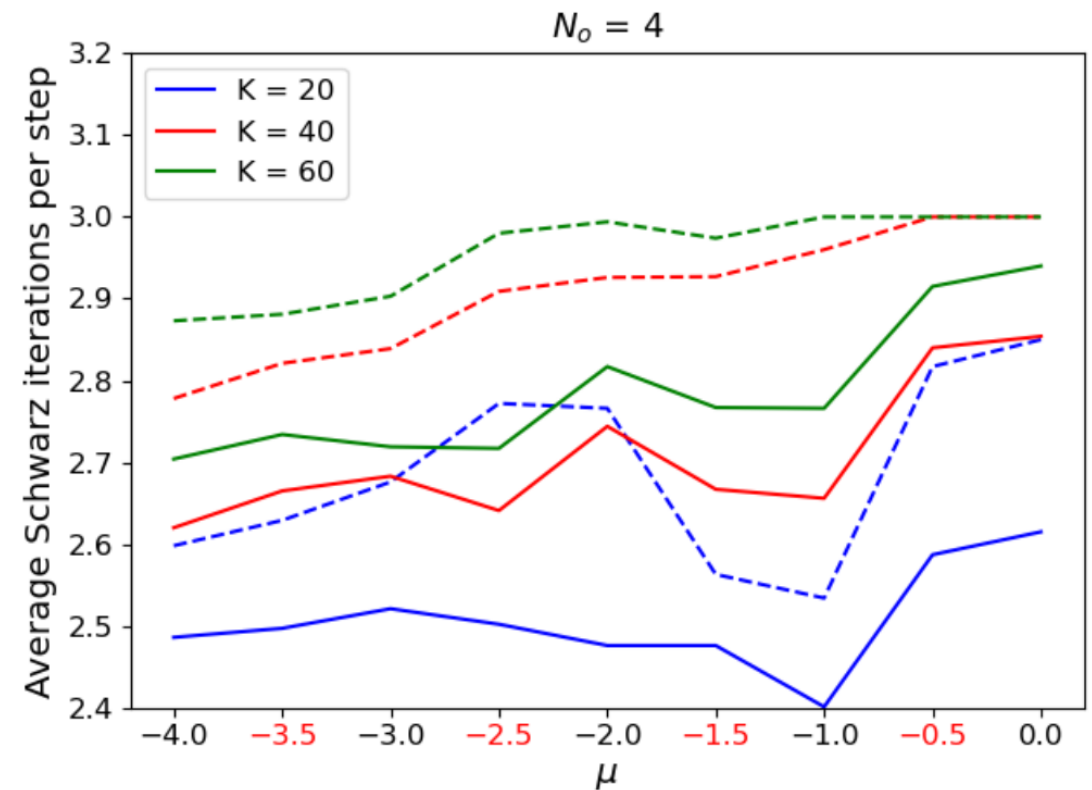
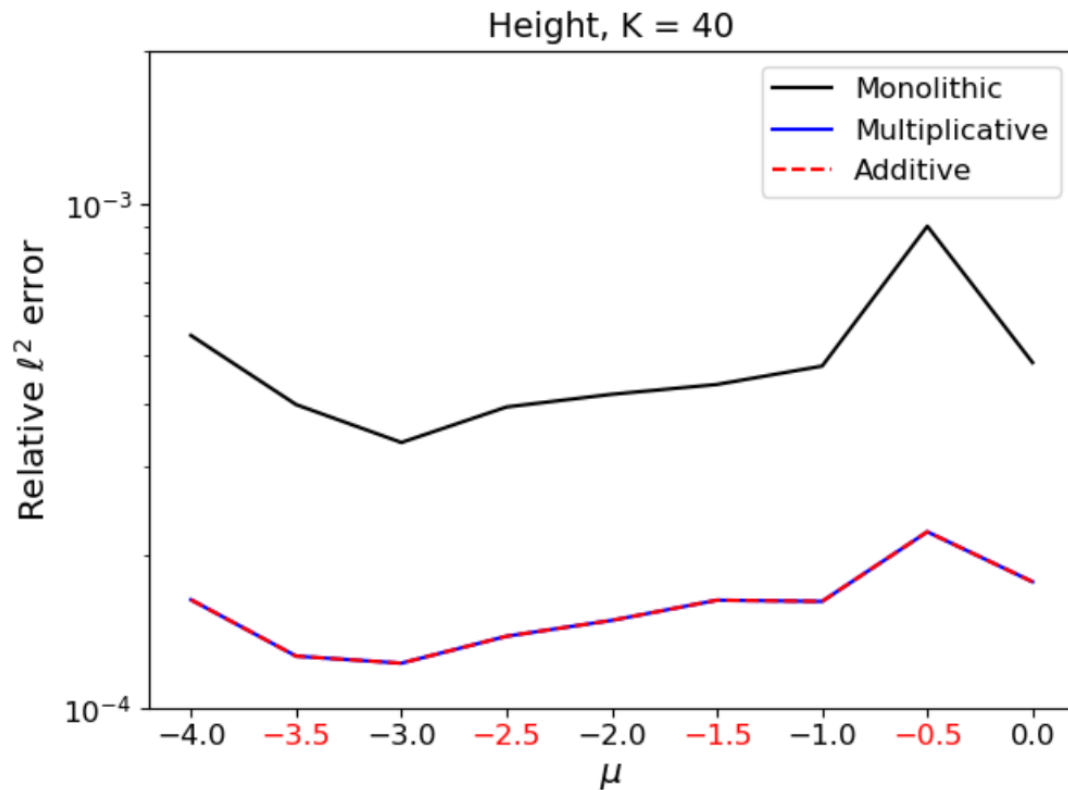
2D SWE: Takeaways

- Resolving overlap region discrepancy is critical
- Additive Schwarz exacerbates PROM dimension costs
- Available parallel cost savings
- Unexpected overlap error requires further investigation



2D SWE: PROMs, additive Schwarz

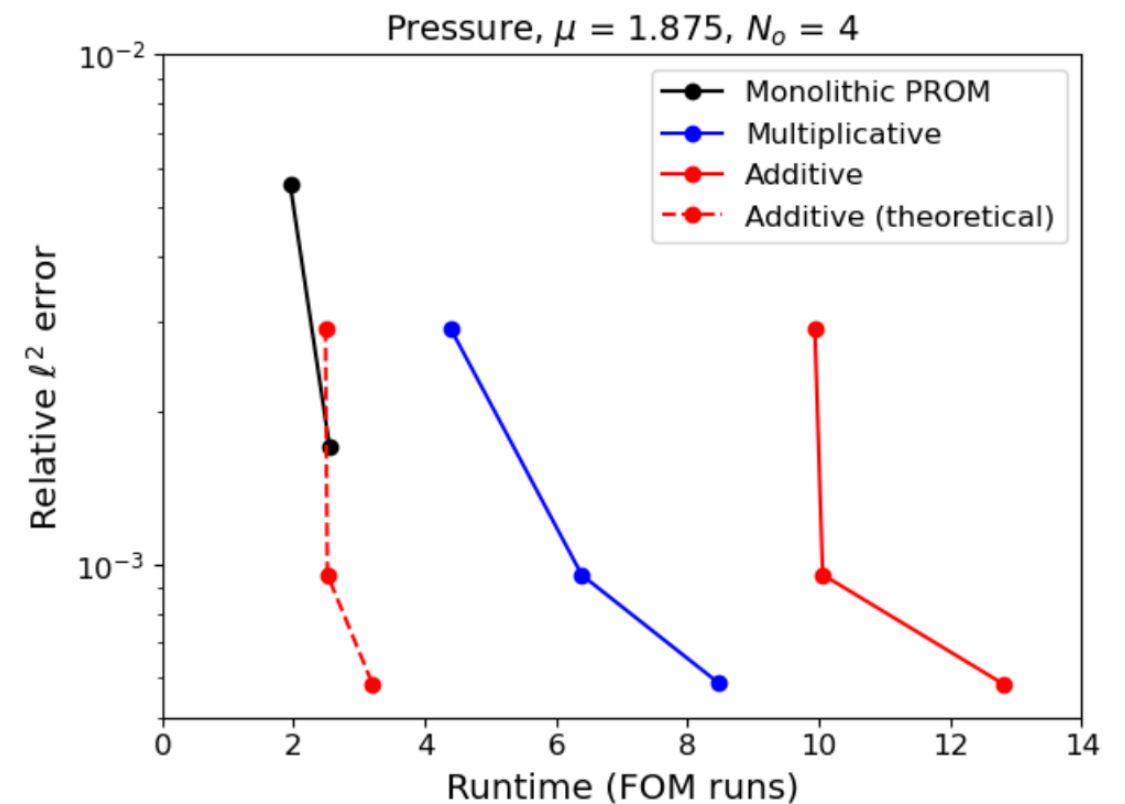
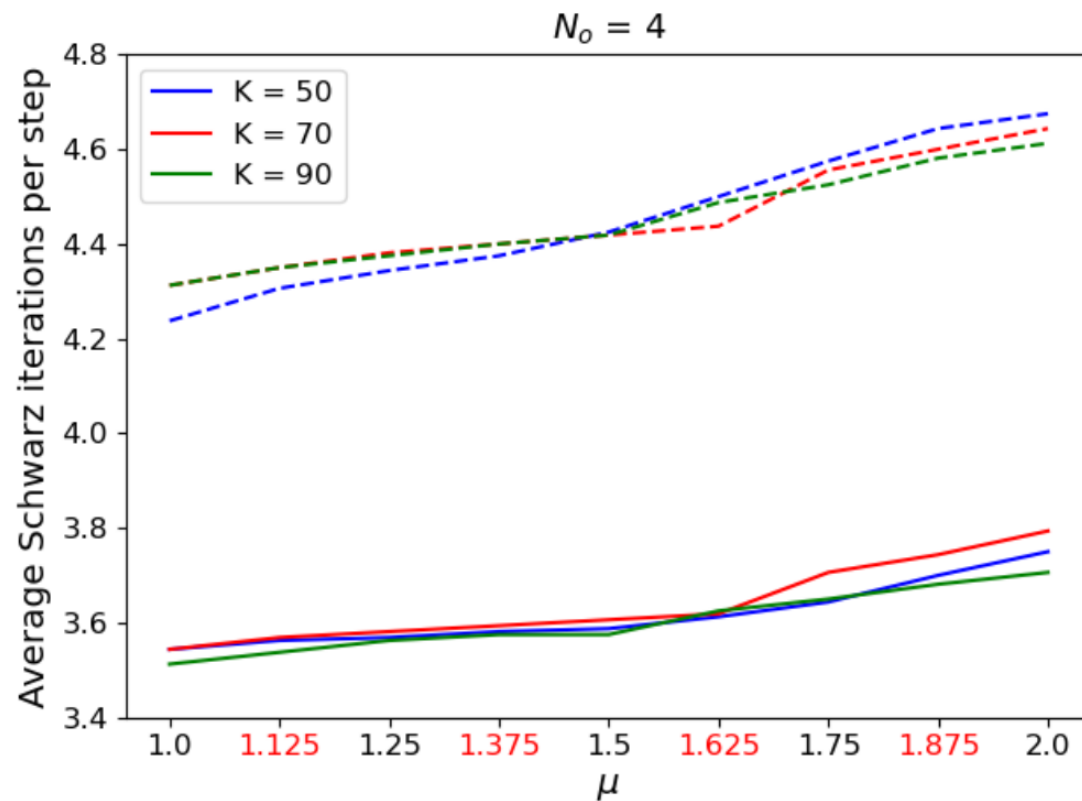
- Additive does not affect accuracy, converging to same result
- As expected, additive incurs additional Schwarz iterations
- Increased PROM dimension also degrades convergence



Solid: multiplicative, Dashed: additive

2D Euler: Schwarz PROMs

- PROM dimension has **less** effect on convergence, additive has **more**
- True cost savings unachievable without hyper-reduction



Solid: multiplicative, Dashed: additive

Work in Progress: Accelerating Non-Overlapping Schwarz



G. Sambataro

- **Risk:** non-overlapping Schwarz can be slow to converge w/ Dirichlet-Neumann TCs.
- **Mitigation:** explore accelerating Dirichlet-Neumann Schwarz via Aitken and Anderson acceleration.

Non-overlapping Dirichlet-Neumann Schwarz

$$\begin{cases} \text{Div } \mathbf{P}_1^{(n+1)} + \rho \mathbf{B}(t_i) = \mathbf{0}, & \text{in } \Omega_1 \\ \boldsymbol{\varphi}_1^{(n+1)} = \boldsymbol{\chi}, & \text{on } \partial\Omega_1 \setminus \Gamma \\ \boldsymbol{\varphi}_1^{(n+1)} = \boldsymbol{\lambda}_{n+1} & \text{on } \Gamma \end{cases}$$

$$\begin{cases} \text{Div } \mathbf{P}_2^{(n+1)} + \rho \mathbf{B}(t_i) = \mathbf{0}, & \text{in } \Omega_2 \\ \boldsymbol{\varphi}_2^{(n+1)} = \boldsymbol{\chi}, & \text{on } \partial\Omega_2 \setminus \Gamma \\ \mathbf{P}_2^{(n+1)} \mathbf{n} = \mathbf{P}_2^{(n+1)} \mathbf{n}, & \text{on } \Gamma \end{cases}$$

Aitken acceleration can reduce the # of Schwarz iterations by 3× and has virtually no tuning knobs.



Minimal tuning knobs improves usability.

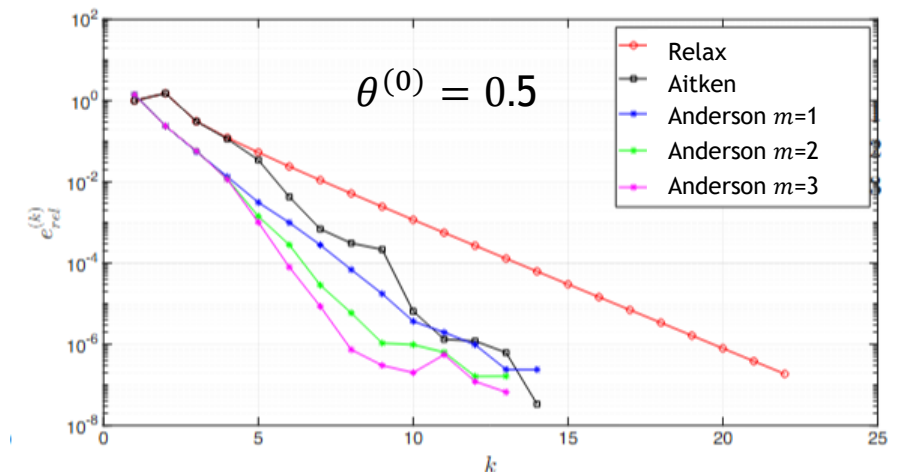
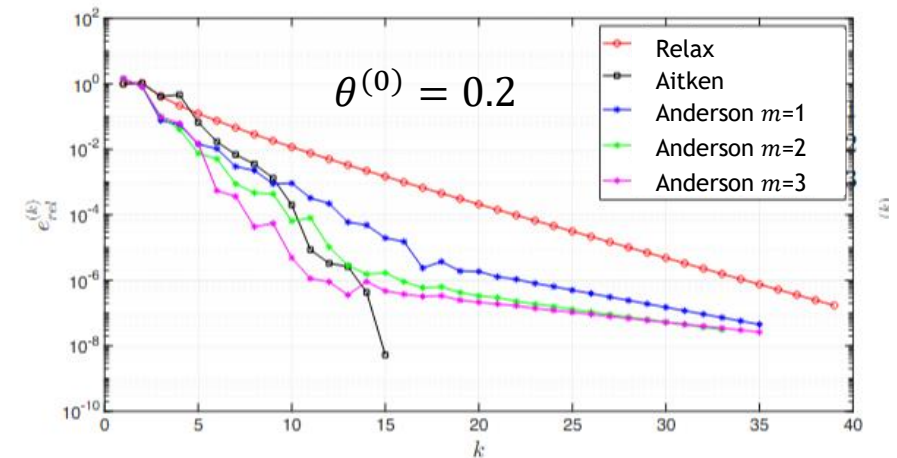
Classical relaxation: $\boldsymbol{\lambda}_{n+1} = \theta \boldsymbol{\varphi}_2^{(n)} + (1 - \theta) \boldsymbol{\lambda}_n$, on Γ , for $n \geq 1$

Aitken acceleration: $\boldsymbol{\lambda}_{n+1} = \boldsymbol{\varphi}_1^{(n)} + \theta^{(n-1)} (\boldsymbol{\varphi}_2^{(n-1)} - \boldsymbol{\varphi}_1^{(n-1)})$

$$\theta^{(n)} = - \frac{(\boldsymbol{\varphi}_2^{(n)} - \boldsymbol{\varphi}_1^{(n)} - \boldsymbol{\varphi}_2^{(n-1)} - \boldsymbol{\varphi}_1^{(n-1)}) \cdot (\boldsymbol{\varphi}_1^{(n)} - \boldsymbol{\varphi}_1^{(n-1)})}{\|\boldsymbol{\varphi}_2^{(n)} - \boldsymbol{\varphi}_1^{(n)} - \boldsymbol{\varphi}_2^{(n-1)} - \boldsymbol{\varphi}_1^{(n-1)}\|^2}$$

Anderson acceleration: $\boldsymbol{\lambda}_{n+1} = \sum_{j=0}^m \theta^{(n)} T(\boldsymbol{\lambda}_{k-m+j})$,

$\theta^{(n)}$ from optimization problem



Work in Progress: SAM-based Coupling for Non-Intrusive NN-based Models



E. Parish



A. Gruber



Motivation: finite deformation mechanics *does not* admit a *polynomial structure*

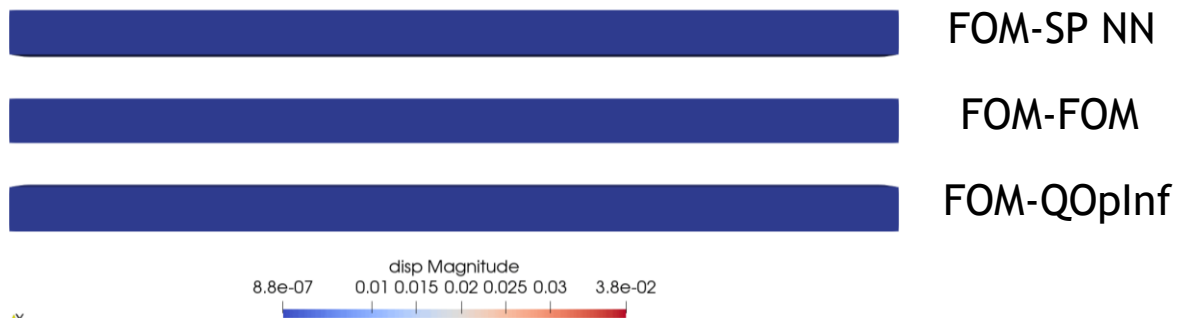
- Limits capacity of polynomial-based OpInf models

Approach: Develop a *neural-network-based OpInf* model-reduction strategy

- Can represent *general nonlinearities*
- Enforces *structure* by designing NN operators to parameterize a positive definite stiffness matrix
- Fully differentiable ML software* enables standard and dynamics-constrained training

Pros: Enables accurate models for *strong nonlinearities*

Cons: Higher *offline cost*



NN modeling strategy

$$\ddot{\hat{q}}^{NN} + \hat{K}(\hat{q}^{NN}; \mathbf{w}_K) - \hat{B}(\mathbf{u}_i, \hat{q}^{NN}; \mathbf{w}_B) = \mathbf{0}$$

\hat{K}, \hat{B} : NN models for stiffness and boundary forcings

$\mathbf{w}_K, \mathbf{w}_B$: Learnable parameters

Structure is enforced via SPD parameterization of stiffness:

$$\hat{K} = \hat{L}\hat{D}\hat{L}^T$$

Enforced structure significantly improves performance

Future work: Hamiltonian parameterizations

Training paradigms

Offline (traditional) training

$$\min_{\mathbf{w}_K, \mathbf{w}_B} \sum_{i=1}^N (\ddot{\hat{q}}_i + \hat{K}(\hat{q}_i; \mathbf{w}_K) - \hat{B}(\mathbf{u}_i, \hat{q}_i; \mathbf{w}_B))^2$$

Dynamics-constrained training (rollout)

$$\min_{\mathbf{w}_K, \mathbf{w}_B} \sum_{i=1}^N (\hat{q}(t_i) - \hat{q}^{NN}(t_i))^2$$

$$\text{s.t. } \ddot{\hat{q}}^{NN} + \hat{K}(\hat{q}^{NN}; \mathbf{w}_K) - \hat{B}(\mathbf{u}_i, \hat{q}^{NN}; \mathbf{w}_B) = \mathbf{0}$$